CHARACTERIZATION & TREATMENT OF LARGE SENSORY FIBER PERIPHERAL NEUROPATHY IN DIABETIC MICE

By

Karra Anne Muller

B.S., Emory University, 2003

Submitted to the graduate degree program in Anatomy and Cell Biology and the Graduate Faculty of the University of Kansas in partial fulfillment of the requirements for the degree of Doctor of Philosophy

Dissertation Committee:

_____
Douglas E. Wright, PhD
Committee Chairperson

_____
Dianne Durham, PhD

_____
Stephen C. Fowler, PhD

_____
Patricia Kluding, PhD

_____
Hiroshi Nishimune, PhD

Date Defended: August 13, 2008

I. ACCEPTANCE PAGE

The Dissertation Committee for Karra Anne Muller certifies that this is the approved version of the following dissertation:

THE CHARACTERIZATION & TREATMENT OF LARGE SENSORY FIBER PERIPHERAL NEUROPATHY IN DIABETIC MICE

Dissertation Committee:

_____
Douglas E. Wright, PhD
Committee Chairperson

_____
Dianne Durham, PhD

_____
Stephen C. Fowler, PhD

_____
Patricia Kluding, PhD

_____
Hiroshi Nishimune, PhD

Date Accepted:

TABLE OF CONTENTS

Contents **Page**

II. ACKNOWLEDGEMENTS

I would like to start out by saying that none of this would have been possible without the enormous amount of support, education, and laughs that many people have provided over the years. First of all, I would like to thank my mentor, Dr. Douglas Wright, for all of his guidance. Also, I really appreciate Doug for not allowing me to take myself too seriously all of the time. He granted me the utmost freedom and trusted in my work even when I sometimes did not – and for that Doug, thank you. I also want to thank all of the members of the Wright Lab that I have had the joy to work and play with. Thanks go out to Janelle Ryals and Dr. Susan Smittkamp for having patience with me as a rotating and new graduate student. Thanks to Dr. Rohan Gandhi for the fun times before you left us for sunny San Diego. Thanks to Dr. Melinda Arnett for support and love. Thanks to Dr. Neena Sharma for your insight and physical therapy skills! Thanks to Dr. Megan Johnson for...oh my...I can't even write it all down on paper (you know!)

Thank you to everyone in my comprehensive exam and dissertation committees, Dr. Dianne Durham, Dr. Stephen Fowler, Dr. Patricia Kluding, and Dr. Hiroshi Nishimune, for their insight and assistance with everything from statistics to behavior. I would also like to thank the MD/PhD program and Dr. Joseph Bast for helping me all along the way. In addition, all of my MD/PhD student colleagues have been a huge support and a constant source of fun! Thanks also go out to MDs, PhDs and MD/PhDs that have inspired and assisted me along the way: Dr. Michael Decker, Dr. David Rye, Dr. Allan Levey, Dr. Donna Sweet, Dr. Eva Feldman, and Dr. Joan Hunt.

Also, thank you to members of the R.L. Smith Intellectual & Developmental Disabilities Research Center for their assistance with equipment, particularly the confocal microscopes – thanks to Dr. Don Warn, Doug Brownyard, and Eric Grimes.

Thank you to the Department of Anatomy and Cell Biology for their administrative assistance and stimulating seminars and discussions.

Very special thanks go out to my family – Mom and Dad, thank you for your unconditional love and support. You gave me a great base from which to climb and have believed in me all along the way. Thanks to my brother, Matthew, for being an inspiration every day to go out and pursue my dreams. Lastly, thanks go out to my constant of all constants, my husband Robb. He has given me love, support, and laughs throughout this whole process. Thank you Robb for your calming nature that brings me back to peace every day that I come home. Also, thanks cannot be forgotten for his graphic design skills and amazing posters and images that he created for me, and are even used here in this body of work.

This research was funded by the National Institutes of Health Grant R01NS43314 (DEW), the Juvenile Diabetes Research Foundation (DEW, ELF), the Biomedical Research Training Program at the University of Kansas Medical Center (KAM), and the R.L. Smith Intellectual & Developmental Disabilities Research Center NICHD HD02528.

This work is dedicated to Inez Solomon.

III. LIST OF TABLES

LIST OF TABLES

IV. LIST OF FIGURES

LIST OF FIGURES

V. CHAPTER ONE

Introduction

1. Diabetic neuropathy

Diabetes Mellitus

Diabetes mellitus (DM) encompasses multiple metabolic disorders that are ultimately associated with hyperglycemia. In 2007, 23.6 million Americans (7.8% of the population) were affected with one form of diabetes while an estimated 5.7 million Americans were undiagnosed (National Institute of Diabetes and Digestive and Kidney Diseases (NIDDK), 2007). The figures from 2007 were increased by 2.6 million people compared to reports from only two years ago (CDC, 2005). In 2002, it was estimated that diabetes cost the United States approximately $132 billion when medical expenses and the price of lost productivity were combined (Hogan et al., 2003). Moreover, the figure from 2002 was likely underestimated as patients with diabetes also have greater contact with other healthcare-related providers such as optometrists, dentists, etc. In addition, recent reports estimate that in 2007 the direct and indirect costs of diabetes in the United States had increased to $174 billion (NIDDK, 2007). Clearly there is an increase in the incidence of diabetes, and it calls for research in the prevention, cure, and treatment of patients with the disease.

Types 1 and 2 are the two main forms of diabetes, and both can result in progressive β-cell failure in pancreatic islets (Cnop et al., 2005); however, the pathogenesis differs. Type 1 diabetes is an autoimmune disease in which there is selective destruction of β-cells, while type 2 diabetes has a varied progression with β-cell failure resulting, in some patients, from the increased demand for insulin due to peripheral insulin resistance (Cnop et al., 2005; Tuomi, 2005). Clinically, diabetes is commonly diagnosed by a fasting blood glucose concentration greater than 6.9 mM (American Diabetes Association, 2006). Insulin is a hormone made and released

from pancreatic β-cells in response to increased blood glucose levels. Insulin's primary action is to increase uptake and storage of blood glucose by peripheral cells. When decreased β-cell activity occurs in type 1 and 2 diabetes, it leads to decreased insulin production, which disrupts glucose homeostasis. Although, it is important to note that type 2 diabetic patients can have hyperinsulinemia, which is thought to be a response to peripheral insulin resistance (Smith and Singleton, 2008). Therefore, the metabolic status of patients with diabetes always involves hyperglycemia, but can have either hypoinsulinemia or hyperinsulinemia.

Neuropathy Overview

The altered metabolic state in patients with DM leads to multiple diabetes-related long-term complications, such as retinopathy, nephropathy, cardiovascular disease, and neuropathy (American Diabetes Association, 2004). Diabetic neuropathy has many sub-classifications, but overall, approximately 70% of patients will diabetes will develop some form of nervous system damage throughout the course of their disease (Centers for Disease Control and Prevention, 2005). In patients with diabetes, neuropathy is the most common long-term complication (Vinik et al., 2000). In fact, diabetes is known as the leading cause of neuropathy in the United States and Western countries (Duby et al., 2004). Of the diabetic neuropathy subtypes, the most common is diabetic sensorimotor polyneuropathy (DPN) (Sinnreich et al., 2005). Interestingly, DPN has many names: distal symmetrical sensory greater than motor polyneuropathy, distal peripheral neuropathy, sensorimotor neuropathy, and distal symmetrical polyneuropathy (Duby et al., 2004; Sinnreich et al., 2005; Dobretsov et al., 2007). In this body of work we were interested in studying the DPN

subtype of diabetic neuropathy specifically, and will simply use the nomenclature DPN.

Pathophysiology

Many theories have been explored for the pathophysiology of DPN, and most involve prolonged hyperglycemia as the overriding cause (Duby et al., 2004; Vinik and Mehrabyan, 2004; Tomlinson and Gardiner, 2008). It has been shown that reversing hyperglycemia by treatment with insulin can improve symptoms and/or delay the progression of DPN (Skyler, 2004). When insulin is present in the blood, it directs some glucose into cells for immediate use and the remaining glucose into storage in muscle, fat, and the liver (Tomlinson and Gardiner, 2008). However, in the setting of diabetes and hypoinsulinemia, blood glucose concentrations increase dramatically. Neurons are known for insulin-independent glucose uptake that is proportionate to extracellular concentrations of glucose. Therefore, the hyperglycemia translates into dangerously large increases in neuronal glucose (Tomlinson and Gardiner, 2008). High neuronal glucose levels result in glucose neurotoxicity, which is characterized by increased oxidative stress, advanced glycation end-product (AGE) formation, and polyol pathway flux, as depicted in **Figure V-1** (Duby et al., 2004; Dobretsov et al., 2007; Tomlinson and Gardiner, 2008).

Oxidative stress is the result of glucose participation in pathological processes due to its higher than normal concentration (Duby et al., 2004). Increased oxidative stress results in increased free-radical generation, impaired antioxidant/detoxification pathways, and an increase in precursors for nitrosylation and lipoxidation (van Dam et al., 1995; Duby et al., 2004; Tomlinson and Gardiner, 2008).

Figure V-1. Hypothesized pathogenesis of diabetic neuropathy. Hyperglycemia leads to glucose neurotoxicity, which manifests as seen in this figure (adapted from AC Kappelle, ISNO Dutch Neuromuscular Research Support Centre, www.isno.nl). Glucose-induced metabolic alterations include increased polyol pathway flux, increased oxidative stress, and an increase in protein glycation, which all affect one-another. These alterations can, in turn, have an effect on microvasculature, and all of the pathways together can impact nerve function. In addition, decreased neurotrophin support can also lead to nerve dysfunction.

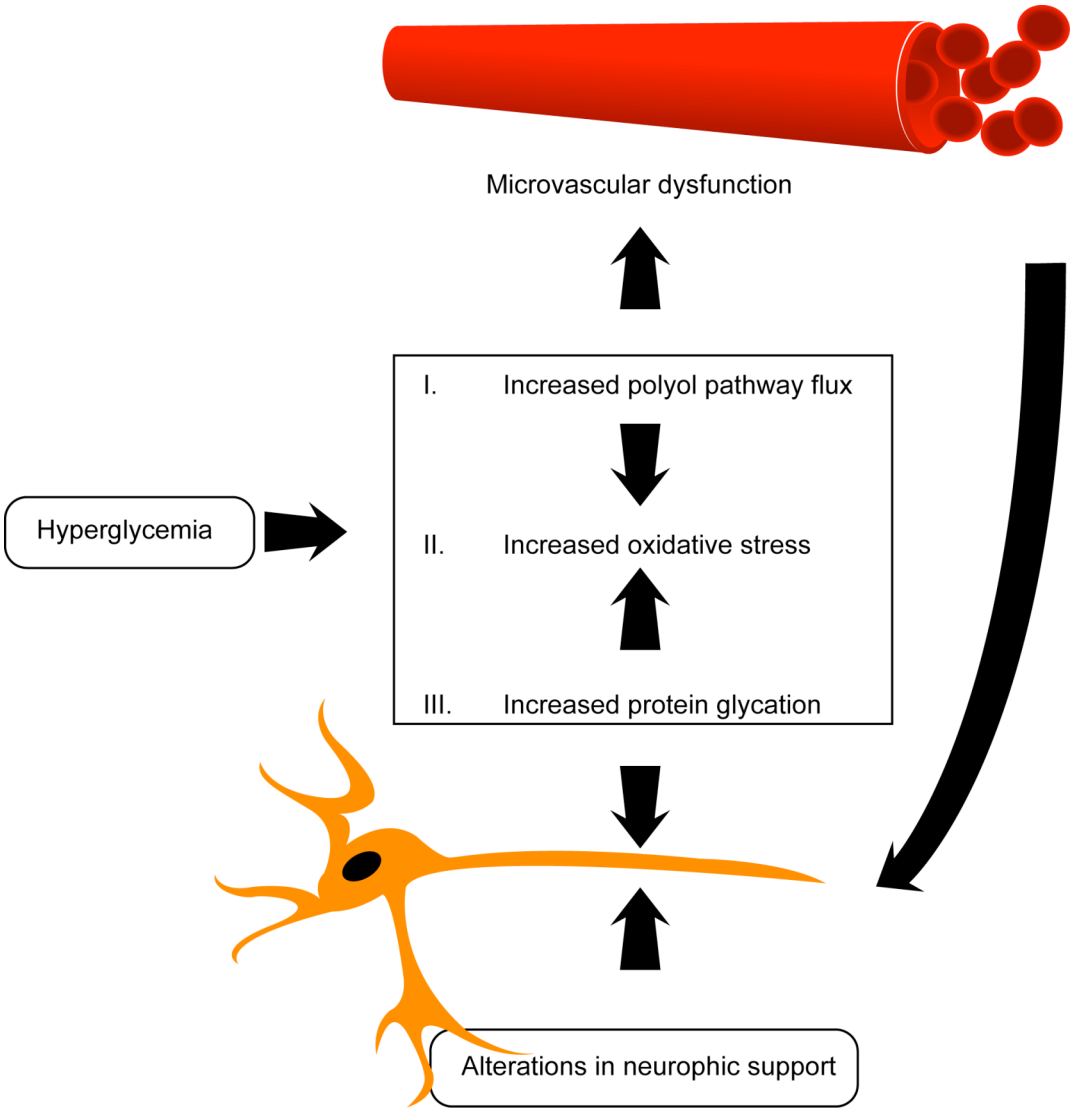
Microvascular dysfunction
I. Increased polyol pathway flux
II. Increased oxidative stress
III. Increased protein glycation
Hyperglycemia
Alterations in neurophic support

In addition, oxidative stress increases substrates for protein glycation, which occurs through nonenzymatic covalent bonds between glucose and proteins through the Maillard reaction. This, in turn, produces Schiff bases that undergo Amadori rearrangement to form stable AGEs (Duby et al., 2004; Tomlinson and Gardiner, 2008). AGE formation has deleterious effects on proteins by impairing their structure and function (Duby et al., 2004). In addition, extra glucose in nerves can be shunted into the polyol pathway, which is normally limited by low glucose concentrations. Increased polyol pathway flux leads to the pathogenic accumulation of sorbitol and fructose and increased turnover of NADPH and NAD+, which are needed for glutathione reduction (Tomlinson, 1993; Duby et al., 2004).

Neuronal damage in the setting of diabetes can also be due to microvascular complications and/or decreased neurotrophin support (Duby et al., 2004; Dobretsov et al., 2007). Nerves and blood vessels have physiological interdependence, and damage to one can affect the function of the other. Microvascular alterations have been documented in diabetes, such as pathologic vasoconstriction and hypoperfusion, and are implicated in damage to peripheral nerves (Cameron et al., 2001). Additionally, multiple studies have reported diabetes-induced decreased neurotrophic support to neurons (Brewster et al., 1994; Ishii, 1995; Dyck, 1996), which is hypothesized to lead to nerve dysfunction and damage. Importantly, insulin has also been shown to act as a trophic factor for nerves (Recio-Pinto et al., 1986; White, 2003; Brussee et al., 2004; Toth et al., 2006), and insulin levels are decreased in some diabetic patients. Therefore, insulin deficiency itself may lead to neuropathy.

DPN

As mentioned above, diabetic neuropathy has many sub-classifications as diabetes can affect peripheral sensory, motor, and autonomic neurons. Our focus is on diabetic sensorimotor polyneuropathy (DPN), which can affect both large and small sensory afferent nerve fibers. Large sensory nerve fibers are heavily myelinated and involved in proprioception, reflexes, sensorimotor function (balance and gait), touch, and vibration sense (Waxman, 2003). Small nerve fibers are either lightly myelinated or have no myelination and involved in pain, temperature sense, and some light touch (Waxman, 2003). Typically, DPN is characterized by a distal symmetrical nerve degeneration pattern, referred to as a glove-and-stocking distribution (Duby et al., 2004; Sinnreich et al., 2005). Some of the typical fiber changes found in DPN are axonal degeneration, regeneration, demyelination, and remyelination (Sinnreich et al., 2005). The majority of research focuses on small-fiber neuropathy leading to increased or decreased cutaneous pain and temperature sensations. Using different animal models of diabetes (mainly rat and mouse), allodynia, hyperalgesia, and hypoalgesia in DPN have been widely characterized (Calcutt et al., 1996; Drel et al., 2006; Johnson et al., 2007; Sullivan et al., 2007). However, there is a shortage of animal model research exploring large-fiber DPN, which can cause deficits in lower limb proprioception, decreased tactile sensitivity and vibration sense, and incoordination due to gait and balance abnormalities (Duby et al., 2004; Casellini and Vinik, 2007).

Large-Fiber DPN

The sensorimotor deficits due to large-fiber DPN, while sometimes subtle in nature, can lead to significant impairment. Numerous human studies have reported

that patients with DPN are at increased risk for falls due to decreased postural control, altered gait and balance, and increased body sway (Cavanagh et al., 1992; Uccioli et al., 1995; Richardson et al., 2001). Cavanagh et al. (1993) found that patients with DPN were 15 times more likely to report an injury/fall during walking and/or standing compared to diabetic patients without neuropathy. Falls are particularly dangerous as they are a main source for morbidity and mortality in the elderly and diabetic (Richardson, 2002; Malik, 2003; Cimbiz and Cakir, 2005).

Sensorimotor functions include proprioception, gait, and balance, all controlled by the use of large sensory nerve fibers, motor nerves, and skeletal muscles. The muscle spindle is an important regulator of sensorimotor function, and will be discussed later in this chapter. Muscle weakness and atrophy are known to occur in patients with DPN (Cotter et al., 1989; Andersen et al., 1996; Andersen et al., 2004), and it has been hypothesized that problems with gait and postural control were due to these motor/skeletal muscle alterations (Courtemanche et al., 1996). However, many studies have suggested the combination of altered motor and sensory nerve information, perhaps in the muscle spindle, may cause the DPN patient's dysfunction in gait and balance (Bergin et al., 1995; van Deursen et al., 1998; Sacco and Amadio, 2003; Nardone and Schieppati, 2004; Menz et al., 2004).

Interestingly, disrupted ankle movement, in particular, has been implicated as leading to altered gait and balance in DPN patients (Mueller et al., 1994; Kwon et al., 2003). During walking, the ankle performs both dorsiflexion and plantarflexion, using different muscle groups in order to complete the full stance and swing phases comprising gait. Kwon et al. (2003) reported decreased peak ankle dorsiflexion in patients with DPN compared to controls, which they hypothesized to be due to

premature activation of the soleus and medial gastrocnemius muscles that make up the plantar flexion phase. In order for these flexor muscles to be activated, it takes coordinated firing of both sensory and motor nerves and functional muscle spindles. Kwon et al. (2003) attributed the premature activation of flexor muscles to be a compensatory mechanism for patients to improve balance. However, an alternate hypothesis is that premature activation of soleus and medial gastrocnemius muscles is a result of altered muscle spindle firing of sensory and/or motor nerves.

Nerve conduction studies have been used a great deal in the diagnosis of DPN clinically, and decreased nerve conduction velocity (NCV) can indicate nerve dysfunction even before the patient displays symptoms of DPN (Dyck et al., 2005). Motor and sensory NCV can be decreased experimentally in diabetic mice (Moore et al., 1980), and they are common measurements used as a criterion for DPN in many neurology clinics. However, as discussed above, DPN can affect small and large sensory nerve fibers, in addition to motor nerves, and NCV is used to diagnose general DPN. This becomes a problem clinically because NCV is a better measure of large sensory and motor nerve function, and does not accurately reflect the activity of Aδ and C fibers (Sinnreich et al., 2005; Horowitz, 2006). In contrast, for our studies of large-fiber DPN, nerve conduction studies add important information of the status of large peripheral nerves.

Overall, the underlying neurologic mechanisms involved in large-fiber DPN remain poorly understood. It has been hypothesized, based on clinical studies in humans, that large-fiber DPN instability could be caused by altered sensorimotor function, specifically damaged group Ia and II sensory afferent fibers in muscle spindles (Simoneau et al., 1996; van Deursen et al., 1998; Nardone et al., 2007).

However, visualization of muscle spindles in humans is extremely difficult, and only through indirect testing of muscle spindle afferents, can any information be gained in support of the hypothesis.

2. Muscle Spindle

Anatomy

Muscle spindles found within skeletal muscle are rapidly adapting sensorimotor receptors. Spindles in mice are surrounded by extrafusal muscle fibers and consist of a capsule containing 2 bag and 2-4 chain intrafusal fibers that run parallel with the extrafusal fibers. In humans, spindles can contain up to 10 intrafusal fibers (Ganong, 2005). Nuclear bag intrafusal fibers are dilated in the center and have a dynamic response to extrafusal fiber stretch, while nuclear chain intrafusal fibers are thinner and shorter and have more of a static response to stretch. Muscle spindle sensory afferents are often called proprioceptors. Three subtypes of nerves innervate the intrafusal fibers: group Ia and II large sensory axons and gamma motor axons (**Figure V-2A**). Group Ia fibers are rapidly conducting and terminate with an annulospiral morphology in the equatorial (central) region of intrafusal fibers. Group II fibers terminate in a flower-spray morphology either side of the group Ia fibers. The gamma motor neurons terminate on motor end plates at the polar ends of the intrafusal fibers.

During development, muscle spindle intrafusal fibers and sensory afferents require the trophic support of neurotrophin 3 (NT-3; Wright et al., 1997). NT-3 is expressed by fetal extrafusal fibers pre-natally and acts as the main ligand for tyrosine kinase C (trkC) receptors found on Ia and II sensory afferents (Wright et al.,

1997). Recently it was reported that, post-natally, muscle spindle intrafusal fibers release NT-3 in order to maintain sensory afferent connections with the spindles themselves and motor neurons (Chen et al., 2002).

Function

Muscle spindles are involved in multiple sensorimotor behaviors such as the regulation of proprioception, balance, gait, and the postural response (Stapley et al., 2002; Waxman, 2003). **Figure V-2B** outlines muscle spindle firing. When the muscle spindle intrafusal fibers are stretched, it leads to sensory nerve ending distortion, which allows for an increase in receptor potentials to then cause sensory nerve firing. Because the intrafusal fibers are in parallel with extrafusal fibers, if the extrafusal fibers stretch from relaxation, this causes the intrafusals to stretch and, concomitantly, the sensory nerves to fire. Action potentials generated from sensory nerves are at frequencies proportional to the amount of intrafusal and extrafusal fiber stretching. Because muscle spindle proprioceptors make monosynaptic connections with alpha motor neurons in the ventral horn of the spinal cord, spindle firing leads to motor neuron firing, which results in contraction of the extrafusal fibers of the same muscle and, through spinal cord inhibitory interneuron connections of reciprocal innervation, relaxation of the extrafusal fibers of the opposing or antagonistic muscle. In addition, gamma motor neurons receive input from descending motor pathways and sensitize the intrafusal fibers so that less stretch will lead to greater firing of spindle afferents, and vice versa. All of this results in coordinated reflexes, proprioception, and sensorimotor function allowing for normal gait and balance.

Figure V-2. Muscle spindle innervation and firing pathways. (A) Representation of a muscle spindle. Intrafusal fibers are shown in blue in parallel to the extrafusal fibers in gray. The Ia afferent fibers in green have an annulospiral morphology in the equatorial region of the spindle. On either side of the equatorial region are group II afferent fibers with a flower-spray morphology. At the ends of the intrafusal fibers are gamma motor neurons synapsing at neuromuscular junctions. (B) Representation of muscle spindle firing pathways. Spindles (in red) stretch proportionately to the amount and rate of stretch in extrafusal fibers (in gray) leading to sensory afferent (in green) firing. The sensory afferent signal travels through the cell body in the dorsal root ganglia through to the spinal cord where the fibers synapse with alpha motor neurons (in yellow) in the ventral horn. This induces alpha motor neuron firing, which sends the signal to extrafusal fibers of the same muscle telling it to contract. In addition, gamma motor neurons (in blue) bring their signal from descending motor pathways to the intrafusal fiber in order to sensitize it.

A

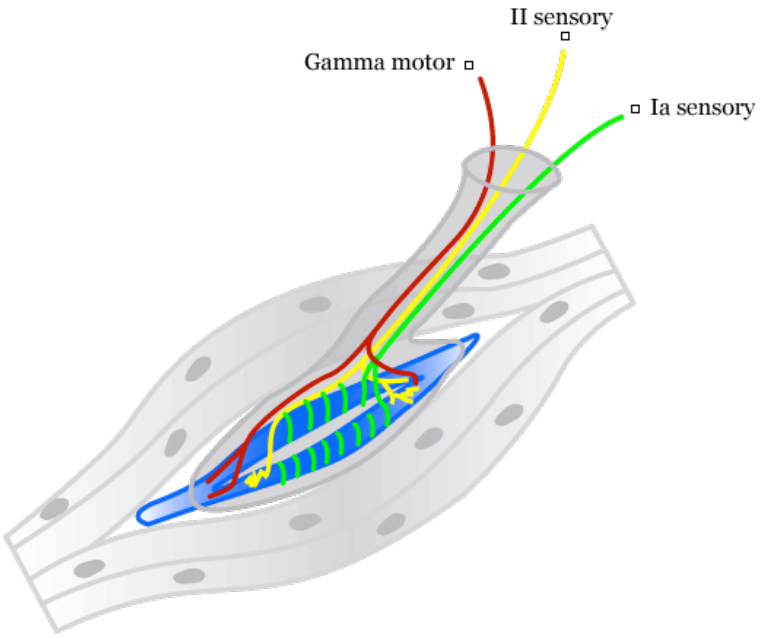

B

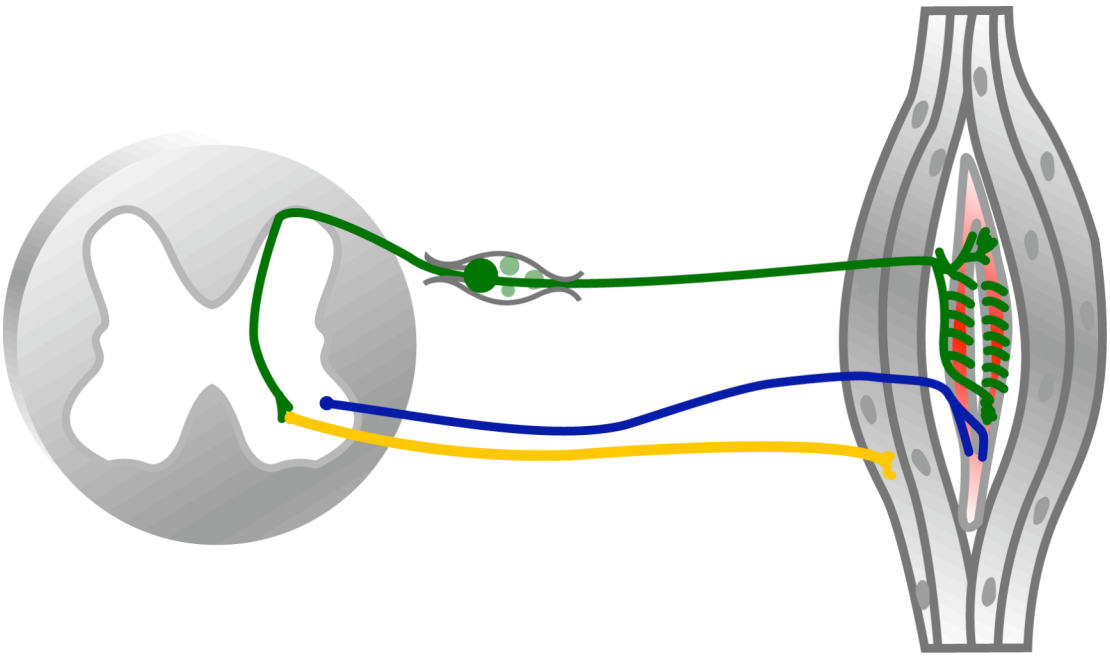

Muscle Spindle Pathology

Muscle spindle damage can lead to problems with proprioception, balance, and/or ataxic gait. Multiple studies in humans have reported changes to muscle spindle morphology during aging that could contribute to the increase in falls and ataxia seen in the elderly (Swash and Fox, 1972; Kararizou et al., 2005). Specifically, Swash and Fox (1972) found that aged spindles had a decreased number of intrafusal fibers per spindle and axonal swellings, and suggested that some spindles were denervated. In rodents, Egr3 null mutant mice have muscle spindle degeneration postnatally, which results in an ataxic gait and proprioceptive deficits (Chen et al., 2002). In addition, after nerve crush injury in mice, muscle spindle afferents degenerate with subsequent reinnervation resulting in altered sensorimotor function (Taylor et al., 2005). Therefore, it is plausible that symptoms of large-fiber DPN, such as altered sensorimotor function, could result from damage to muscle spindle large afferent fibers.

Muscle Spindle and Diabetes

It has been hypothesized that alterations in large sensory nerve fibers innervating muscle spindles (group Ia and II fibers) in diabetic patients contribute to their manifested gait disturbances (Weis et al., 1995; Nardone et al., 2007). An indirect analysis of muscle spindles in the setting of diabetes was performed by Kishi et al. (2002). They analyzed dorsal root ganglia from STZ-treated diabetic rats and found that the neurons of largest size were reduced in number by 41%, which was the greatest decrease out of all sensory nerve populations. The largest sensory neurons found in the DRG correspond to the group Ia population of spindle afferents. Therefore, it can be inferred that after 12 months of diabetes in rats, the large spindle

afferents are the most highly affected population of sensory neurons. Direct analysis of diabetic muscle spindles was performed by Weis et al. (1995). They reported that STZ-induced diabetes in rats leads to spindle sensory axon dilation, sporadic axonal dystrophy, and axonal blebs that they described as “myelinlike cytoplasmic globules”. In addition, some intrafusal fibers presented with abnormal nuclei. Weis and colleagues (1995) also recorded decreased motor and sensory NCVs compared to nondiabetic rats, which is reflective of large sensory and motor nerve fiber function. However, it should be noted that the diabetic rats received small doses of insulin in order to prevent a catabolic state, which could have had an effect on the results of their study.

As discussed above, NT-3 is a trophic factor involved in the development of muscle spindles, and it continues to be expressed by intrafusal fibers into adulthood in order to support sensory afferents (Copray and Brouwer, 1994). Fernyhough et al. (1998) showed that NT-3 expression in skeletal muscle was decreased in the STZ-induced diabetic rat. In addition, treatment with insulin prevented a pathologic decrease in NT-3. They hypothesized that large nerve fibers in muscle expressing trkC receptors could be receiving decreased trophic support during diabetes. Fernyhough and Tomlinson then went on to examine NT-3 production in the dorsal root and found that it was increased in the setting of diabetes (Cai et al., 1999). They suggest that because of decreased NT-3 production in muscle, its expression is increased in the dorsal root ganglia in order to maintain proprioceptors. Interestingly, it was also reported that NT-3 levels are significantly increased in the epidermis of diabetic patients compared to nondiabetics, and is concomitant with epidermal denervation (Kennedy et al., 1998). Taken together, these studies reveal that altered

NT-3 expression could be a potential mechanism for aberrant muscle spindle function in the setting of diabetes.

Intrafusal bag fibers contain primarily the slow tonic myosin heavy chain (MyHC) isoform, while chain fibers contain primarily fast tonic MyHC (Soukup et al., 1990). Myosins are molecular motors involved in extrafusal and intrafusal contraction, and their heavy chains are characterized (slow versus fast tonic) by their oxidative capacity. Interestingly, Cotter et al. (1989) reported that STZ-induced diabetes in rats lead to a decrease in fast twitch MyHC extrafusal fibers in the extensor digitorum longus muscle, which was in agreement with a study from Armstrong et al. (1975) that found the same decrease in fast fibers in the gastrocnemius muscle with preservation of slow twitch fibers. To date, only MyHC diabetic alterations in extrafusal fibers have been reported; however, it is important to note that changes in extrafusal fibers could be reflected by the same pathology in intrafusal fibers due to both fibers containing the same MyHCs. In fact, Liu et al. (2005) examined aging muscle spindles and found that chain fibers were preferentially lost, which could be interpreted as fast twitch MyHC loss over slow twitch. Therefore, it is possible that diabetes induces a loss in not only extrafusal fast twitch fibers, but also intrafusal fast twitch fibers (the nuclear chain fibers).

3. Insulin

As briefly mentioned above, one of the main functions of insulin is glucose homeostasis through increasing glucose uptake from the blood and acting on insulin receptors (IRs) in the liver, skeletal muscle, and adipose tissue. Moreover, IRs are also located on perikarya of neurons, spinal nerve roots, and on peripheral axons

(Sugimoto et al., 2002; Toth et al., 2006). After treatment with insulin intrathecally, locally, and even systemically, multiple reports have shown improvements in DPN (Singhal et al., 1997; Huang et al., 2003; Brussee et al., 2004; Christianson et al., 2007; Hoybergs and Meert, 2007). Specifically, Christianson et al. (2007) reversed diabetes-induced cutaneous mechanical insensitivity with treatment of systemic insulin. Additionally, in a rat model of diabetes, cutaneous allodynia was normalized after low-dose insulin therapy, even in the presence of sustained hyperglycemia (Hoybergs and Meert, 2007). Electrophysiologic deficits in diabetes can also be corrected by low-dose insulin treatment (Singhal et al., 1997). Therefore, it is clear that different paradigms of insulin treatment can result in a variety of improved symptoms of DPN; however, the mechanisms of action are not quite as clear.

Importantly, insulin has actions aside from glucose homeostasis. Data reveal that insulin itself can act as a neurotrophic factor to support peripheral nerves by signaling through IRs, and even through insulin-like growth factor 1 (IGF-1) receptors (Recio-Pinto et al., 1986; Toth et al., 2006). Perhaps insulin is not only needed for glucose homeostasis in diabetic patients, but also for trophic support. It has been suggested that hyperglycemia may not be the only or main cause of DPN, and insulin may have a greater role than previously thought (Romanovsky et al., 2006; Dobretsov et al., 2007). In fact, Romanovsky and colleagues (2006) examined STZ-treated rats that were normoglycemic, but insulinopenic. These animals developed mechanical hyperalgesia that could be attributed to low insulin levels due to their lack of hyperglycemia.

4. Exercise

Exercise and Diabetes

The American Diabetes Association (2007) recommends aerobic exercise for diabetic patients to help prevent diabetes-related complications, such as DPN. Exercise therapy has been evaluated recently as a treatment for DPN in humans, with multiple different protocols (aerobic exercise, resistance training, or exercise counseling) resulting in a variety of conclusions. A number of studies have reported improved clinical measurements of diabetic and pre-diabetic neuropathy after exercise therapy including intraepidermal nerve fiber (IENF) density, balance control, nerve conduction velocities (NCV), and vibration perception thresholds (Richardson et al., 2001; Balducci et al., 2006; Smith et al., 2006). Additionally, diabetic exercise studies have reported inconsistencies in regards to the metabolic parameters of the patients. Some papers report a lowering of fasting blood glucose concentrations (Sigal et al., 2004), while others found no changes in fasting blood glucose (Balducci et al., 2006; Smith et al., 2006).

Exercise's Mechanism of Action

Overall, the molecular mechanisms behind treating DPN with exercise therapy have not been elucidated, but several hypotheses exist. Exercise can have positive effects directly on the cardiovascular system, on the musculoskeletal system, and even directly on nerves themselves. A natural physiological codependence exists between the peripheral nervous system and the microvascular system (Duby et al., 2004). Therefore, it has been theorized that exercise-induced increases in blood flow improve nerve function. In general, it has been shown that intense exercise can lower blood glucose levels and hemoglobin A_{1C} values in human diabetic patients

(Sigal et al., 2004). Moreover, exercise therapy increases overall skeletal muscle strength (Praet et al., 2008). In the nervous system, exercise therapy can act directly on nerves through production of neurotrophins. Molteni et al. (2004) reported that exercise-conditioned animals had increased nerve regeneration after peripheral sciatic nerve crush that was attributed to increased mRNA levels of brain-derived neurotrophic factor (BDNF) and NT-3 in L4-5 dorsal root ganglia of exercise mice compared to sedentary mice. In addition, a more recent study from the same group reported that exercise facilitated the recovery of locomotion following hemisection of the spinal cord through the regulation of BDNF (Ying et al., 2005). Recently we found that aerobic exercise in mice increased NT-3 in skeletal muscle (Sharma et al., unpublished results), which could have a positive effect on NT-3-deficient diabetic muscle and muscle spindles. Lastly, exercise therapy has also been reported to decrease oxidative stress (Villa-Caballero et al., 2007; Nojima et al., 2008), which is implicated as one of the main mechanisms for the development of diabetic neuropathy (Duby et al., 2004; Tomlinson and Gardiner, 2008).

5. Study Significance

It is increasingly apparent that DPN is a large problem for patients and the healthcare system in general. As mentioned above, approximately 70% of patients with diabetes will develop diabetic neuropathy. In addition, large-fiber neuropathy leading to altered gait and balance is a major cause of morbidity and mortality in diabetic patients. Currently, no treatments have been developed for large-fiber neuropathy. This is partially due to the fact that the literature discussing large-fiber DPN explores the disease in human patients. It is obviously important to research

the human condition; however, the findings are hindered by inability to directly examine the hypotheses generated from such work.

Accordingly, the overall goal of this body of work was to characterize large-fiber diabetic sensorimotor polyneuropathy in a widely-used animal model of diabetes, and explore the hypothesis shared by many that the symptoms of large-fiber DPN could be due, in part, to aberrant muscle spindle innervation. Only a few studies, to our knowledge, had examined muscle spindles in the setting of diabetes, and each one did so in a largely descriptive fashion. With this work, we have joined together two fields of study – diabetic neuropathy and muscle spindles – and have tried to bring more insight into the human condition of large-fiber DPN. In addition, we have explored a relatively understudied area of DPN by looking at large-fiber neuropathy in animal models. It is our hope that with this and subsequent studies, the mechanisms of large-fiber neuropathy will be revealed and treatments will be identified and implemented. Overall, this work provides novel techniques for the assessment of muscle spindle innervation and function and uncovers inadequacies in our scientific knowledge that can be further addressed.

In Chapter 2 ("**Diabetic Mice Display Sensorimotor Deficits and Altered Muscle Spindle Ia Afferent Innervation**") we developed a novel method for quantifying muscle spindle Ia afferent innervation using immunohistochemistry and confocal microscopy that allows for visualizing very detailed morphologic alterations. In addition, a behavior task was identified that successfully measured sensorimotor deficits in diabetic mice. Importantly, muscle spindle sensory afferents were found to have altered morphology, lending support to many clinicians' suspicions that deficits in gait and balance in DPN patients could be due to muscle spindle dysfunction.

In Chapter 3 ("**Insulin Treatment Modifies Development of Sensorimotor Deficits and Repairs Muscle Spindle Ia Afferent Innervation in Diabetic Mice**") we used slow-release insulin pellets to treat the large-fiber neuropathy that was characterized in Chapter 2. Our findings lent support to the results of Chapter 2 because insulin reversed the diabetes-induced hyperglycemia and resulted in concomitant behavioral and anatomical repair. However, it also raised questions about insulin's mechanism of action, and will lead to future studies using insulin treatment directly on peripheral axons.

In Chapter 4 ("**Aerobic Exercise Therapy Improves Sensorimotor Deficits and Has No Effect on Variability in Muscle Spindle Ia Afferent Innervation in Diabetic Mice**") we were successful at creating a low-intensity aerobic exercise paradigm for diabetic mice and tested the effects of exercise on large-fiber DPN. Interestingly, exercise improved sensorimotor function, but had no effect on muscle spindle afferent morphology. This study will lead to future studies addressing the mechanism of behavioral repair, and addressing the use of other higher-intensity exercise protocols.

VI. CHAPTER TWO

Diabetic Mice Display Sensorimotor Deficits and Altered Muscle Spindle Ia Afferent Innervation

1. Abstract

Large-fiber DPN leads to balance and gait abnormalities, placing patients at extreme risk for falls. Large sensory axons innervating muscle spindles provide important feedback for balance and gait and, when damaged, can cause altered sensorimotor function. The current study was aimed at determining whether the symptoms of large-fiber DPN in type 1 and 2 diabetic mouse models are related to alterations in muscle spindle innervation.

Behavioral assessments were carried out in streptozotocin (STZ)-injected C57BL/6 mice to quantitate diabetes-induced deficits in balance and gait. Nerve conduction velocities were measured to better understand the electrophysiologic parameters of peripheral motor and sensory nerves in diabetes. In addition, quantitative assessment of group Ia axon innervation of muscle spindles was carried out using immunohistochemistry and confocal microscopy on STZ-injected C57BL/6 and leptin receptor-null mutant (*db/db*) mice.

STZ-injected C57BL/6 mice displayed significant and progressive sensorimotor dysfunction associated with balance and gait. Likewise, electrophysiologic deficits were progressive in diabetic mice, but differed between motor and sensory nerves. The analysis of Ia innervation of diabetic C57BL/6 spindles revealed a range of abnormalities in innervation patterns suggestive of Ia axon degeneration and/or regeneration. The multiple distinct and abnormal Ia fiber morphologies resulted in substantial variability in Ia axonal width and inter-rotational distance (IRD). Likewise, diabetic *db/db* mice displayed significant variability in their IRDs compared to heterozygotes (*db*+), suggesting that damage to Ia axons occurs in both type 1 and 2 models of DPN.

Similar to small sensory fibers, Ia axons are vulnerable to diabetes, and damage to these axons may contribute to balance and gait deficits. In addition, these studies provide a novel method to assist in assaying therapeutic interventions designed for diabetes-induced large-fiber dysfunction.

2. Introduction

As discussed in Chapter 1, DPN affects both large and small sensory afferent nerve fibers. There has been a shortage of animal model research exploring large-fiber DPN, which can lead to deficits in lower limb proprioception, decreased tactile sensitivity and vibration sense, and incoordination due to gait and balance abnormalities (Duby et al., 2004; Casellini and Vinik, 2007). The sensorimotor deficits due to large-fiber DPN, while sometimes subtle in nature, can lead to significant impairment; however, the underlying neurologic mechanisms remain poorly understood. Nardone et al. (2007) hypothesized that large-fiber DPN instability could be caused specifically by damaged group Ia and II sensory afferent fibers in muscle spindles.

Muscle spindle damage has been shown to lead to problems with proprioception, balance, and/or ataxic gait. Multiple studies in humans have reported changes to muscle spindle morphology during aging that could contribute to the increase in falls and ataxia seen in the elderly (Swash and Fox, 1972; Kararizou et al., 2005). In rodents, Egr3-null mutant mice have muscle spindle degeneration postnatally, resulting in an ataxic gait and proprioceptive deficits (Tourtellotte and Milbrandt, 1998; Chen et al., 2002). Therefore, it is plausible that symptoms of large-fiber DPN could result from damage to muscle spindle large afferent fibers. Here, we examined

STZ-induced type 1 and leptin receptor-null mutant (*db/db*) type 2 diabetic mouse models for evidence of large-fiber DPN and muscle spindle alterations. These novel studies provide evidence that disrupted muscle spindle innervation in both type 1 and 2 diabetic models may be involved, at least in part, in the sensorimotor deficits displayed in STZ-induced DPN.

3. Experimental Procedures

Male C57BL/6 mice were purchased at 7 weeks of age from Charles River (Wilmington, MA) and housed 2 mice/cage on a 12:12-hour light/dark cycle in the animal facility at the University of Kansas Medical Center under pathogen-free conditions. Male *db/db* mice (strain name: BKS.Cg-*m*+/+Lepr^{db}/J, stock number: 000642, background strain C57BLKS/J) were purchased from Jackson Laboratories (Bar Harbor, ME), and were housed at the University of Michigan under pathogen free conditions on a 12:12-hour light/dark cycle. A breeding colony was established, and the mice were genotyped 4 weeks after birth. All animals had free access to water and mouse chow (C57BL/6 mice: Harlan Teklad 8604, 4% kcal derived from fat; *db/db* and *db*+ mice: LabDiet 5001, 12% kcal derived from fat), and their use was in accordance with NIH guidelines and approved by the University of Kansas Medical Center Animal Care and Use Committee or the University of Michigan Committee on the Care and Use of Animals, respectively.

STZ-injected C57BL/6 mice. Diabetes was induced in 8 week-old C57BL/6 mice in experimental week 0 by a single intraperitoneal injection of STZ (Sigma, St. Louis, MO) at 180 mg/kg body weight. The STZ was prepared in pH 4.5 10mM sodium citrate buffer (Wang et al., 1993), and the nondiabetic mice were injected with 400 μl

of the vehicle buffer. prior to the STZ or vehicle injections, mouse chow was removed for 4-5 hours and was not replaced until 3 hours after the injections in order to improve STZ uptake in pancreatic β cells. Hyperglycemia and diabetes was defined as a blood glucose level greater than 16mM (~288 mg/dl), and STZ-injected mice with blood glucose levels below the standard were not included in this study. Weight and tail vein blood glucose levels were measured using glucose diagnostic reagents (Sigma) throughout the protocol and analyzed using a two-way repeated measures analysis of variance (RM ANOVA) with Fisher's protected least significant difference (PLSD) post hoc test.

***db/db* mice.** Diabetes was confirmed in the *db/db* mice at 8 weeks of age. In order to compare the muscle spindle innervation between type 1 and 2 diabetes models, immunohistochemical analysis and quantification of muscle spindles were performed on medial gastrocnemius muscles from 24 week old homozygous (*db/db*; n=3) and heterozygous (*db*+; n=3) leptin receptor-null mutant mice.

Beam-walk. The beam-walk utilizes an elevated wooden balance beam to test sensorimotor deficits. Mice were trained during week 2 and 3 post-STZ to traverse a 1 m long beam with a diameter of 1.2 cm in order to reach a dark, enclosed safety box containing food and bedding (adapted from Taylor et al., 2001; Taylor et al., 2005). The animals were recorded for 3 trials/session while traversing a demarcated 70 cm section of the beam on weeks 3, 5 and 10 post-STZ injection. A digital video camera was used to record the 3 trials. A footslip was counted if either the left or right hindpaw slipped off the beam. The number of footslips/mouse was averaged, and the data was analyzed using a two-way RM ANOVA with Fisher's PLSD post hoc test.

Footprint analysis. Footprinting was used to analyze hindlimb gait as previously described in Taylor et al. (2001). Briefly, the rear paws of C57BL/6 mice were inked and the mice were trained to then walk along a 6 cm X 70 cm track lined with paper at 10 weeks post-STZ injection. Prints were scanned and analyzed using NIH ImageJ 1.38x software (http://rsb.info.nih.gov/ik/). For each tracking, 3-5 prints were analyzed for 4 parameters: step length, toe spread (distance between toes 1 through 5), intermediate toe spread (inter-toe spread; distance between toes 2 through 4), and print length. Means were calculated for each animal and analyzed using an unpaired t-test.

Grid-walk. The grid-walk apparatus was used to analyze sensorimotor function as modified from Onyszchuk et al. (2007). Briefly, the apparatus consisted of an elevated 1.1 cm wire grid that was 20 cm X 35 cm. Animals were recorded with a digital video camera for 5 minutes while walking on the grid at 10 weeks post-STZ injection. Afterwards, the video was reviewed and every hindpaw step was counted, in addition to the number of hindpaw foot faults, or slips. Slips were counted when a mouse attempted to bear weight on a foot, but missed the grid and passed the foot through the plane of the grid. The % slips were calculated for each animal (hindpaw slips/total hindpaw steps x 100), and analyzed using an unpaired t-test.

Rotorod. The rotorod (AccuRotor Rota Rod, AccuScan Instruments Inc.; Columbus, OH) was used to measure coordination and balance, as previously described in Taylor et al. (2001). Briefly, STZ-induced C57BL/6 mice were tested on the rotorod at a constant speed of 12 rpm for 3 trials at 9 weeks post-STZ injection. The latency of the mice to remain on the rotorod (in seconds) was recorded, and mean latencies were analyzed using an unpaired t-test.

Gait analysis. Using a more sophisticated approach than footprinting, gait analysis was performed using the DigiGait Imaging System (Mouse Specifics, Inc., Boston, MA). Mice were initially acclimatized in the treadmill with the motor speed set to zero. The speed was steadily increased to 16.7 cm/s, at which point about 4 seconds of running was recorded through a 16 mm lens by the DigiGait Acquisition software. Video from each animal was then processed through the DigiGait Analysis software, and stance and steps were manually corrected if needed by comparing the plotted temporal history of paw placement with the actual video. All gait outcome measures produced by the analysis software were analyzed using un-paired t-tests.

Nerve conduction velocity. Both motor and sensory nerve conduction velocities were recorded in the diabetic and nondiabetic mice at 6 and 10 weeks post-STZ injection (separate animals) using methods described in Stevens et al. 2000. Anesthesia was induced with an intraperitoneal injection of Avertin (1.25% v/v tribromoethanol, Sigma; 2.5% *tert*-amyl alcohol, Sigma; 200 μL/10 g body weight), and body temperature was monitored with a rectal probe and maintained at 37°C. In order to perform sciatic-tibial motor conduction, we stimulated distally at the ankle and proximally at the sciatic notch using supramaximal stimulation (~9.9 mA). The compound muscle action potential latencies were recorded from recording electrodes placed in the first interosseous muscle of the hind paw. The latency was calculated from the stimulus artifact to the onset of negative M-wave deflection. Motor nerve conduction velocity (MNCV) was calculated by dividing the difference between the proximal and distal latencies by the distance between the stimulating and recording electrodes. Digital sensory nerve conduction velocity (SNCV) was recorded in the digital nerve of the second toe with a 0.5 ms square wave pulse using the smallest

current to elicit a response (~2.7 mA). The recording electrode was placed behind the medial malleolus to record the action potential. Ten sensory nerve action Potentials (SNAPs) was recorded and averaged. SNCV was calculated by dividing the average latency by the distance between the stimulating and recording electrodes. Diabetic and nondiabetic nerve conduction velocities were analyzed using two-way ANOVAs with Fisher's PLSD post hoc tests.

Experimental design. Beam-walk testing was performed on 10 diabetic and 3 nondiabetic mice on weeks 3, 5, and 10 post-STZ injection. Footprinting, grid-walk, and rotorod were performed on 8 diabetic and 3 nondiabetic mice at weeks 9-10 post-STZ injection. Gait analysis was performed on 3 diabetic and 5 nondiabetic mice at week 6 post-STZ injection. NCV was performed at 6 weeks post-STZ on 7 diabetic and 6 nondiabetic mice and at 10 weeks post-STZ on 6 diabetic and 6 nondiabetic mice. Immunohistochemical analysis was performed on 10 diabetic and 8 nondiabetic mice. Mice were sacrificed after beam-walk analysis on week 10 and immunohistochemical analysis and quantification of muscle spindles followed.

Immunohistochemistry. Diabetic and nondiabetic C57BL/6 mice were deeply anesthetized at 10 weeks post-STZ with inhaled isoflurane (Abbott Laboratories, Abbott park, IL) to areflexia and decapitated prior to the removal of the right and left medial gastrocnemius muscles. *db/db* and *db+* mice gastrocnemius muscles were dissected after an overdose of sodium pentobarbital and flash frozen in liquid nitrogen in 24 week old animals. Medial gastrocnemius muscles were fresh frozen on dry ice, sectioned with a cryostat in longitudinal serial sections at 50 μm, mounted on Superfrost plus slides (Fisher Scientific, Chicago, IL), and stored at -20°C. All immunohistochemistry was performed under humidified conditions. Following a 5 min

thaw, slides were incubated for 2 hours at room temperature in blocking solution (0.5% porcine gelatin, 1.5% normal donkey serum, and 1% Triton X-100 in SuperBlock Blocking Buffer [pH 7.4; Pierce, Rockford, IL]). Intrafusal bag fibers were visualized using a mouse anti-slow-tonic myosin heavy chain antibody (S46; 1:50; generous gift of Dr. Frank Stockdale, Stanford, CA). Sensory axons were visualized using a rabbit anti-neurofilament H antibody (NFH; 1:500; Chemicon, Temecula, CA). The NFH primary antibody used (#AB1991) is not affected by neurofilament phosphorylation. All primary antibodies were diluted in blocking solution and incubated with sections for 24 hours at 4°C. For fluorescence visualization, sections were washed 2x5 min with 0.1 M phosphate-buffered saline (PBS; pH 7.4) followed by incubation for 2 hours with fluorochrome-conjugated secondary antibodies (donkey anti-mouse Alexa 555, 1:2000; donkey anti-rabbit Alexa 488, 1:2000; Molecular Probes, Eugene, OR) in PBS. Prior to viewing, slides were washed 2 times with PBS and coverslipped.

Muscle spindle quantification. Fluorescent digital images were acquired using a Nikon Digital Eclipse C1si confocal microscope. Z stacks were obtained at a 1 μm step size (EZ-C1 Software). Approximately 3 - 6 muscle spindles per muscle were imaged for spindle innervation quantification. Digital Z-stack images of spindles were transferred to Nikon Imaging Software-Elements (NIS-Elements; Melville, NY). For each spindle the mean width of 3 or more axonal rotations and the mean inter-rotational distance (the space in between the axonal rotations) between 3 or more rotations were calculated and recorded by a blinded observer using NIS-Elements. Mean axonal width and mean inter-rotational distance were analyzed using unpaired t-tests.

4. Results and Figures

Body weight and blood glucose. One week following STZ injection, C57BL/6 mice displayed characteristic symptoms of diabetes, including polydipsia and polyuria. Diabetic mice had significantly reduced weight gain and significantly higher blood glucose levels as early as 1 week post-STZ, which persisted through the end of the study until week 10 (**Table VI-1**). In addition, *db/db* mice displayed significantly higher body weights and blood glucose levels from week 15 through the terminal week 24 (**Table VI-1**).

Beam-walk performance. The number of hindpaw slips counted as mice crossed the beam-walk apparatus was used to access sensorimotor ability. For a slip to be counted, the foot had to lose contact with the balance beam with the leg extended (**Figure VI-1A**). At week 3 post-STZ injection there was no significant difference between the mean number of slips that were counted for nondiabetic (0.9 +/- 0.11 SEM) and diabetic (0.8 +/- 0.18 SEM; **Figure VI-1B**) mice. Likewise, at 5 weeks post-STZ there was no significant difference in footslips between nondiabetic (0.4 +/- 0.29 SEM) and diabetic (1.1 +/- 0.19 SEM) mice; however, a trend towards a poorer performance in diabetic mice compared to the nondiabetic mice (**Figure VI-1B**). After 10 weeks of hyperglycemia, the diabetic mice displayed a significantly greater number of footslips (1.3 +/- 0.27 SEM) compared to nondiabetic mice (0.2 +/- 0.11 SEM; $p < 0.05$; **Figure VI-1B**). These results suggest that STZ-induced diabetes in C57BL/6 mice leads to a sensorimotor dysfunction that is detectable by the beam-walk apparatus.

Table VI-1. Body weight and blood glucose concentrations in C57BL/6 and leptin receptor-null mutant mice

	Early		Terminal	
	Weight	Blood Glucose	Weight	Blood Glucose
Nondiabetic C57BL/6	23 +/- 0.8	6.1 +/- 0.49	28 +/- 0.4	6.6 +/- 0.55
Diabetic C57BL/6	19 +/- 0.5*	18.9 +/- 1.40**	22 +/- 1.0*	29.1 +/- 1.18**
db+	NA	NA	28 +/- 0.9	8.0 +/- 0.64
db/db	NA	NA	51 +/- 1.5*	28.7 +/- 2.29*

Weight and blood glucose levels measured at an early time point (1 week post-STZ for C57BL/6 mice or 15 weeks of age for leptin receptor null mutant mice) and the final time point (10 weeks post-STZ or 24 weeks of age). Weight is in grams; glucose concentration is in mmol/L. Data are represented as means +/- standard error of mean. NA represents data that were not available. * $p < 0.05$ vs. nondiabetic or *db*+ mice; ** $p < 0.0001$ vs. nondiabetic or *db*+ mice. Table from Muller et al., 2008.

Figure VI-1. Sensorimotor evaluation on beam-walk in STZ-treated C57BL/6 diabetic mice. (A) Photograph of a nondiabetic C57BL/6 mouse performing the beam-walk task. White arrow denotes a slip of the left hindpaw. (B) Quantification of mean hindpaw footslips for diabetic and nondiabetic mice at 3, 5, and 10 weeks post-STZ injection. Diabetic mice had significantly more slips at 10 weeks post-STZ. Data are presented as means +/- SEM. * $p < 0.05$ vs. nondiabetic mice. Figure from Muller et al., 2008.

A

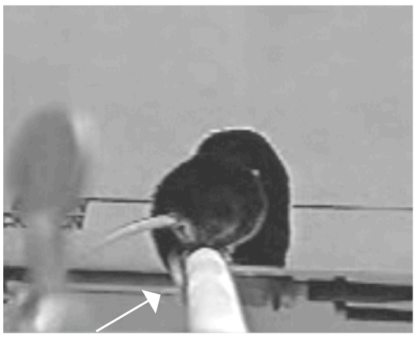

B

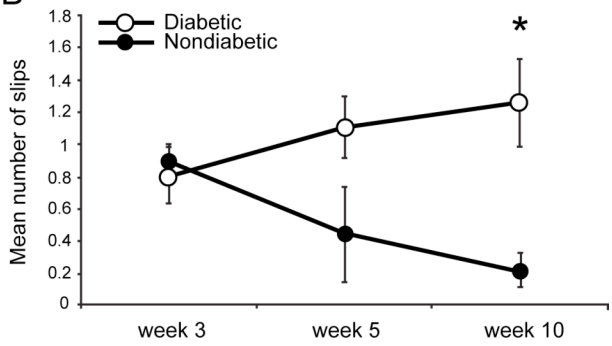
Diabetic
Nondiabetic
*
Mean number of slips
1.8
1.6
1.4
1.2
1
0.8
0.6
0.4
0.2
0
week 3
week 5
week 10

Footprinting, grid-walk, and rotorod performance. To examine additional measures of sensorimotor function, footprinting, grid-walk, and rotorod tests were performed in STZ-induced C57BL/6 mice. Interestingly, none of the behavior tasks were sensitive enough to detect the sensorimotor deficits that were found during the beam-walk tests. All footprinting parameters were not different between nondiabetic and diabetic mice (**Table VI-2**). In addition, the grid-walk % slips and rotorod latencies of diabetic mice were not significantly different than nondiabetic mice (**Table VI-2**). These results suggest that the beam-walk apparatus exposes sensorimotor dysfunction in STZ-induced diabetes.

Gait analysis. Many gait parameters were calculated using the DigiGait Analysis software. There are two main phases of gait: stance is made up of braking and propulsion and occurs when the paw is in contact with the surface, while swing takes place when the paw is not in contact with the surface. At 6 weeks post-STZ in C57BL/6 mice there were no significant differences between diabetic and nondiabetic mice for stride length, paw angle, swing, or the breaking component of stance ($p > 0.05$). Diabetic mice displayed a significantly shorter propel time (0.13 s +/- 0.01 SEM) for rear paws when compared to nondiabetic mice (0.15 s +/- 0.01 SEM; $p < 0.05$; **Figure VI-2A**); however, the front paws did not show significant differences ($p > 0.05$; **Figure VI-2A**). In addition, diabetic mice had a greater front paw area (0.30 cm^2 +/- 0.02 SEM) compared to nondiabetic mice (0.25 cm^2 +/- 0.01 SEM; $p < 0.05$; **Figure VI-2B**). There were no significant differences found in the rear paw area of diabetic and nondiabetic mice ($p > 0.05$; **Figure VI-2B**). These data suggest that at 6 weeks post-STZ there are minimal gait alterations in diabetic mice.

Table VI-2. Footprinting, grid-walk, and rotorod tests failed to detect sensorimotor deficits in C57BL/6 diabetic mice

	Nondiabetic	Diabetic
Footprinting		
Step Length	8.5 +/- 0.20	7.7 +/- 0.43
Toe Spread	0.8 +/- 0.05	0.7 +/- 0.02
Inter-Toe Spread	0.3 +/- 0.01	0.3 +/- 0.03
print Length	0.7 +/- 0.04	0.7 +/- 0.03
Gridwalking	0.7 +/- 0.19	0.9 +/- 0.46
Rotorod Latency	172 +/- 60.3	222 +/- 51.0

Results from three behavioral tasks at 9-10 weeks post STZ-injection in C57BL/6 mice. Footprinting parameters included step length, toe spread (toes 1-5), inter-toe spread (toes 2-4), and print length, and these analyses did not detect differences between nondiabetic and diabetic mice ($p > 0.05$). Likewise, the grid-walk did not detect a difference in the % slips between diabetic and nondiabetic mice ($p > 0.05$). Diabetic mice had a similar latency on the rotorod compared to nondiabetic mice ($p > 0.05$). Footprinting parameters are in centimeters; gridwalking is the % slips in 5 minutes on the grid; rotorod latency is in seconds. Data are represented as means +/- SEM. Table from Muller et al., 2008.

Figure VI-2. Gait analysis in STZ-treated C57BL/6 diabetic and nondiabetic mice. (A) Quantification of the amount of time diabetic and nondiabetic mice spend in the propel phase of their gait (seconds) at 6 weeks post-STZ injection. Diabetic mice had a significantly shorter propel duration in their rear paws. (B) Quantification of the amount of paw surface area (cm^2) during locomotion in diabetic and nondiabetic mice at 6 weeks post-STZ injection. Diabetic mice had a significantly greater paw area for their front paws. Data are presented as means +/- SEM. * $p < 0.05$ vs. nondiabetic mice.

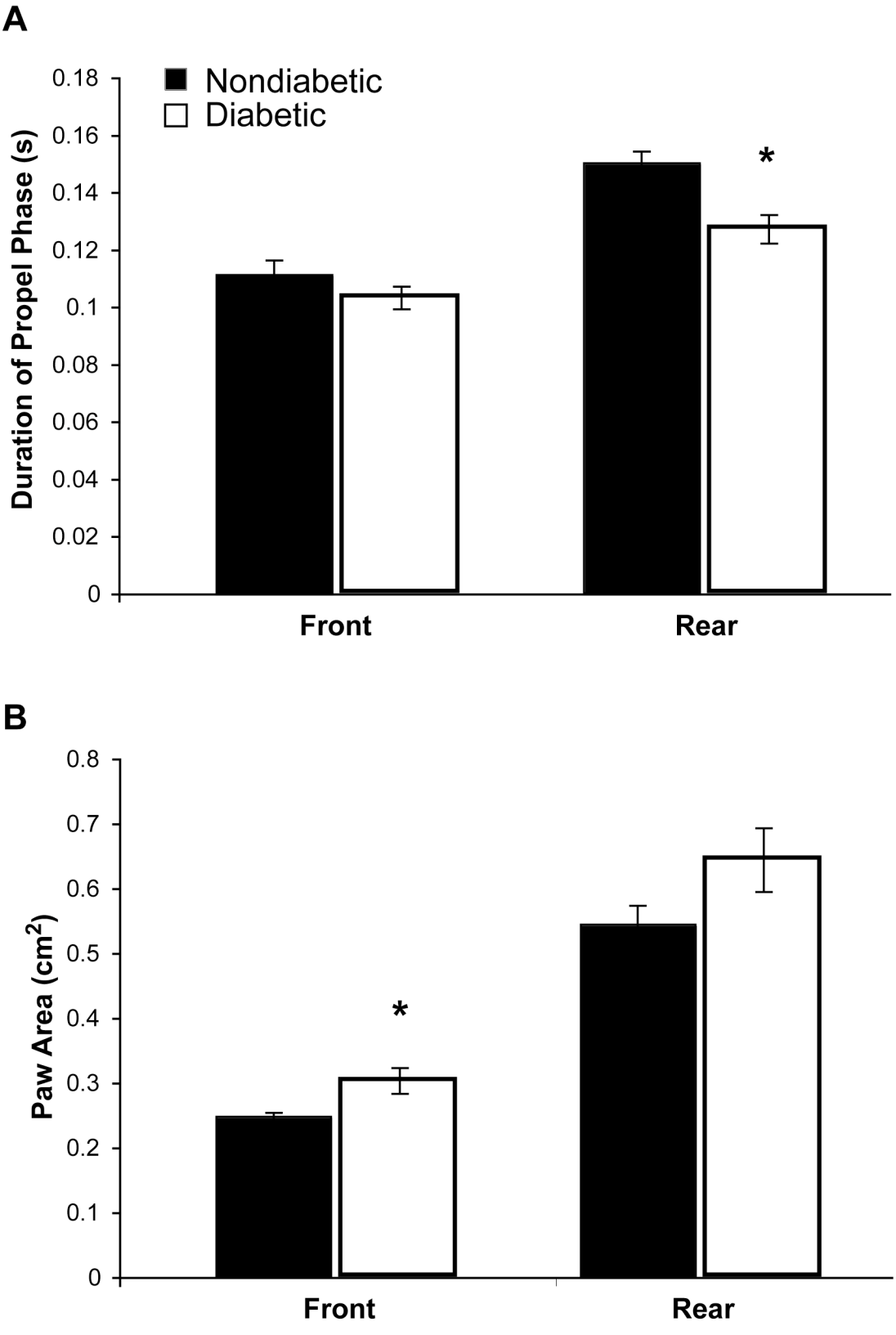
A
Nondiabetic
Diabetic
Duration of Propel Phase (s)
0.18
0.16
0.14
0.12
0.1
0.08
0.06
0.04
0.02
0
*
Front
Rear
B
Paw Area (cm2)
0.8
0.7
0.6
0.5
0.4
0.3
0.2
0.1
0
*
Front
Rear

Nerve conduction velocity measurements. Conduction velocities of motor and sensory nerve fibers were accessed in nondiabetic and diabetic C57BL/6 mice 6 and 10 weeks post-STZ injection. For MNCV, at 6 weeks post-STZ injection diabetic mice (41.6 m/s +/- 1.6 SEM) were not significantly different than nondiabetic mice (44.3 m/s +/- 1.8 SEM; $p > 0.05$; **Figure VI-3A**). However, after 10 weeks of hyperglycemia, diabetic mice had significantly lower MNCV (49.5 m/s +/- 2.2 SEM) compared to nondiabetic mice (59.7 m/s +/- 2.6 SEM; $p < 0.0001$; **Figure VI-3A**). In comparison, digital SNCV was not different between diabetic and nondiabetic mice at either 6 (30.3 m/s +/- 1.2 SEM vs. 33.3 m/s +/- 1.1 SEM) or 10 weeks (32.6 m/s +/- 1.1 SEM vs. 31.7 m/s +/- 0.9 SEM) post-STZ injection ($p > 0.05$ for ANOVA week and group differences; **Figure VI-3B**).

Muscle spindles in nondiabetic mice. To quantify muscle spindle group Ia innervation, the muscle spindles from nondiabetic mice were visualized on a confocal microscope and 2 axonal parameters were measured: axonal width and inter-rotational distance (IRD). IRD was defined as the distance between the Ia axonal annulospiral rotations. Within the nondiabetic group of mice, there was a mean axonal width of 1.3 μm with very low variability (+/- 0.19 SD) and a mean inter-rotational distance of 3.6 μm with low variability (+/- 0.98 SD). Up to 12 muscle spindles can be found within 1 mouse gastrocnemius muscle, and the mean axonal width and IRD were very consistent not only overall in the nondiabetic group, but also within individual muscles (**Figure VI-4A, B, C, D**). These results indicate that within nondiabetic muscle spindles there is a high degree of homogeneity in axonal width and IRD.

Figure VI-3. Nerve conduction velocities in C57BL/6 diabetic and nondiabetic mice. (A) Sciatic MNCV in diabetic and nondiabetic mice at 6 and 10 weeks post-STZ injection. Diabetic mice have significantly decreased MNCV at 10 weeks post-STZ, but not at 6 weeks. (B) Digital SNCV in diabetic and nondiabetic mice at 6 and 10 weeks post-STZ injection. Diabetic mice have no significant differences in their SNCV at 6 or 10 weeks. Data are presented as means +/- SEM. ** $p < 0.0001$ vs. nondiabetic mice.

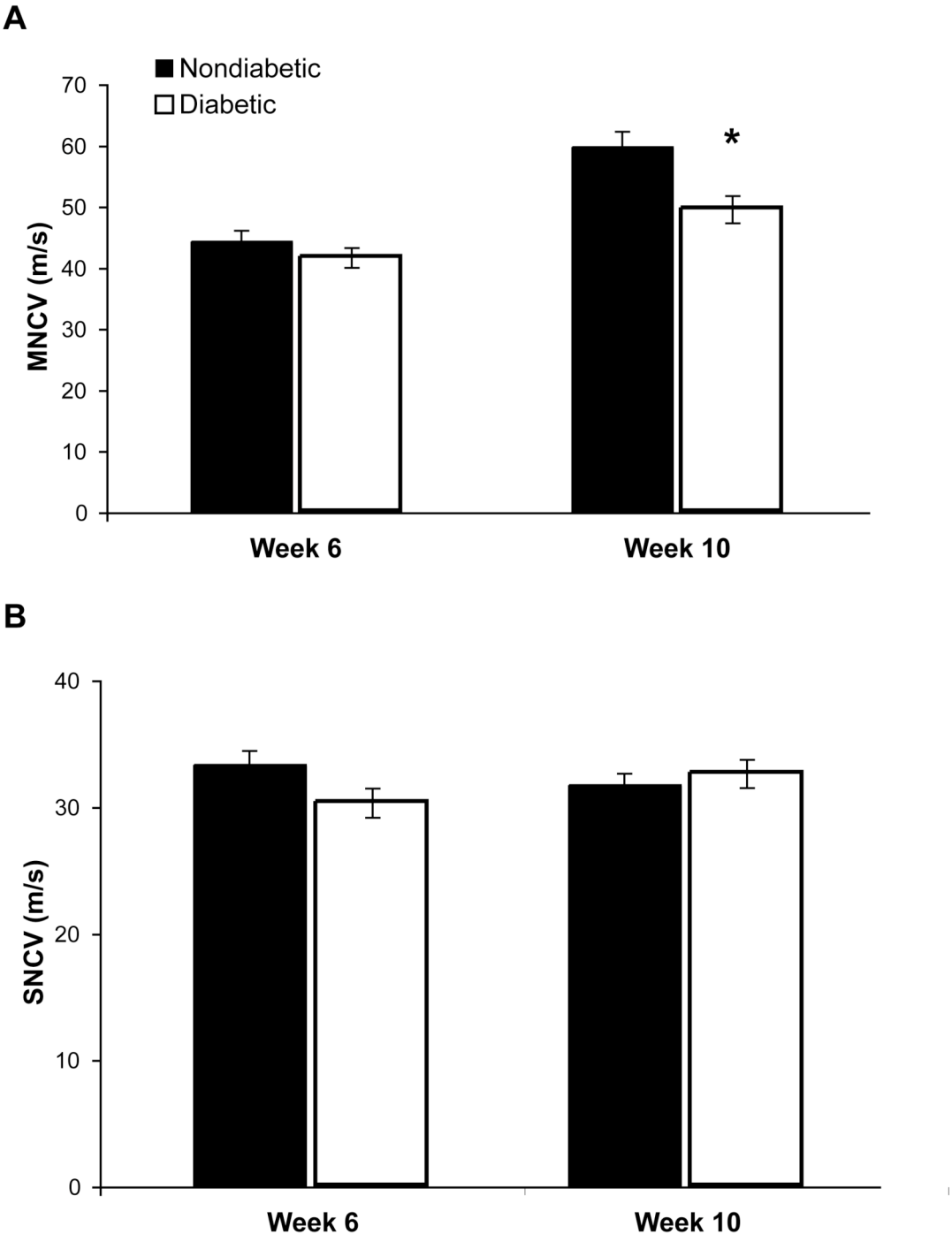
A
Nondiabetic
Diabetic
MNCV (m/s)
70
60
50
40
30
20
10
0
*
Week 6
Week 10
B
SNCV (m/s)
40
30
20
10
0
Week 6
Week 10

Figure VI-4. Typical muscle spindle Ia innervation in nondiabetic C57BL/6 mice. Confocal optical images from the equatorial region of medial gastrocnemius muscle spindles from a nondiabetic mouse (A, B) illustrate consistent axonal width and inter-rotational distance (IRD) within one muscle. In addition, spindles from 2 other nondiabetic mice (C, D) display similar consistency in axonal width and IRD, reflective of all nondiabetic animals. Red visualizes slow tonic myosin heavy chain (S46) expression within spindle bag fibers, and green represents NF-H positive Ia axons with their characteristic annulospiral morphology. Figure from Muller et al., 2008.

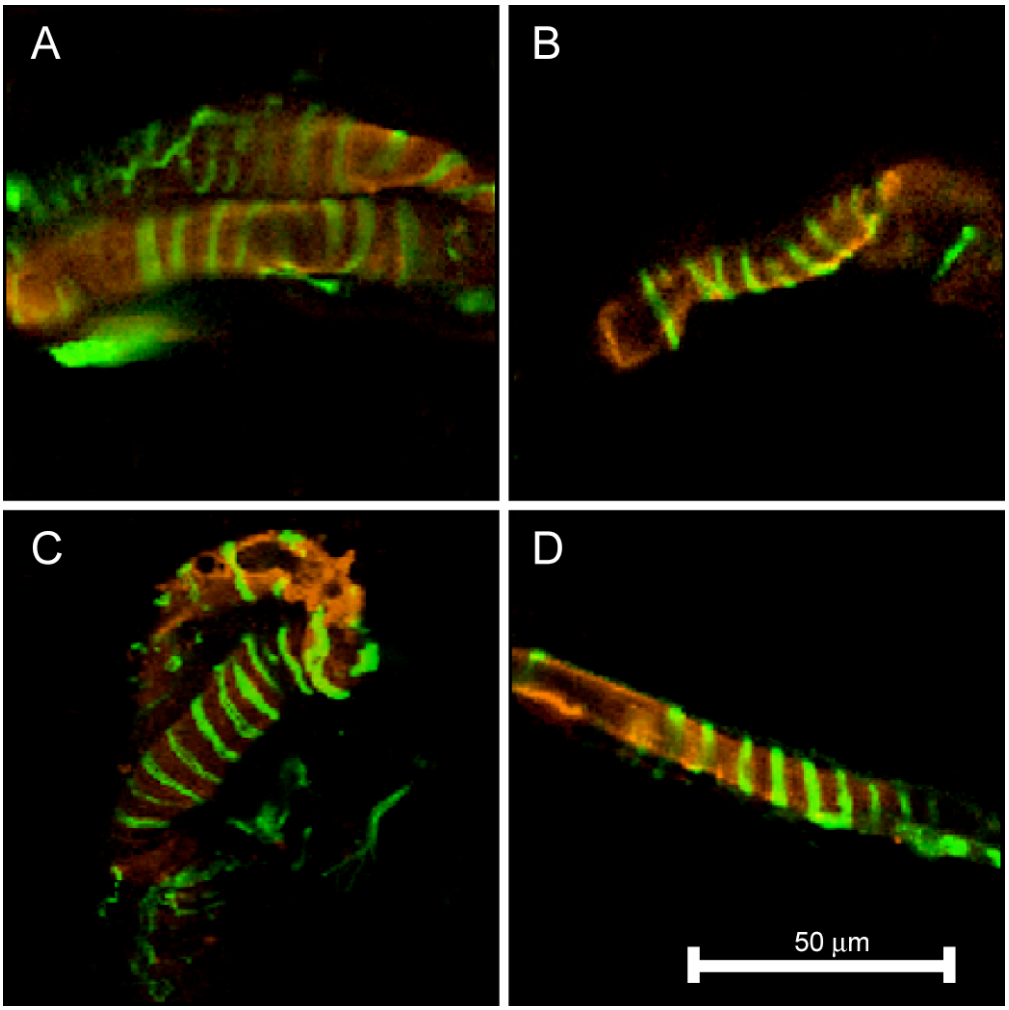
A
B
C
D
50 μm

Muscle spindles in C57BL/6 diabetic mice. Axonal width and IRD were also measured in muscle spindles from diabetic mice. The mean axonal width of diabetic mice (1.3 μm +/- 0.42 SD) was not significantly different from nondiabetic mice ($p > 0.05$). In addition, the mean IRD of diabetic mice (3.9 μm +/- 1.59 SD) was not significantly different from nondiabetic mice ($p > 0.05$). However, a clear pattern began to appear when analyzing the values for the two spindle parameters in diabetic and nondiabetic mice. As described above, the nondiabetic mice had reliable consistency with each spindle parameter within their group and within individual muscles. In contrast, this consistency was not seen in the diabetic mice. Multiple distinct and abnormal morphologies were identified in diabetic mice that resulted in a high degree of variability. In diabetic mice, the mean axonal width of Ia axons was sometimes more narrow, sometimes wider, or sometimes average compared to the nondiabetic mice (**Figure VI-5A, B, C; Figure VI-6A**). Axonal width in nondiabetic mice ranged from only 0.9 μm to 1.6 μm, whereas axonal width in diabetic mice ranged from 0.8 μm to 2.6 μm. Similarly, Ia axons in diabetic mice sometimes had smaller IRDs (axon rotations closer together), sometimes larger IRDs (axon rotations further apart), or sometimes average IRDs compared to the nondiabetic mice (Figure VI-6B). IRD in nondiabetic mice ranged from only 1.3 μm to 6.0 μm, whereas IRD in diabetic mice ranged from 1.2 μm to 8.2 μm. Although the size difference for small IRDs was minimal (1.2 – 1.3 μm), many diabetic animals displayed this small phenotype.

Figure VI-5. Altered muscle spindle Ia innervation in diabetic C57BL/6 mice. Confocal optical images from the equatorial region of medial gastrocnemius muscle spindles from diabetic mice (A, B, C) show that within one diabetic muscle, both thinner and thicker axons are evident. These images highlight the variability in diabetic muscle spindle innervation morphology. Red visualizes slow tonic myosin heavy chain (S46) expression within spindle bag fibers, and green represents NF-H positive Ia axons with their characteristic annulospiral morphology. The white arrows denote very thin axons and the white arrowheads denote very thick axons. Figure from Muller et al., 2008.

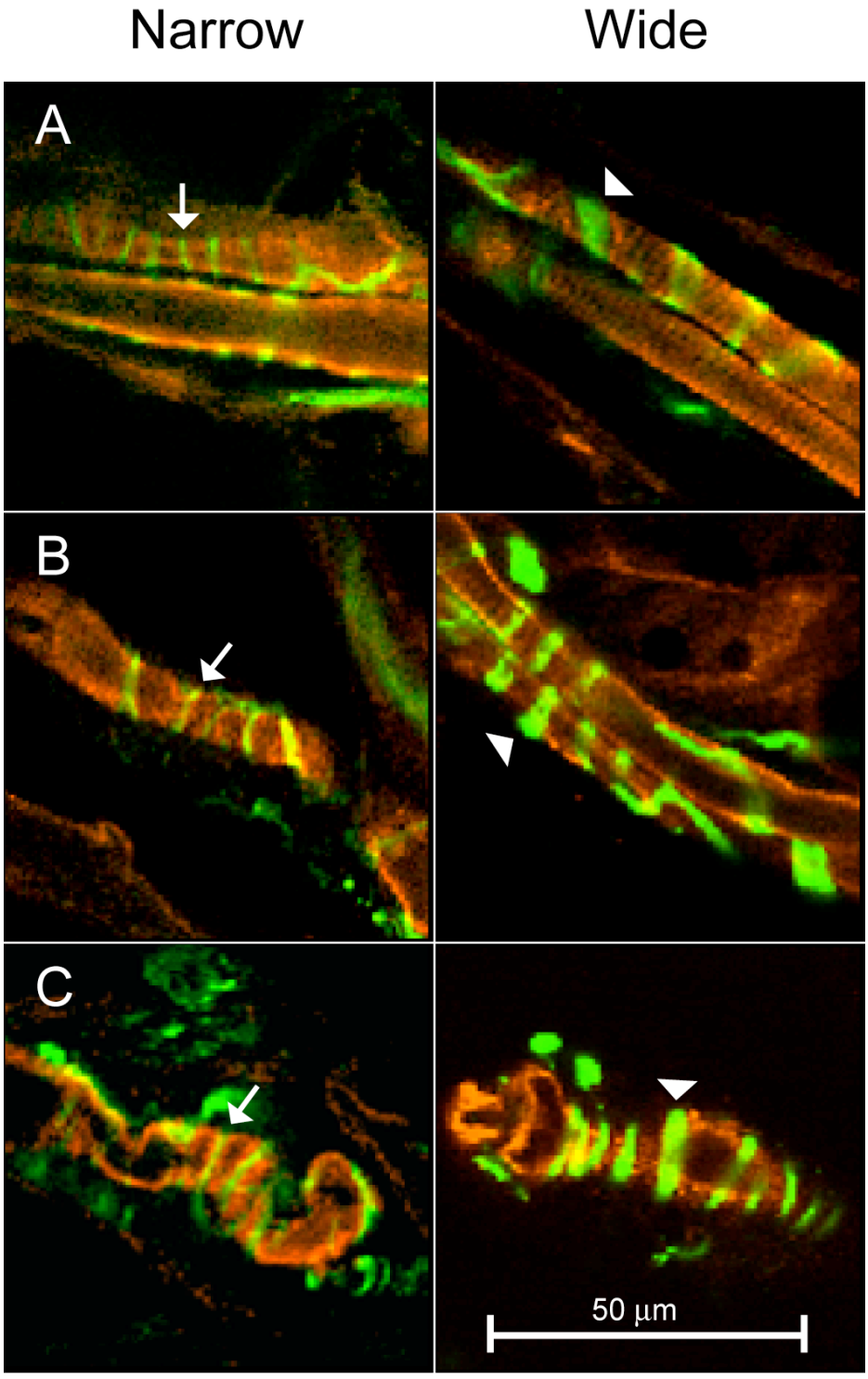
Narrow
Wide
A
B
C
50 µm

Figure VI-6. Ia axonal width and inter-rotational distance (IRD) in diabetic and nondiabetic C57BL/6 mice. (A) Mean axonal width was more variable in diabetic mice compared to nondiabetic mice. Nondiabetic mice have a tighter range of widths compared to diabetic mice. The variability in diabetic mice is also higher for IRD (B) where nondiabetic mice have a tighter range of IRDs compared to diabetic mice. Note that there are increased numbers of smaller or larger Ia axons in diabetic mice compared to nondiabetic mice (A), and there are rotations that are spaced closer together or further apart in diabetic mice compared to nondiabetic mice (B). Diabetic mice have increased variability in axonal width in muscles of individual animals compared to nondiabetic mice (C). Diabetic mice also have increased variability in IRD in individual muscles compared to nondiabetic mice (D). CoV is the coefficient of variation. Black circles represent 1 muscle and black lines represent the mean CoV in each group (C, D). Figure from Muller et al., 2008.

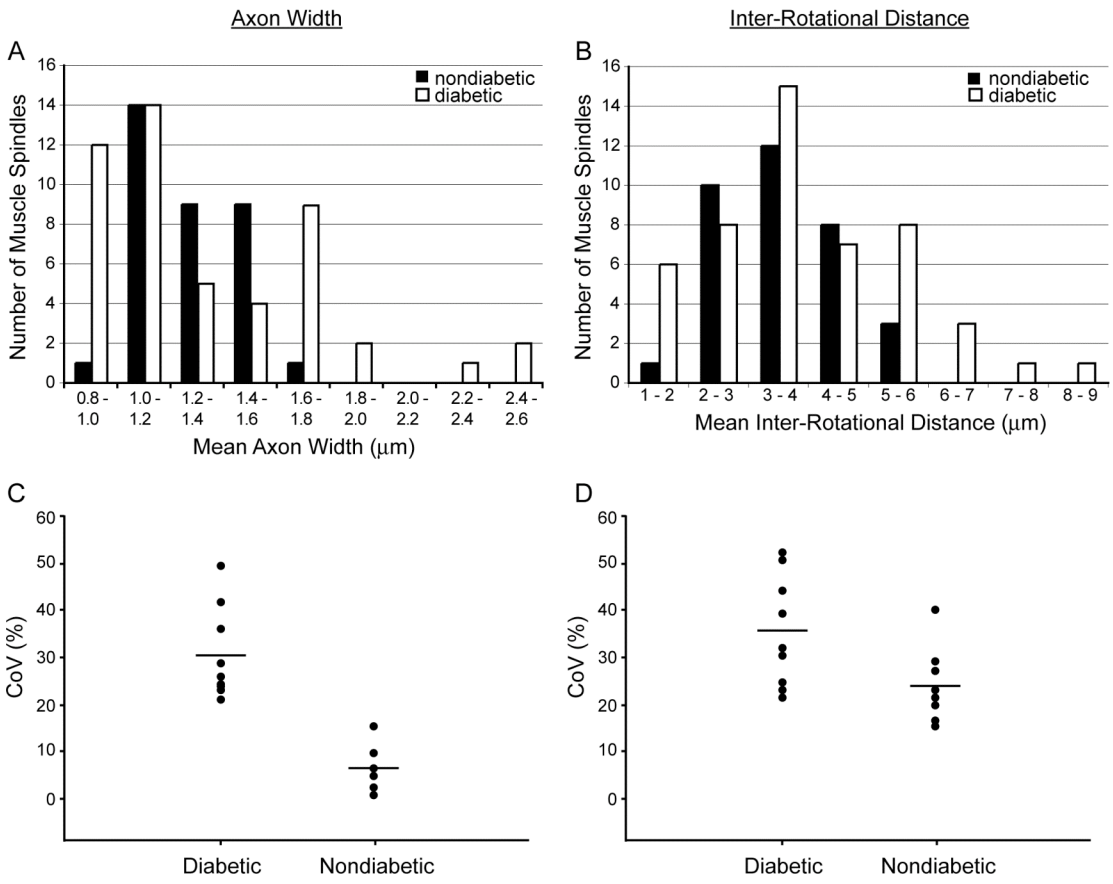
Axon Width
Inter-Rotational Distance
A
B
C
D
nondiabetic
diabetic
Number of Muscle Spindles
0.8 - 1.0
1.0 - 1.2
1.2 - 1.4
1.4 - 1.6
1.6 - 1.8
1.8 - 2.0
2.0 - 2.2
2.2 - 2.4
2.4 - 2.6
Mean Axon Width (μm)
1 - 2
2 - 3
3 - 4
4 - 5
5 - 6
6 - 7
7 - 8
8 - 9
Mean Inter-Rotational Distance (μm)
CoV (%)
Diabetic
Nondiabetic

Not only were axonal width and IRD variable between animals of the diabetic group (**Figure VI-6A, B**), but also within muscles of individual animals. The coefficient of variation was calculated (CoV (%) = SD/mean x 100) for each diabetic and nondiabetic muscle as a marker of variability. For axonal width, diabetic mice had a mean CoV of 30.8%, which is 7 times more variable than nondiabetic mice (6.5%; **Figure VI-6C**). For IRD, the CoV of diabetic mice also indicated more variability (36.1%) than nondiabetic mice (CoV = 24.5%; **Figure VI-6D**), but not to as great of an extent (1.5 times more variable). There was no correlation between axonal width and IRD in diabetic mice ($r^2 = 0.05$, $p = 0.737$), but there is a slight trend towards a significant correlation in nondiabetic mice ($r^2 = 0.33$, $p = 0.057$). Overall, these results suggest that diabetic muscle spindle Ia fibers have high variability in their axonal width and IRD both as a group, and within individual muscle spindles.

Muscle spindles from *db+* and *db/db* mice were analyzed to determine whether Ia axon variability observed in the STZ-induced type 1 mice was also present in a type 2 diabetes model. There was no difference in axonal width between *db+* and *db/db* mice (data not shown). However, similar to STZ-induced C57BL/6 diabetic mice, *db/db* mice displayed a high degree of variability in their mean IRDs compared to *db+* mice. Ia axons in *db/db* mice sometimes had smaller IRDs, sometimes larger IRDs, or sometimes average IRDs compared to the *db+* mice (**Figure VI-7A, B, C**). IRD in *db+* mice ranged from 1.4 μm to 3.5 μm, where IRD in *db/db* mice ranged from 1.2 μm to 9.0 μm (**Figure VI-7D**). This data indicates that *db/db* mice display greater variability in their IRDs compared to *db+* mice, suggesting that alterations in Ia axon morphology occur in both type 1 and type 2 models of DPN.

Figure VI-7. Variable inter-rotational distance (IRD) in *db/db* and *db*+ mice. Confocal optical images from the equatorial region of medial gastrocnemius muscle spindles from a *db*+ mouse showing the average IRD in the control mice (A). IRD values from *db/db* mice ranged from being smaller than *db*+ IRD to being much larger than *db*+ IRD (B, C). These images highlight the variability in *db/db* muscle spindle innervation morphology. Red visualizes slow tonic myosin heavy chain (S46) expression within spindle bag fibers, and green represents NF-H positive Ia axons with their characteristic annulospiral morphology. The white arrows denote small IRDs and the white arrowheads denote large IRDs. (D) IRD was more variable in diabetic than in nondiabetic mice (E) *db/db* mice displayed an increased variability in IRD in muscles of individual animals compared with diabetic mice. CoV is coefficient of variation. Black circles represent one muscle, and black lines represent the mean coefficient of variation in each group (E). Figure from Muller et al., 2008.

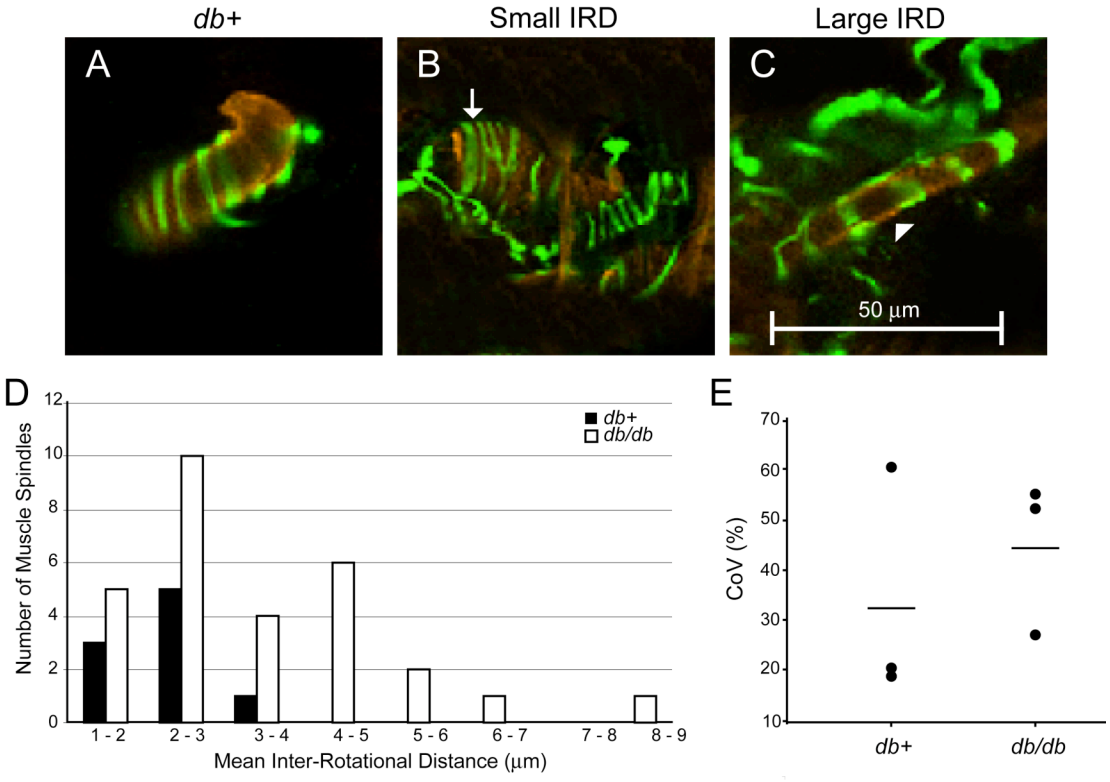
db+
Small IRD
Large IRD
A
B
C
50 µm
D
Number of Muscle Spindles
db+
db/db
Mean Inter-Rotational Distance (µm)
1 - 2
2 - 3
3 - 4
4 - 5
5 - 6
6 - 7
7 - 8
8 - 9
E
CoV (%)
db+
db/db

5. Discussion

In this study, type 1 and type 2 mouse models of diabetes were used to examine large-fiber diabetic sensorimotor polyneuropathy. Our results reveal that STZ-induced diabetes leads to sensorimotor behavioral deficits involving balance and gait detectable by the beam-walk apparatus and DigiGait Analyzer. These behavioral abnormalities are hypothesized to be due, in part, to the irregularities and variability in muscle spindle group Ia innervation. In addition, similar alterations in innervation were identified in a type 2 diabetes mouse model. Collectively, these results suggest that diabetic mice undergo damage to large sensory axons that may contribute to deficits in large-fiber sensory feedback associated with balance and gait.

Behavior testing. The beam-walk apparatus has been widely used to assess sensorimotor function deficits following traumatic brain injury and other conditions resulting in altered gait, balance, and/or proprioception (Fox et al., 1998; Sherbel et al., 1999; Ferrer et al., 2005). Baskin et al. (2003) suggested that the beam-walk task is effective in detecting sensorimotor deficits resulting primarily from hindlimb dysfunction. In previous studies, we have used the beam-walk apparatus to evaluate sensorimotor function in relation to hindlimb muscle spindle innervation, and the performance of mice using this approach reliably mirrored the reinnervation of muscle spindles following nerve crush (Taylor et al., 2005). Importantly, the beam-walk apparatus was found to be the most sensitive measure for diabetes-induced sensorimotor changes, as footprinting, the grid-walk, and rotorod were not able to detect altered behavior. The balance changes observed in the diabetic mice were subtle, suggesting that the beam may challenge the mice to rely on sensorimotor feedback more so than the other tasks discussed above. In addition, we became

interested in more sophisticated measures of gait analysis compared to footprinting, which lead us to test the mice on the DigiGait Analyzer. Unfortunately, we were only able to run STZ-induced C57BL/6 mice 6 weeks after diabetes induction, which coincides with just the beginning of sensorimotor deficits (based on beam-walk data). The results suggest that diabetic mice do have slight gait disturbances compared to nondiabetic mice, particularly during the propel phase of walking. In addition, diabetic mice had greater paw surface area compared to nondiabetics, indicating nerve injury and/or pain status. It has been reported that rats with chronic pain have decreased paw area (Coulthard et al., 2002), and interestingly, we know that our STZ-induced C57BL/6 mouse model is an insensate model of DPN. Altogether, we hypothesize that gait analysis at 10 weeks post-STZ would uncover greater gait disturbances, similar to the beam-walk data. Collectively, behavioral testing suggests that diabetic mice have altered sensorimotor function related to balance and gait, and that beam-walking performance and gait analysis provide reliable indicators of these abnormalities in diabetic mice.

Nerve conduction velocity. SNCV has been widely studied in rodent models of diabetic neuropathy, and it is thought that slowed CVs likely reflect deficits in conduction predominantly in large nerve fibers. However, reports of diabetes-induced slowed SNCV can be variable, with some studies reporting decreases (Mizisin et al., 1999), while others report no change (Jefferys and Brismar, 1980). This may be due to inherent animal model differences, just as some models display cutaneous insensitivity while others report allodynia. Our studies revealed no reductions in SNCV in STZ-induced diabetic mice. It is not surprising that our model did not have decreased SNCV simply due to the subtle large-fiber morphologic alterations in

which, perhaps, some fibers compensate for others while in different states of flux. It is plausible to predict that rodents with significantly slowed SNCV may have a more severe phenotype related to spindle innervation. Ramji et al. (2007) examined motor nerve anatomy and electrophysiology in STZ-induced diabetic mice and found distal motor axon retraction and slowed MNCV. Our study did reveal slowly progressive decreases in MNCV in diabetic mice, which is in agreement with many other studies (Cameron and Cotter, 2007; Drel et al., 2007; Russell et al., 2008).

Visual and vestibular systems. In addition to muscle spindle feedback, visual and vestibular systems also contribute to sensorimotor functions, and together, this information is integrated within central neural systems (Hirschfeld and Forssberg, 1992). However, based on studies with pyridoxine toxicity, Stapley et al. (2002) reported that intact large afferent fibers from muscle spindles are necessary for the timing of balance/postural responses, and when damaged, the visual and vestibular systems cannot compensate. Thus, our results are consistent with the view that damage to large sensory afferent fibers innervating muscle spindles contributes significantly to behavioral deficits.

Visualization of muscle spindles. Typically, muscle spindle quantification has involved cross section or transverse views of the muscle spindle capsule through light or electron microscopy (Wang et al., 1997; Wright et al., 1997; Chen et al., 2002). This method of visualizing the spindle has been very beneficial for many areas of study; however, it does not allow for the intricate analysis of axon morphology or spacing. Visualizing muscle spindle fibers and their afferents longitudinally provides more information about spindle innervation, particularly related to axonal width and IRD. To our knowledge, our study is the first to quantify

Ia annulospiral endings on muscle spindle intrafusal fibers in diabetic mice, and this technique now provides a new assay to determine the efficacy of therapeutic interventions aimed at improving large-fiber diabetic neuropathy. Small-fiber neuropathy has benefited greatly from quantitative assessments in epidermal innervation, and an analogous approach has been lacking for large fibers.

Degeneration/regeneration. Fiber changes commonly reported in DPN include axonal degeneration, regeneration, demyelination, and remyelination (Sinnreich et al., 2005). A previous study examined muscle spindles in STZ-treated diabetic rats and visually observed nonspecific changes in the nerve terminals of intrafusal fibers, such as axonal dilation and axonal dystrophy (Weis et al., 1995). Using electron microscopy analysis, diabetic rats revealed enlarged sciatic nerve axon terminals, intrafusal fiber nuclear disintegration, and increased numbers of Schwann cells, all suggestive of previous degeneration and subsequent regeneration (Weis et al., 1995). This study is consistent with our more detailed observations of thicker, thinner, closer spaced, and further spaced axons and supports the proposed view that Ia axons undergo degeneration and subsequent regeneration in diabetic mice.

Extrafusal fibers. It is plausible that extrafusal fiber atrophy could drive changes in spindle innervation. Although muscle wasting was not measured here, it is likely that muscle wasting occurs in STZ-induced diabetic mice. It may be worthwhile to assess spindle innervation in other muscle wasting diseases such as muscular dystrophy or myasthenia gravis. In human muscle spindles from patients with Duchenne muscular dystrophy, changes were apparent in capsule thickness, intrafusal fiber number and diameter (Swash and Fox, 1976). No measures of

quantifiable spindle innervation were documented; however, certain spindles were reported to be devoid of axons.

Intrafusal fibers. Likewise, it is possible that changes in intrafusal bag fibers may influence Ia axon innervation. Bag fibers are typically enlarged in the equatorial region due to the accumulation of nuclei, and these diameter changes make it difficult to measure intrafusal fiber size. However, our observations suggest that some intrafusal fibers in diabetic mice appeared abnormal (Figure 3C), and it is reasonable to suggest that annulospiral innervation is influenced by intrafusal fiber morphology.

Altered spindle output. Irrespective of the cause leading to altered annulospiral morphology, a plausible outcome of the Ia afferent fiber abnormalities reported in this study may be altered electrophysiological output from spindles. Muscle spindle afferent axons fire when the extrafusal fiber and subsequent intrafusal fiber stretch, leading to the distortion of Ia endings and increased activity of the Ia axon. It is reasonable to suggest that when Ia axon morphology is disrupted, it leads to changes in the firing patterns of the spindle afferent. Collectively, the varied Ia innervation in spindles from diabetic mice could lead to changes in overall Ia firing patterns and result in asynchronous Ia firing within diabetic muscles when stretched, as in the model shown in **Figure VI-8**. Furthermore, this variation in sensory input could affect motor neuron function as well. This hypothesis could be tested using electrophysiologic approaches such as H-reflex measurements and acute isolated spinal cord preparations focused on motor neuron output.

Type 2 diabetes model. Our results reveal that both axonal width and inter-rotational distance were more varied in STZ-diabetic mice compared to nondiabetic

mice. However, in the type 2 diabetes mouse model, axonal width was the same in *db/db* and *db+* mice while inter-rotational distance varied substantially in the *db/db* but not *db+* mice. The difference between *db/db* and STZ-induced diabetes may be related to the severity of neuropathy in the type 2 model or the rate of progression of the neuropathy. It is possible that the altered inter-rotational distance is the first sign of axonal damage and precedes variability in axonal width.

Human studies. Previous studies have examined muscle spindle function in human neuromuscular disorders. Swash and Fox (1974) found sensory neuropathy led to a degeneration of Ia afferents, and they noted an attempt at regeneration of the sensory afferents in the form of swelling and attenuation of the Ia fibers. In addition, multiple studies have hypothesized that instability and postural sway in human diabetic neuropathy are due to poor muscle spindle function or changes in spindle afferents (van Deursen et al., 1998; Nardone et al., 2007). However, there has been little experimental research into this area due to the difficulty in accessing muscle spindles from human biopsies. This problematic issue reinforces the need to develop animal model studies to help address the pathogenesis of human large-fiber diabetic neuropathy.

In conclusion, we have identified behavioral and pathological large sensory nerve fiber-related changes in diabetic mice. Future studies could provide new insight into the treatment and prevention of large-fiber complications that develop in humans suffering from diabetes.

Figure VI-8. This figure is a working hypothesis of how altered spindle morphology could lead to disruptions in the spindle electrophysiologic output. If a nondiabetic spindle with homogeneous Ia afferent morphology is stretched, the black arrows lead to the hypothesized spindle electrophysiologic discharges, which are synchronous. However, if a diabetic spindle with heterogeneous Ia afferent morphology is stretched, the black arrows lead to the hypothesized discharges, which are inherently asynchronous due to the altered morphology. Overall, this could lead to problems with balance, gait, and other sensorimotor functions, as well as hyporeflexia.

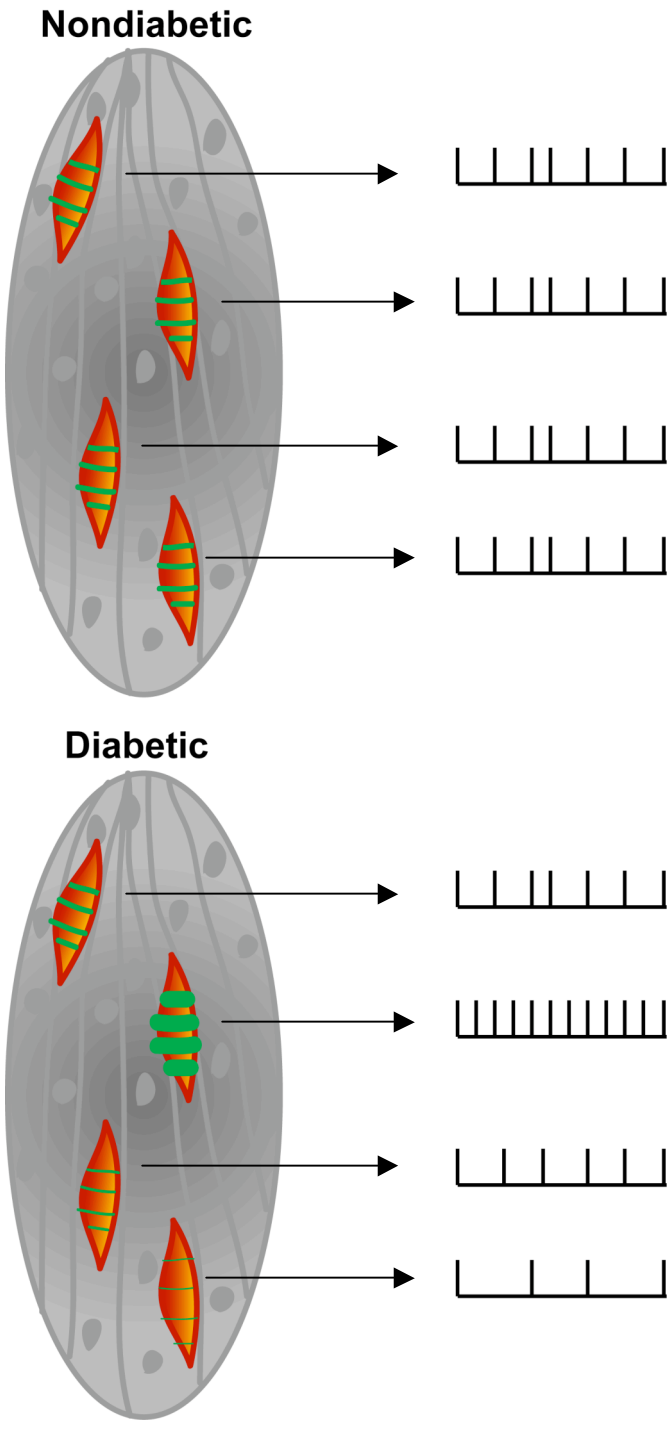
Nondiabetic
Diabetic

VII. CHAPTER THREE

Insulin Treatment Modifies Development of Sensorimotor Deficits and Repairs Muscle Spindle Ia Afferent Innervation in Diabetic Mice

1. Abstract

Muscle spindle group Ia afferent fibers are exquisitely sensitive to diabetes-induced hyperglycemia, and their damage can lead to altered sensorimotor function. Insulin, or lack thereof, has multiple roles in the setting of diabetes. Not only can insulin increase uptake of blood glucose, but also poor insulin support to peripheral nerves has been implicated in the progression of DPN. The current study was aimed at determining whether sensorimotor and spindle deficits in a large-fiber type 1 diabetes mouse model are reversible after treatment with insulin.

Insulin was delivered for 4 weeks through slow-release pellets implanted subcutaneously in STZ-injected C57BL/6 mice. Behavioral assessments were carried out at baseline and after insulin treatment to quantitate deficits in balance and gait. Nerve conduction velocities were measured after insulin treatment to determine if insulin had an effect on peripheral motor and sensory nerve electrophysiology. In addition, quantitative assessment of group Ia axon innervation of muscle spindles was carried out using immunohistochemistry and confocal microscopy following 4 weeks of insulin treatment.

Insulin treatment significantly decreased blood glucose concentrations and significantly increased insulin concentrations in diabetic mice. In addition, insulin repaired electrophysiologic deficits in motor nerves and altered nerve conduction velocity in sensory nerves. Importantly, sensorimotor behavior was restored after insulin treatment with concomitant restoration of muscle spindle Ia afferent innervation patterns to levels similar to nondiabetic mice.

Insulin therapy in STZ-induced type 1 diabetic mice completely repaired behavioral and neuroanatomical impairments that were associated with large-fiber

neuropathy. These studies provide a treatment for large-fiber neuropathy that will lead to further mechanistic studies in order to better understand the beneficial actions of insulin on nerves.

2. Introduction

As shown in Chapter 2, large-fiber diabetic neuropathy in mice results in sensorimotor dysfunction, progressive motor nerve conduction velocity deficits, and concomitant alterations in muscle spindle Ia axonal morphology. Overall, these changes are hypothesized to be due to diabetes-induced hyperglycemia. Therefore, it follows that reversing high blood glucose concentrations could improve the symptoms of large-fiber neuropathy.

As described in Chapter 1, insulin is a prime candidate for decreasing hyperglycemia; its most widely known function is inducing glucose uptake throughout the body. However, insulin has also been found to have actions as a potent neurotrophic factor (Recio-Pinto et al., 1986; White, 2003; Brussee et al., 2004; Toth et al., 2006). Dobtretsov and colleagues (2007) suggest that insulin treatment in human patients may have actions to both correct hyperglycemia and independently have effects on peripheral nerves.

Here, we have tested the hypothesis that insulin treatment in STZ-induced C57BL/6 type 1 diabetic mice could improve the symptoms of large-fiber neuropathy, such as altered sensorimotor function and disrupted neuroanatomy. This study provides evidence that insulin treatment reverses sensorimotor dysfunction and peripheral nerve alterations, irrespective of its mechanism of action.

3. Experimental Procedures

Mice. Male C57BL/6 mice were purchased at 7 weeks of age from Charles River (Wilmington, MA) and housed 2 mice/cage on a 12:12-hour light/dark cycle in the animal facility at the University of Kansas Medical Center under pathogen-free conditions. All animals had free access to water and mouse chow (Harlan Teklad 8604, 4% kcal derived from fat), and their use was in accordance with NIH guidelines and approved by the University of Kansas Medical Center Animal Care and Use Committee.

Diabetes induction. Diabetes was induced as previously described in Chapter 2 in 8 week-old C57BL/6 mice (n=11) by a single intraperitoneal injection of STZ (Sigma, St. Louis, MO) at 180 mg/kg body weight. The nondiabetic mice (n=6) were injected with 400 μl of the vehicle. Hyperglycemia and diabetes was defined as a blood glucose level greater than 16mM (~288 mg/dl), and STZ-injected mice with blood glucose levels below the standard were not included in this study. Weight and tail vein blood glucose levels using glucose diagnostic reagents (Sigma) were measured throughout the protocol and analyzed using a two-way RM ANOVA with Fisher's PLSD post hoc test.

Experimental design. In order to evaluate the effects of insulin on hyperglycemia-induced changes in sensory nerve fibers, mice were randomly assigned to 3 groups: nondiabetic (n=6), diabetic + sham pellets (n=6), or diabetic + insulin pellets (n=5). Baseline beam-walk behavioral testing was performed on weeks 1 and 5 post-STZ injection. Insulin replacement therapy began in week 6 and continued for a total of 4 weeks, while beam-walk performance was evaluated post-

insulin at 10 weeks post-STZ. Mice were sacrificed after nerve conduction studies in week 10, and immunohistochemical analysis of muscle followed.

Beam-walk apparatus. The beam-walk apparatus was used as described in Chapter 2, and briefly, the animals were recorded for 3 trials/session while traversing a demarcated 70 cm section of the beam on weeks 1, 5 and 10 post-STZ injection. The number of footslips/mouse was averaged, and the data was analyzed using a two-way RM ANOVA with Fisher's PLSD post hoc test.

Insulin Administration. Insulin pellets were administered to 5 STZ-induced C57BL/6 diabetic mice, while 6 diabetic and 6 nondiabetic mice received sham palmitic acid pellets. Insulin replacement therapy began 6 weeks post-STZ injection via LinBit sustained release insulin pellets (13 +/- 2 mg each; 0.1 U/24 hours/pellet; LinShin Canada, Inc., Scarborough, Ontario, Canada) implanted subcutaneously in the dorsal skin (2 pellets for the first 20g body weight and an additional pellet for every additional 5g body weight). All pellets remained in the mice for 4 weeks, and an additional insulin pellet was added if blood glucose levels failed to drop below 16mM after one week.

Serum insulin concentration. To determine insulin levels, serum was separated out from tail vein blood through centrifugation. The serum insulin concentration in nondiabetic, diabetic + sham, and diabetic + insulin mice was measured at 10 weeks post-STZ injection using an Ultrasensitive Mouse Insulin ELISA (Mercodia AB, Uppsala, Sweden). Briefly, equal amounts of serum samples (5 μL) were analyzed in duplicate, and enzyme activity was measured with a spectrophotometer. Insulin concentrations in unknown samples were derived by interpolation from a reference curve that was generated using insulin standards of

known concentrations in the same assay. Insulin concentration was analyzed using a one-way ANOVA with Fisher's PLSD post-hoc test.

Nerve conduction velocity. Both motor and sensory nerve conduction velocities were recorded at 10 weeks post-STZ injection using methods described in Chapter 2. Diabetic and nondiabetic nerve conduction velocities were analyzed by a one-way ANOVA with Fisher's PLSD post hoc test.

Immunohistochemistry. Immediately following NCV testing, diabetic and nondiabetic C57BL/6 mice were decapitated prior to the removal of the right gastrocnemius muscles. Medial gastrocnemius muscles were processed according to methods in Chapter 2.

Muscle spindle innervation. Muscle spindle large-fiber sensory innervation was analyzed using methods described in Chapter 2. Fluorescent digital images were acquired using a Nikon Digital Eclipse C1si confocal microscope. Approximately 3 - 6 muscle spindles per muscle were imaged for spindle innervation quantification. Digital Z-stack images of spindles were transferred to Nikon Imaging Software-Elements (NIS-Elements; Melville, NY). For each spindle the mean width of 3 or more axonal rotations and the mean inter-rotational distance in between 3 or more rotations were calculated and recorded by a blinded observer using NIS-Elements. Mean axonal width and mean inter-rotational distance were analyzed using a one-way ANOVA with Fisher's PLSD post hoc test.

4. Results and Figures

Body weight and blood glucose. One week following STZ injection, diabetic + sham (D-Sham) and diabetic + insulin (D-insulin) mice had significantly reduced weight gain and significantly higher blood glucose levels compared to nondiabetic

(ND) mice (**Table VII-1**). Insulin therapy began at 6 weeks post-STZ injection, and **Figure VII-1** illustrates blood glucose levels in the weeks prior to insulin implantation (week 5) and just after implantation (week 7). At 5 weeks post-STZ injection D-sham and D-insulin mice had significantly higher blood glucose concentrations (19.6 mM +/- 0.4 SEM and 19.7 mM +/- 0.2 SEM, respectively) compared to ND mice (5.7 mM +/- 0.2 SEM; $p < 0.0001$; **Figure VII-1**). After insulin implantation, D-sham mice had significantly higher blood glucose concentrations (19.6 mM +/- 0.4 SEM) compared to ND mice (5.4 mM +/- 0.2 SEM; $p < 0.0001$) and, importantly, compared to D-insulin mice (6.3 mM +/- 1.8 SEM; $p < 0.0001$; **Figure VII-1**). D-insulin mice were no longer statistically different than ND mice after insulin treatment ($p > 0.05$). In addition, at the end of the study (10 weeks post-STZ injection), D-Sham mice continued to have significantly reduced weight gain and significantly higher blood glucose concentrations compared to both ND mice and to N-insulin mice (**Table VII-1**). These data show that insulin treatment in STZ-induced C57BL/6 diabetic mice reversed weight loss and hyperglycemia, bringing the metabolic status of the mice to levels comparable with nondiabetic mice.

Insulin concentration. Serum insulin concentrations were measured in ND, D-Sham, and D-insulin mice 10 weeks post-STZ injection. Diabetic mice with sham pellets had significantly lower blood insulin levels compared to ND mice ($p < 0.05$) and diabetic mice with insulin pellets ($p < 0.05$; **Table VII-2**). Insulin therapy increased insulin concentrations in diabetic mice to levels significantly higher than nondiabetic and D-Sham mice ($p < 0.05$; **Table VII-2**). These results suggest that the STZ-induced diabetes model successfully decreased circulating serum insulin levels, and, importantly, the insulin treatment paradigm administered was successful at

Table VII-1. Body weight and blood glucose concentrations

	1 Week Post-STZ		10 Weeks Post-STZ	
	Weight	Blood Glucose	Weight	Blood Glucose
Nondiabetic	23 +/- 0.3	6.2 +/- 0.1	29 +/- 0.8	7.0 +/- 0.3
Diabetic + Sham (D-Sham)	19 +/- 0.3*	17.8 +/- 1.0**	21 +/- 0.9	20.2 +/- 0.5
Diabetic + Insulin (D-Insulin)	21 +/- 0.7*	17.0 +/- 0.8**	26 +/- 0.7#	13.1 +/- 2.3#

Weight (g) and blood glucose levels (mM) measured at 1 week post-STZ and 10 weeks post-STZ. Data are represented as means +/- standard error of mean. * $p < 0.05$ vs. nondiabetic; ** $p < 0.0001$ vs. nondiabetic; # $p < 0.05$ vs. diabetic + sham.

Figure VII-1. Blood glucose concentrations pre-insulin and during insulin treatment. Quantification of mean blood glucose concentrations weeks 5 (pre-insulin) and 7 (during insulin treatment) post-STZ. At 5 weeks post-STZ both diabetic + sham and diabetic + insulin mice had significantly higher blood glucose levels compared to nondiabetic mice. After insulin treatment began, diabetic + sham mice had significantly higher blood glucose levels compared to both nondiabetic and diabetic + insulin treated mice. Data presented as means +/- SEM. * $p < 0.0001$ vs. nondiabetic; # $p < 0.0001$ vs. diabetic + insulin.

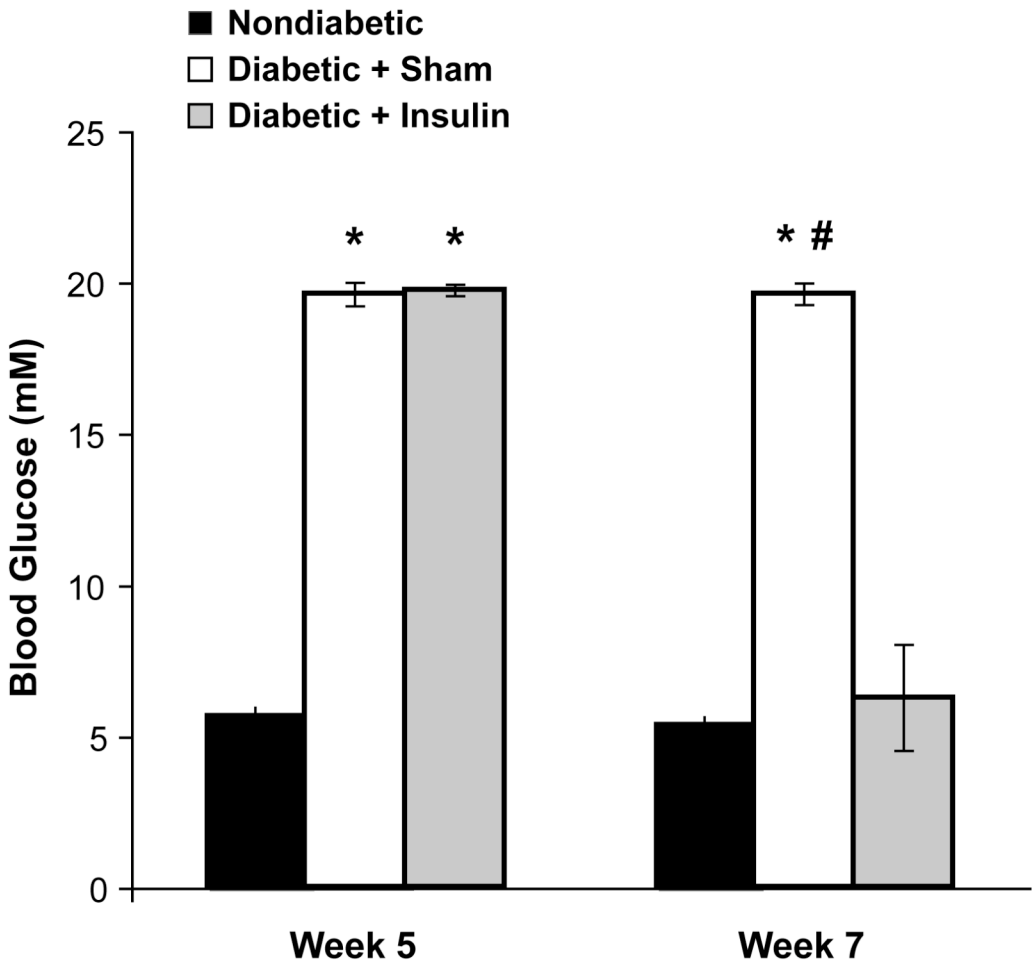
Nondiabetic
Diabetic + Sham
Diabetic + Insulin
Blood Glucose (mM)
25
20
15
10
5
0
* *
* #
Week 5
Week 7

Table VII-2. Serum Insulin Concentrations

	Mean Insulin Concentration (μg/L)	SEM
Nondiabetic	2.1	0.7
Diabetic + Sham	0.6*	0.1
Diabetic + Insulin	12.2#	3.8

Serum insulin levels measured at 10 weeks post-STZ, after 4 weeks of insulin treatment. Diabetic + sham mice have significantly lower insulin levels compared to nondiabetic and diabetic + insulin mice. Additionally, diabetic + insulin mice have significantly higher insulin levels compared to nondiabetic and diabetic + sham mice. * $p < 0.05$ vs. nondiabetic and diabetic + insulin. # $p < 0.05$ vs. nondiabetic and diabetic + sham.

increasing serum insulin concentrations in treated mice.

Beam-walk performance. Insulin replacement therapy was administered to determine if the behavioral and anatomical changes in STZ-induced diabetic mice were reversible. At 1 and 5 weeks post-STZ injection, no significant differences in beam-walk slips were apparent between ND, D-Sham, and D-Insulin mice ($p > 0.05$; **Figure VII-2**). However, after 10 weeks post-STZ, the D-Sham mice displayed significantly more slips (1.2 +/- 0.07 SEM) compared to ND mice (0.5 +/- 0.20 SEM, $p = 0.05$). Importantly, diabetic mice treated with insulin improved their beam performance, and had significantly fewer slips (0.3 +/- 0.07 SEM) compared to D-Sham mice ($p < 0.05$) and were not significantly different than ND mice ($p > 0.05$; **Figure VII-2**). These data indicate that insulin replacement therapy in diabetic mice can reverse the progression of sensorimotor deficits.

Peripheral nerve electrophysiology. Sciatic motor nerve conduction velocity (MNCV) was significantly decreased at 10 weeks post-STZ injection in D-sham mice compared to ND and D-Insulin mice ($p < 0.05$; **Figure VII-3A**). Insulin therapy was able to increase MNCV to levels comparable with nondiabetic mice. Similar to Chapter 2, there was no difference in the nerve conduction velocity of the digital nerve (SNCV) between diabetic + sham and nondiabetic mice ($p > 0.05$ D-Sham vs. ND; **Figure VII-3B**). Interestingly, insulin treatment in diabetic mice resulted in a significantly lower SNCV compared to nondiabetic and diabetic + sham mice ($p < 0.05$; **Figure VII-3B**). These results suggest that insulin treatment in diabetic mice repairs MNCV to levels comparable with nondiabetic mice and altered SNCV.

Figure VII-2. Sensorimotor evaluation on beam-walk in nondiabetic, diabetic + sham, and diabetic + insulin mice. Quantification of mean hindpaw footslips at weeks 1, 5, and 10 post-STZ injection. Diabetic + sham mice had significantly more slips at 10 weeks post-STZ compared to nondiabetic and diabetic + insulin mice. Arrow denotes time of insulin pellet administration at 6 weeks post-STZ. Data are presented as means +/- SEM. * $p < 0.05$ diabetic + sham vs. nondiabetic and diabetic + insulin. Figure from Muller et al., 2008.

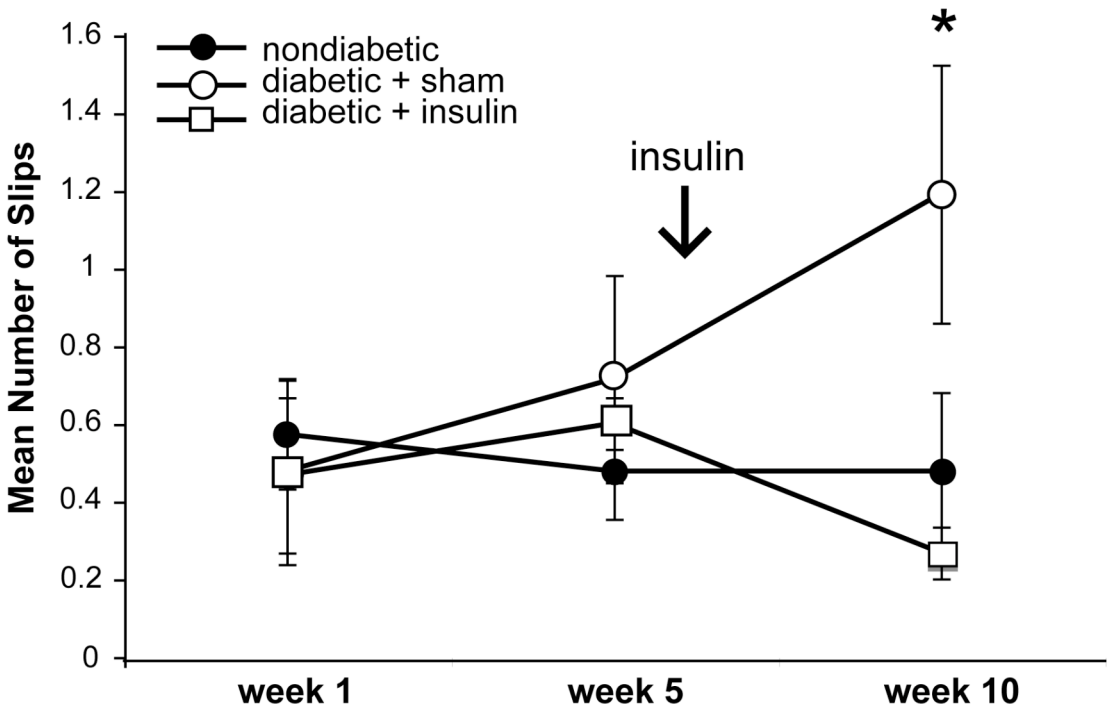
nondiabetic
diabetic + sham
diabetic + insulin
insulin
*
Mean Number of Slips
1.6
1.4
1.2
1
0.8
0.6
0.4
0.2
0
week 1
week 5
week 10

Figure VII-3. Nerve conduction velocity in nondiabetic, diabetic + sham, and diabetic + insulin mice. (A) Quantification of mean sciatic motor nerve conduction velocity at 10 weeks post-STZ injection. Diabetic + sham mice had significantly lower conduction velocity compared to nondiabetic and diabetic + insulin mice. (B) Quantification of mean digital sensory nerve conduction velocity at 10 weeks post-STZ injection. Diabetic + insulin mice had significantly lower conduction velocity compared to nondiabetic and diabetic + sham mice. Data presented as means +/- SEM. * $p < 0.05$ vs. nondiabetic and diabetic + insulin. # $p < 0.05$ vs. nondiabetic and diabetic + sham.

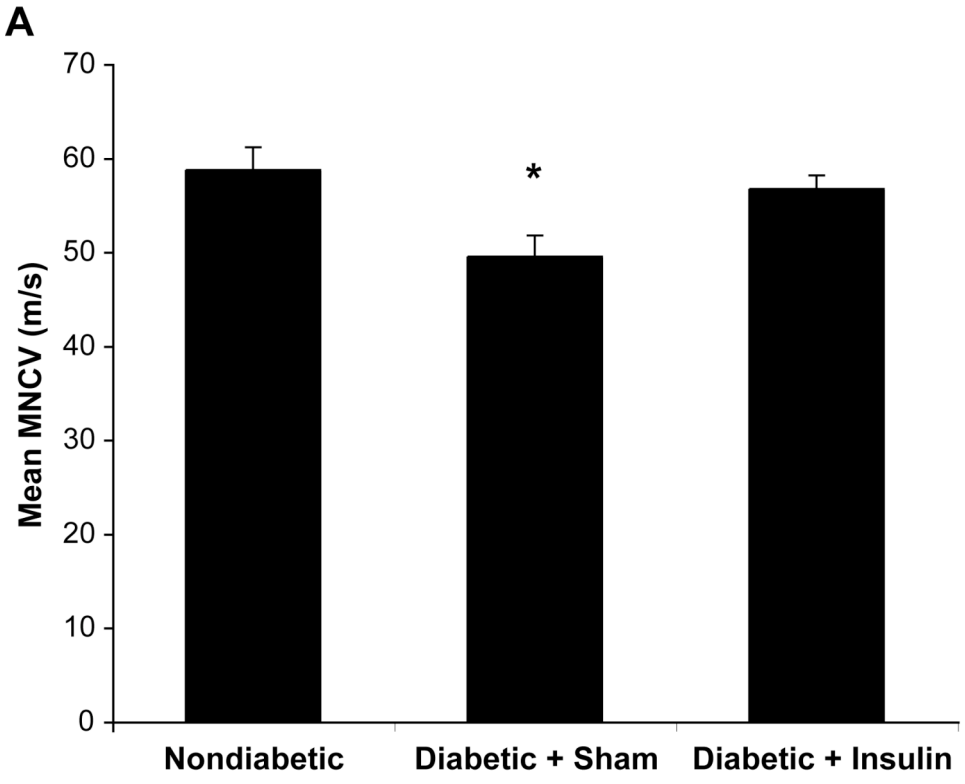
A
70
60
50
40
30
20
10
0
Mean MNCV (m/s)
*
Nondiabetic
Diabetic + Sham
Diabetic + Insulin

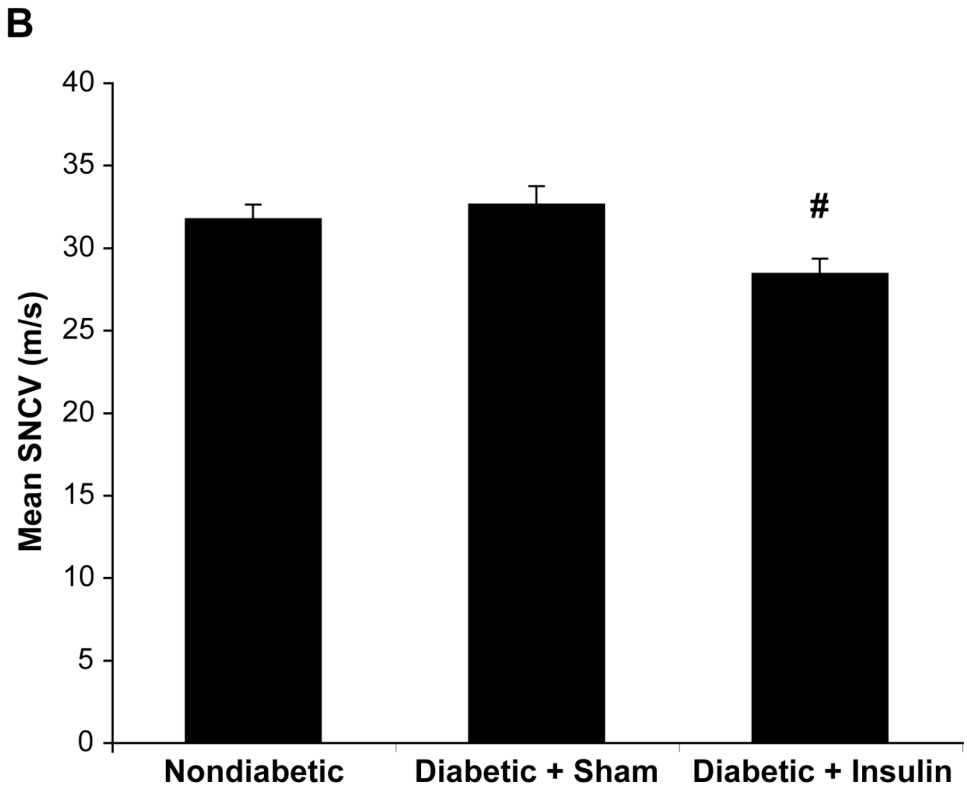
B
40
35
30
25
20
15
10
5
0
Mean SNCV (m/s)
#
Nondiabetic
Diabetic + Sham
Diabetic + Insulin

Muscle spindles after treatment with insulin. In order to evaluate insulin's effect on muscle spindle innervation, axonal width and inter-rotational distance were also measured in muscle spindles from D-Sham vs. D-Insulin mice. The multiple axonal morphologies previously identified in diabetic mice in Chapter 2 that resulted in a high degree of variability were reversed in insulin-treated diabetic mice. In D-Insulin mice, the mean axonal width of Ia axons was more consistent than in D-Sham mice, and was comparable to nondiabetic mice from Chapter 2 (**Figure VII-4A**). Axonal width in D-Insulin mice ranged from only 0.9 μm to 2.0 μm, whereas axonal width in D-Sham mice ranged from 0.8 μm to 2.9 μm. Similarly, IRD variability was decreased in D-Insulin mice (**Figure VII-4B**). IRD in D-Insulin mice ranged from only 1.6 μm to 4.0 μm, whereas IRD in D-Sham mice ranged from 1.2 μm to 8.0 μm.

Not only was axonal width and IRD variability decreased in insulin treated mice, but also within muscles of individual animals. For axonal width, D-Sham mice had a mean CoV of 44.4%, which is 2.5 times more variable than D-Insulin mice (18.0%; **Figure VII-4C**). For IRD, the CoV of D-Sham mice also indicated about 2 times more variability (37.4%) than D-Insulin mice (CoV = 17.6%; **Figure VII-5D**). These results suggest that insulin therapy repairs spindle Ia afferent axonal innervation variability.

5. Discussion

Results from this study reveal that sustained release insulin delivery systemically for 4 weeks in STZ-induced C57BL/6 diabetic mice decreased blood glucose levels, increased body weights, and increased serum insulin concentrations to levels higher than nondiabetic mice. In addition, insulin had positive effects on peripheral nerves through increasing motor nerve conduction velocities, altering sensory nerve

Figure VII-4. Insulin treatment repairs altered muscle spindle innervation in diabetic mice. (A) Mean axonal width was less variable with a tighter range in diabetic + insulin mice compared to diabetic + sham mice. The variability in diabetic + insulin mice was also lower for IRD (B). Diabetic + insulin mice also decreased their internal variability in axonal width and IRD in muscles of individual animals compared to diabetic + sham mice (C and D). CoV is the coefficient of variation. Black circles represent one muscle, and black lines represent the mean CoV in each group (C and D). Figure from Muller et al., 2008.

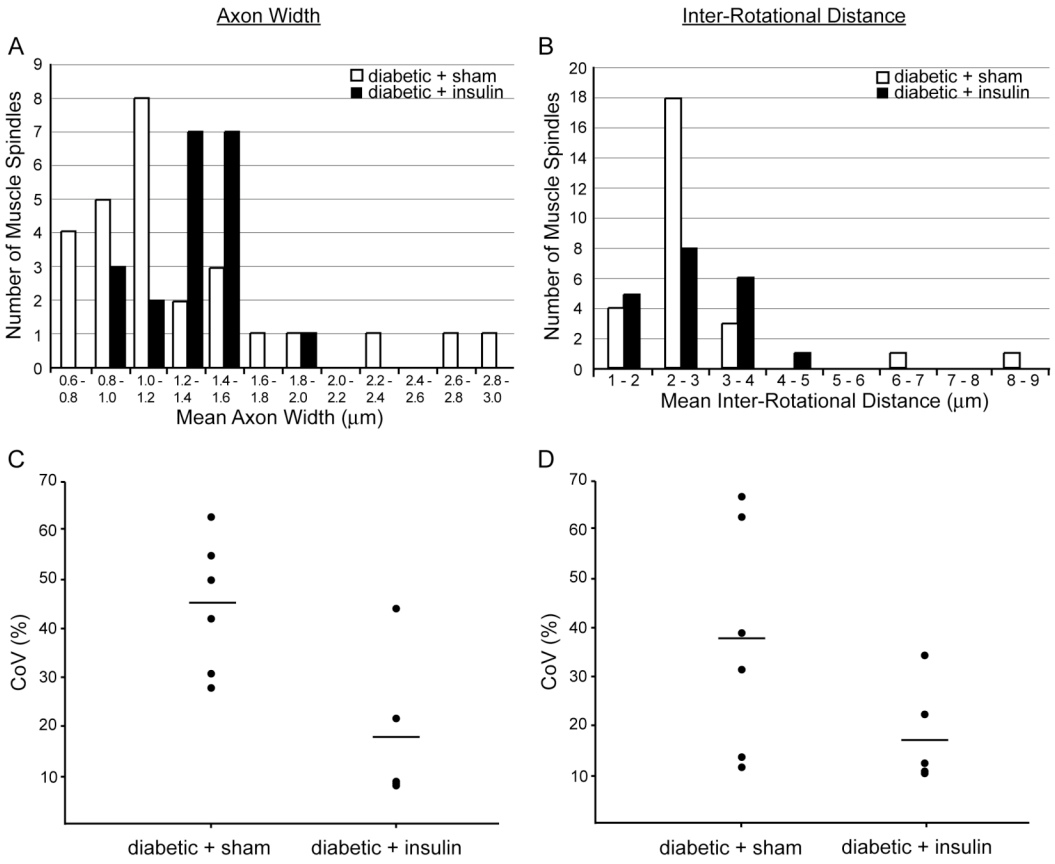
Axon Width
A
diabetic + sham
diabetic + insulin
Number of Muscle Spindles
0
1
2
3
4
5
6
7
8
9
0.6 - 0.8
0.8 - 1.0
1.0 - 1.2
1.2 - 1.4
1.4 - 1.6
1.6 - 1.8
1.8 - 2.0
2.0 - 2.2
2.2 - 2.4
2.4 - 2.6
2.6 - 2.8
2.8 - 3.0
Mean Axon Width (μm)
Inter-Rotational Distance
B
diabetic + sham
diabetic + insulin
Number of Muscle Spindles
0
2
4
6
8
10
12
14
16
18
20
1 - 2
2 - 3
3 - 4
4 - 5
5 - 6
6 - 7
7 - 8
8 - 9
Mean Inter-Rotational Distance (μm)
C
CoV (%)
10
20
30
40
50
60
70
diabetic + sham
diabetic + insulin
D
CoV (%)
10
20
30
40
50
60
70
diabetic + sham
diabetic + insulin

conduction velocities, and decreasing the diabetes-driven pathologic muscle spindle Ia innervation variability. All of these changes resulted in improved sensorimotor function as measured by beam-walk analysis. Collectively, insulin treatment of STZ-induced diabetic mice effectively reversed behavioral and anatomical large-fiber neuropathy deficits.

Insulin and glucose homeostasis and/or neurotrophism. As expected, insulin treatment in diabetic mice resulted in decreased blood glucose levels and reversed weight loss. However, these data are integral to the major pitfall of this study: the inability to tease out the mechanism by which insulin exerted positive effects. It is known that insulin can act as a neurotrophic factor through signaling on insulin receptors (Recio-Pinto et al., 1986; White, 2003; Brussee et al., 2004; Toth et al., 2006). Insulin receptors (IRs) are located on perikarya, nerve roots, and peripheral axons (Sugimotor et al., 2002; Toth et al., 2006). Therefore, in our study insulin could be directly supporting proprioceptive axons or their cell bodies in the DRG, insulin could simply be decreasing blood glucose and concomitant nerve glucose concentrations to reverse glucose toxicity, or it could be acting through both mechanisms simultaneously to result in repaired sensorimotor function, nerve conduction velocity, and muscle spindle innervation morphology. Most likely the latter occurred in this study – a combination of metabolic and neurotrophic mechanisms. Multiple reports have shown improvements in DPN after treatment with insulin intrathecally, locally, and systemically (Singhal et al., 1997; Huang et al., 2003; Brussee et al., 2004; Hoybergs and Meert, 2007). Our results are in agreement with these studies; however, one major difference is that these studies reported no changes in blood glucose concentrations. Therefore, they were able to infer that the

improvements in DPN were due to direct trophic effects of insulin on peripheral nerves. Further studies supplying insulin intrathecally or in low doses directly in the nerves (such as in Singhal et al., 1997) would help narrow down insulin's mechanism of action in repairing large-fiber neuropathy in STZ-induced diabetic mice.

Toth et al. (2006) reported that intrathecal insulin delivery decreased axonal atrophy and lead to increased regeneration after nerve crush injury in rats. In contrast, near-nerve insulin delivery did not have an effect on axonal atrophy or regeneration (Toth et al., 2006). Based on these data, systemic insulin delivery leading to decreased blood glucose levels (such as in our model) might not be expected to have a direct effect on regeneration of peripheral nerves. However, we hypothesize that our diabetes model had inherent differences, when compared to the nerve injury model, which could lead to increased nerve support and/or regeneration even with only an increase in systemic insulin. First of all, our type 1 diabetes mouse model had significantly decreased insulin production, which resulted in lowered insulin trophic support to peripheral nerves. Perhaps because the diabetic nerves were "starved" for insulin, unlike the injury model with normal circulating insulin levels, any contact with insulin to the axon and/or perikarya, could have a positive neurotrophic effect. Secondly, the circulating blood insulin levels in our diabetic + insulin mice were significantly greater than nondiabetic mice with normoinsulinemia. Normally, insulin circulating in the blood will enter the cerebrospinal fluid and have direct contact with the dorsal root ganglia and anterior horn cells. It is possible that with higher than normal levels of circulating insulin, there was a greater amount of insulin acting on IRs supporting the cell bodies of both peripheral sensory and motor neurons.

Insulin and large sensory fibers. Studies have examined the effects of insulin therapy on diabetes-induced peripheral small-fiber neuropathy. In a model of insensate neuropathy, STZ-induced diabetic mice that were treated with sustained release insulin pellets had reversed mechanical insensitivity (Christianson et al., 2007). In addition, in the STZ-induced diabetic rat model of painful neuropathy, low-dose sustained release insulin therapy resulted in normalization of mechanical allodynia, without changes in blood glucose levels (Hoybergs and Meert, 2007). Lastly, insulinopenic STZ-treated rats without hyperglycemia displayed mechanical hyperalgesia that was also reversible with low-dose insulin replacement (Romanovsky et al., 2006). No studies, to our knowledge, have examined large-fiber neuropathy behavioral deficits after insulin therapy. Interestingly, in the current study we have reversed balance sensorimotor dysfunction through treatment with insulin. Therefore, not only does insulin have positive actions on dysfunctional small sensory fibers, but it can also repair large sensory fiber deficits.

Insulin and nerve conduction velocity. Nerve conduction velocity improvements have been reported after insulin therapy in many studies (Singhal et al., 1997; Huang et al., 2003; Brussee et al., 2004). Here, we have also reported that insulin replacement increased sciatic MNCV to levels comparable with nondiabetic mice. Of interest are the changes in SNCV. Reports in diabetic rats and mice have shown decreases in SNCV at different time points (Mizisin et al., 1999; Huang et al., 2003; Brussee et al., 2004). In contrast, Jefferys and Brismar (1980) reported no changes in SNCV due to diabetes. In Chapter 2, we reported no changes in digital SNCV in our animal model of large-fiber diabetic neuropathy, and those results are consistent with the current study. However, unexpectedly, here we have reported

that insulin treatment in the diabetic mice significantly lowered their SNCV. Nerve conduction velocity can be affected by sodium channel expression and function (Yokota et al., 1994; Kearney et al., 2002). Moreover, Craner et al. (2002) examined the expression and protein levels of multiple sodium channels in the setting of STZ-induced diabetes in rats, and found alterations in $Na_V1.3$, $Na_V1.6$, and $Na_V1.8$ levels in both large and small DRG neurons. Administration of growth factors in diabetic and axotomized animals has resulted in the reversal of sodium channel alterations (Fernyhough et al., 1993; Black et al., 1997). Therefore, it is possible that insulin treatment in the current study could have altered sodium channel expression in peripheral sensory nerves. If, in fact, the sensory nerves are going through regeneration after insulin therapy, it could be hypothesized that SNCV was reduced due to sodium channel flux. Perhaps, if the SNCV was measured 1 or 2 weeks later, we would expect to see increases in conduction velocity.

In conclusion, we have reported that 4 weeks of sustained-release insulin treatment in STZ-induced C57BL/6 diabetic mice is successful at reversing large-fiber sensorimotor deficits and restoring muscle spindle Ia afferent innervation variability. Future studies could address the molecular mechanisms by which insulin had positive actions on peripheral sensory and motor nerves. Additionally, studies could test the use of insulin therapy independent of glucose alterations in the large-fiber DPN model. Even though insulin is a common treatment for type 1 and sometimes type 2 diabetes in humans, it is only given to lower blood glucose levels. It is possible that it could be administered locally to nerves in low doses in order to trophically support the peripheral nerves and prevent and/or reverse the symptoms of DPN.

VIII. CHAPTER FOUR

Aerobic Exercise Therapy Improves Sensorimotor Deficits and Has No Effect on Variability in Muscle Spindle Ia Afferent Innervation in Diabetic Mice

1. Abstract

Alterations in group Ia sensory afferent fibers innervating muscle spindles lead to sensorimotor and gait disturbances in STZ-induced type 1 diabetic mice. Sensorimotor and nerve dysfunction can be reversed through insulin treatment. Exercise has been suggested as a therapy for DPN, and we aimed to determine whether symptoms of large-fiber DPN and muscle spindle morphologic variations could be repaired by aerobic exercise therapy.

STZ-induced diabetic and nondiabetic mice performed low-intensity exercise therapy consisting of brisk walking on a treadmill for 4 weeks. Sensorimotor behavioral assessments were made before and after exercise therapy. Electrophysiologic studies and muscle spindle quantification were carried out at the end of the exercise study.

Low-intensity exercise therapy did not have an effect on blood glucose concentrations, body weight, or blood insulin concentrations in diabetic or nondiabetic mice. In addition, exercise had no effect on nerve conduction velocities in peripheral motor or sensory nerves. Interestingly, exercise therapy did improve sensorimotor dysfunction in diabetic mice. Lastly, exercise therapy had no effect on the muscle spindle Ia afferent innervation patterns in diabetic or nondiabetic mice.

Low-intensity exercise therapy can improve sensorimotor deficits in STZ-induced diabetic mice; however, it does not have an effect on the electrophysiologic properties or anatomical structure of peripheral sensory nerves. These studies provide a treatment for large-fiber DPN in type 1 diabetic mice, and will allow for future studies on the mechanisms behind sensorimotor improvement after exercise.

2. Introduction

As discussed in Chapter 1, aerobic exercise therapy is recommended for diabetic patients to help prevent diabetes-related complications, such as DPN. A number of studies have reported improved clinical measurements of diabetic and pre-diabetic neuropathy after exercise therapy including intraepidermal nerve fiber (IENF) density, balance control, nerve conduction velocities (NCV), and vibration perception thresholds (Richardson et al., 2001; Balducci et al., 2006; Smith et al., 2006). Overall, the molecular mechanisms behind treating DPN with exercise therapy have not been elucidated, but several hypotheses exist. Exercise can have positive effects directly on the cardiovascular system, on the musculoskeletal system, and even directly on nerves themselves.

Here we tested the hypothesis that exercise therapy could improve sensorimotor deficits in mice with large-fiber neuropathy, perhaps through repair of Ia axonal morphology. We examined the effects of aerobic low-intensity exercise on STZ-induced type 1 diabetic mice for evidence of large-fiber DPN improvement. These experiments provide evidence that exercise has positive effects on sensorimotor function without altering muscle spindle innervation or metabolic status in STZ-induced diabetic mice.

3. Experimental procedures

Mice. Male C57BL/6 mice were purchased at 7 weeks of age from Charles River (Wilmington, MA) and housed 2 mice/cage on a 12:12-hour light/dark cycle in the animal facility at the University of Kansas Medical Center under pathogen-free conditions. All animals had free access to water and mouse chow (Harlan Teklad

8604, 4% kcal derived from fat), and their use was in accordance with NIH guidelines and approved by the University of Kansas Medical Center Animal Care and Use Committee.

Diabetes induction. Diabetes was induced as previously described in Chapter 2 in 8 week-old C57BL/6 mice (n=21) by a single intraperitoneal injection of STZ (Sigma, St. Louis, MO) at 180 mg/kg body weight. The nondiabetic mice (n=16) were injected with 400 μl of the vehicle. Hyperglycemia and diabetes was defined as a blood glucose level greater than 16mM (~288 mg/dl), and STZ-injected mice with blood glucose levels below the standard were not included in this study. Weight and tail vein blood glucose levels using glucose diagnostic reagents (Sigma) were measured throughout the protocol and analyzed using a two-way RM ANOVA with Fisher's PLSD post hoc test. Blood insulin concentration was measured in 5 μL of serum at 10 weeks post-STZ injection as described in Chapter 3. Insulin concentration was analyzed using a one-way ANOVA with Fisher's PLSD post-hoc test.

Experimental design. In order to evaluate the effects of aerobic exercise on hyperglycemia-induced changes in sensory nerve fibers, mice were randomly assigned to 4 groups: nondiabetic sedentary (n=8), nondiabetic exercise (n=8), diabetic sedentary (n=10), or diabetic exercise (n=11). Baseline beam-walk behavioral testing was performed on weeks 1 and 5 post-STZ injection. Aerobic exercise therapy began in week 6 and continued for a total of 4 weeks, while beam-walk performance was evaluated post-exercise at 10 weeks post-STZ. Mice were sacrificed after nerve conduction studies in week 10, and immunohistochemical analysis of muscle followed.

Beam-walk apparatus. The beam-walk apparatus utilizes an elevated wooden balance beam to test for sensorimotor deficits, and has been found to reveal muscle spindle dysfunction in both a nerve injury model and a diabetic mouse model (Taylor et al., 2003; Muller et al., 2008). It was used as described in Chapter 2, and briefly, the animals were recorded for 3 trials/session while traversing a demarcated 70 cm section of the beam on weeks 1, 5 and 10 post-STZ injection. The number of footslips/mouse was averaged, and the data was analyzed using a two-way RM ANOVA with Fisher's PLSD post hoc test.

Aerobic exercise therapy. Exercise training was carried out on the nondiabetic and diabetic exercise groups 5 weeks post-STZ injection using two 6-lane motorized treadmill (Columbus Instruments, Columbus, OH). Training consisted of 3 days of acclimatization to the treadmill itself, and then subsequent increasing speeds of the treadmill. The exercise protocol began 6 weeks post-STZ injection for 30 minutes/day, 5 days/week for a total of 4 weeks. The mice briskly walked on a level surface at a speed of 10 m/min.

Nerve conduction velocity. Both motor and sensory nerve conduction velocities were recorded at 10 weeks post-STZ injection using methods described in Chapter 2. Diabetic and nondiabetic nerve conduction velocities were analyzed by a one-way ANOVA with Fisher's PLSD post hoc test.

Immunohistochemistry. Immediately following NCV testing, diabetic and nondiabetic C57BL/6 mice were decapitated prior to the removal of the right gastrocnemius muscles. Medial gastrocnemius muscles were processed according to methods in Chapter 2.

Muscle spindle innervation. Muscle spindle large-fiber sensory innervation was analyzed using methods described in Chapter 2. Fluorescent digital images were acquired using a Nikon Digital Eclipse C1si confocal microscope. Approximately 3 - 6 muscle spindles per muscle were imaged for spindle innervation quantification. Digital Z-stack images of spindles were transferred to Nikon Imaging Software-Elements (NIS-Elements; Melville, NY). For each spindle the mean width of 3 or more axonal rotations and the mean inter-rotational distance (the space in between the axonal rotations) in between 3 or more rotations were calculated and recorded by a blinded observer using NIS-Elements. Mean axonal width and mean inter-rotational distance were analyzed using a one-way ANOVA with Fisher's PLSD post hoc test.

4. Results and Figures

Blood glucose concentrations and body weight. STZ-induced diabetes lead to hyperglycemia (> 16 mM) 1 week post-STZ injection and throughout the study that was significantly higher than nondiabetic glucose concentrations ($p < 0.0001$ diabetic sedentary (D-S) vs. nondiabetic sedentary (ND-S) mice; **Figure VIII-1A**). Nondiabetic mice that were exercised (ND-E) continued to display normoglycemia, while diabetic exercise (D-E) mice continued to display hyperglycemia (**Figure VIII-1A**). Therefore, exercise therapy had no effect on blood glucose concentrations ($p > 0.05$ ND-S vs. ND-E mice and D-S vs. D-E mice). Likewise, the body weight of diabetic mice was significantly lower than that of nondiabetic mice starting 1 week post-STZ ($p < 0.05$) and continuing throughout the course of the study (**Figure VIII-1B**). However, exercise did not alter body weight in nondiabetic or diabetic mice ($p > 0.05$ ND-S vs. ND-E mice and D-S vs. D-E mice; **Figure VIII-1B**).

Figure VIII-1. Blood glucose concentrations and body weights in diabetic and nondiabetic sedentary and exercise mice. (A) Quantification of mean blood glucose concentrations weeks 1 and 5 post-STZ (pre-exercise) and weeks 6-10 post-STZ (throughout exercise). Diabetic sedentary and exercise mice had significantly higher glucose levels compared to nondiabetic sedentary and exercise mice throughout the course of the study. (B) Quantification of mean body weights weeks 1 and 5 post-STZ (pre-exercise) and weeks 6-10 post-STZ (throughout exercise). Diabetic sedentary and exercise mice had significantly lower body weights compared to nondiabetic sedentary and exercise mice throughout the course of the study. Data presented as means +/- SEM. * $p < 0.05$ vs. nondiabetic sedentary and exercise mice.

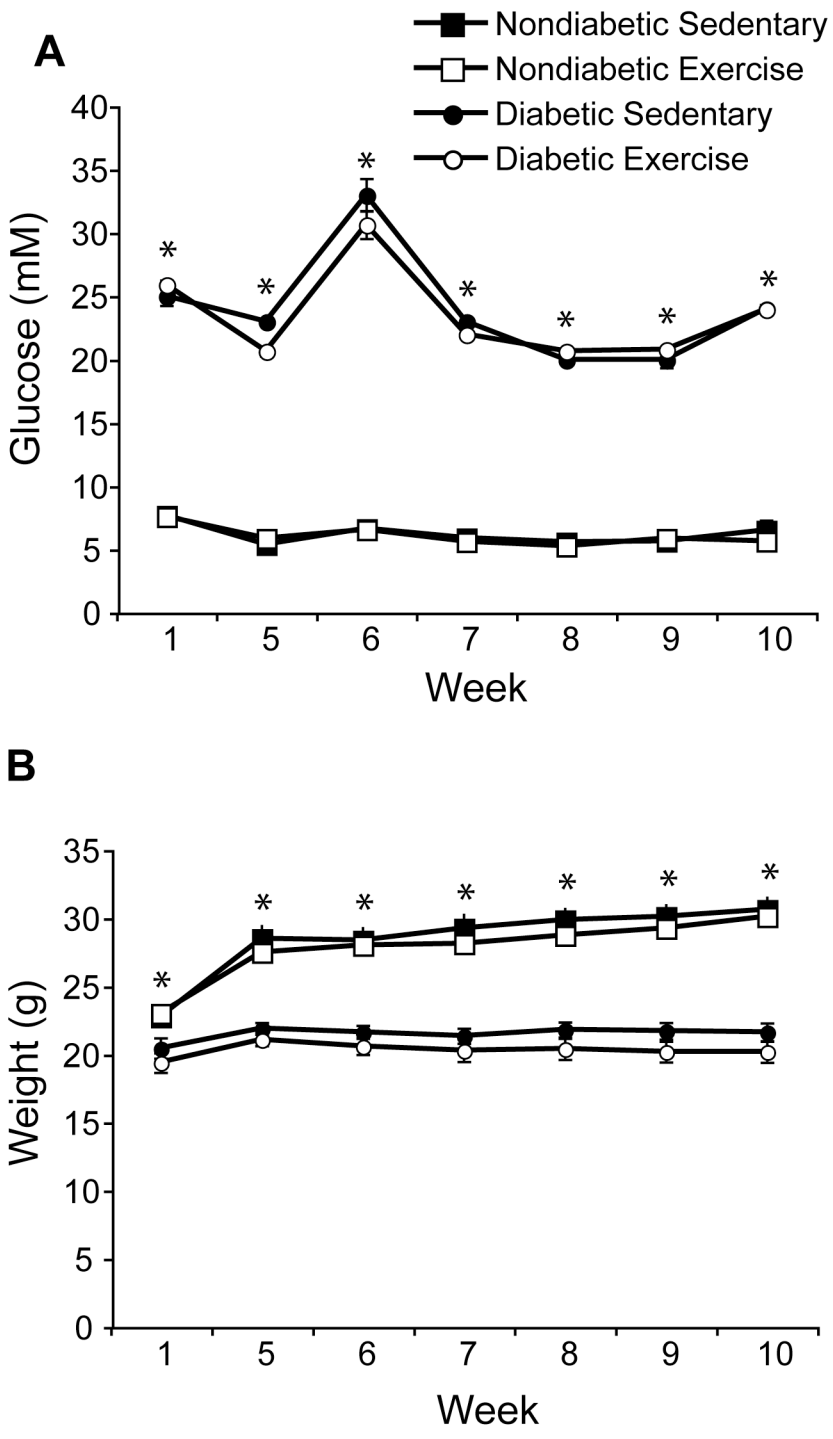
A
Nondiabetic Sedentary
Nondiabetic Exercise
Diabetic Sedentary
Diabetic Exercise
Glucose (mM)
0
5
10
15
20
25
30
35
40
1
5
6
7
8
9
10
Week
B
Weight (g)
0
5
10
15
20
25
30
35
1
5
6
7
8
9
10
Week

Blood insulin concentrations. Blood insulin concentrations were measured in ND-S, ND-E, D-S, and D-E mice 10 weeks post-STZ injection. STZ-induced D-S mice had significantly lower blood insulin levels compared to ND-S mice ($p < 0.05$; **Figure VIII-2**). However, exercise therapy had no effect on insulin concentrations ($p > 0.05$ ND-S vs. ND-E mice and D-S vs. D-E mice; **Figure VIII-2**). These results suggest that the metabolic parameters measured here (blood glucose concentration, weight, and insulin concentration) were all altered by diabetes, but were not changed after 4 weeks of exercise therapy.

Beam-walk performance. In Chapter 2, STZ-induced diabetes leads to sensorimotor dysfunction by 10 weeks post-STZ injection as measured by hindpaw footslips on the beam-walk apparatus. Here, D-S mice displayed a significantly greater number of hindpaw footslips 10 weeks post-STZ injection compared to ND-S mice ($p < 0.05$) and ND-E mice ($p < 0.05$; **Figure VIII-3**). Importantly, 4 weeks of exercise therapy in diabetic mice significantly decreased hindpaw footslips compared to sedentary diabetic mice ($p < 0.05$; **Figure VIII-3**). The number of hindpaw footslips in D-E mice was not statistically different from ND-S ($p > 0.05$) or ND-E ($p > 0.05$) mice. These results suggest that 4 weeks of exercise therapy in diabetic mice improved sensorimotor function as tested on the balance beam to levels comparable to nondiabetic mice. However, exercise had no effect on the sensorimotor performance of nondiabetic mice.

Peripheral nerve electrophysiology. Sciatic motor nerve conduction velocity (MNCV) was significantly decreased at 10 weeks post-STZ injection in D-S compared to ND-S mice ($p < 0.0001$; **Figure VIII-4A**). However, exercise training did

Figure VIII-2. Blood insulin concentrations in diabetic and nondiabetic sedentary and exercise mice. Quantification of mean blood insulin concentrations at 10 weeks post-STZ injection. Diabetic sedentary and exercise mice had significantly lower insulin levels compared to nondiabetic sedentary and exercise mice. Data presented as means +/- SEM. * $p < 0.05$ vs. nondiabetic sedentary and exercise mice.

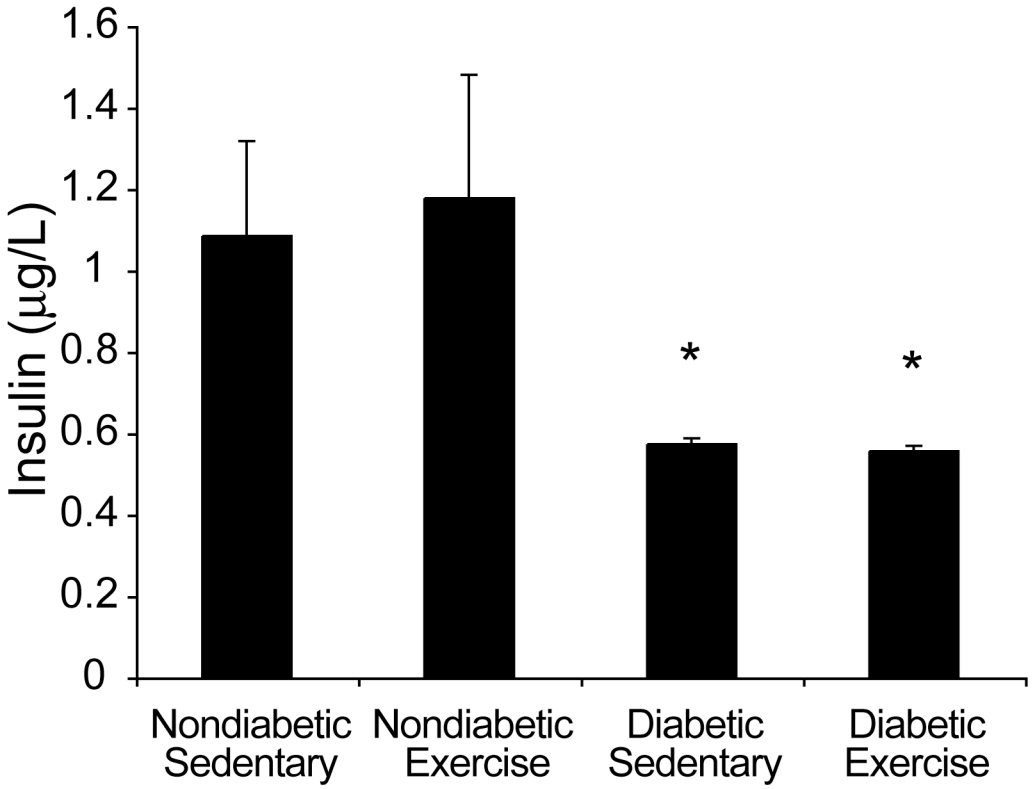
1.6
1.4
1.2
1
0.8
0.6
0.4
0.2
0
Insulin (µg/L)
*
*
Nondiabetic Sedentary
Nondiabetic Exercise
Diabetic Sedentary
Diabetic Exercise

Figure VIII-3. Sensorimotor evaluation on beam-walk in diabetic and nondiabetic sedentary and exercise mice. Quantification of mean hindpaw footslips at weeks 1 and 5 post-STZ (pre-exercise) and 10 weeks post-STZ (terminal exercise week). Diabetic sedentary mice had significantly more slips at 10 weeks post-STZ compared to nondiabetic sedentary, nondiabetic exercise, and diabetic exercise mice. Data are presented as means +/- SEM. * $p < 0.05$ vs. nondiabetic sedentary and exercise and diabetic exercise mice.

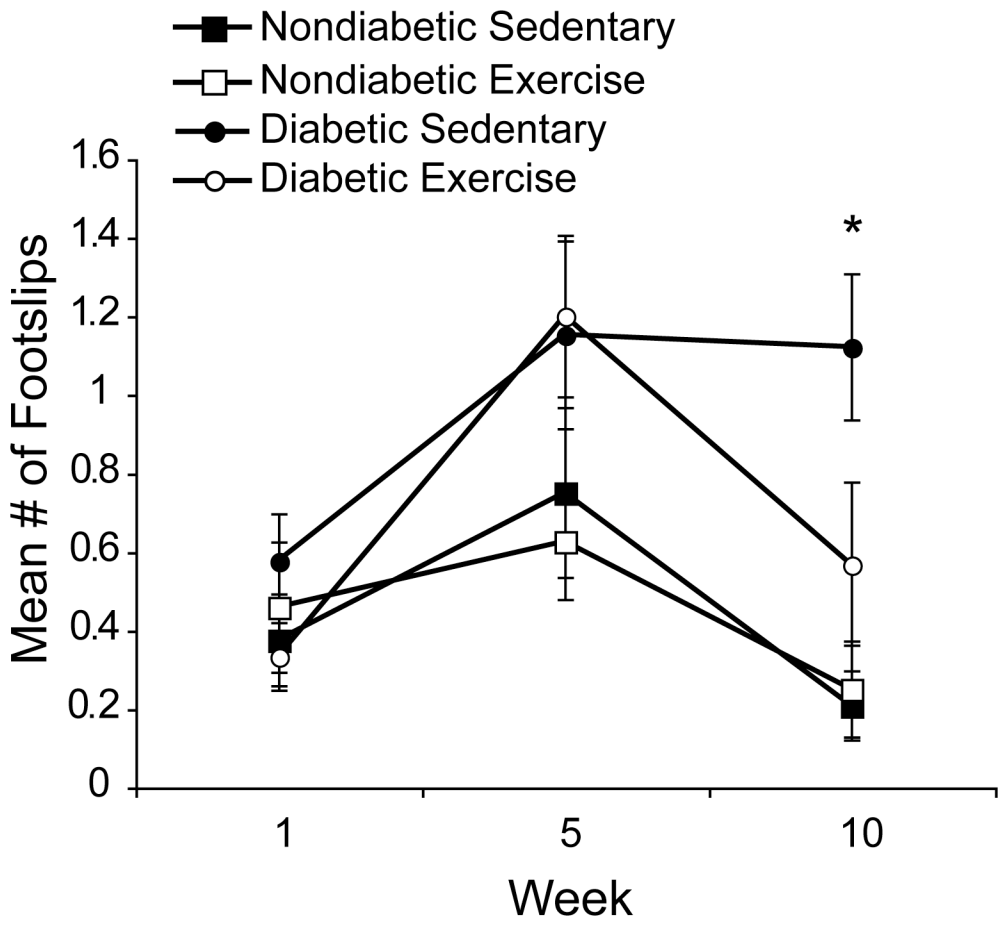
Nondiabetic Sedentary
Nondiabetic Exercise
Diabetic Sedentary
Diabetic Exercise
Mean # of Footslips
1.6
1.4
1.2
1
0.8
0.6
0.4
0.2
0
*
1
5
10
Week

Figure VIII-4. Nerve conduction velocity in diabetic and nondiabetic sedentary and exercise mice. (A) Quantification of mean sciatic motor nerve conduction velocity at 10 weeks post-STZ injection. Diabetic sedentary and exercise mice had significantly lower conduction velocity compared to nondiabetic sedentary and exercise mice. (B) Quantification of mean digital sensory nerve conduction velocity at 10 weeks post-STZ injection. Data presented as means +/- SEM. * $p < 0.05$ vs. nondiabetic sedentary and exercise mice.

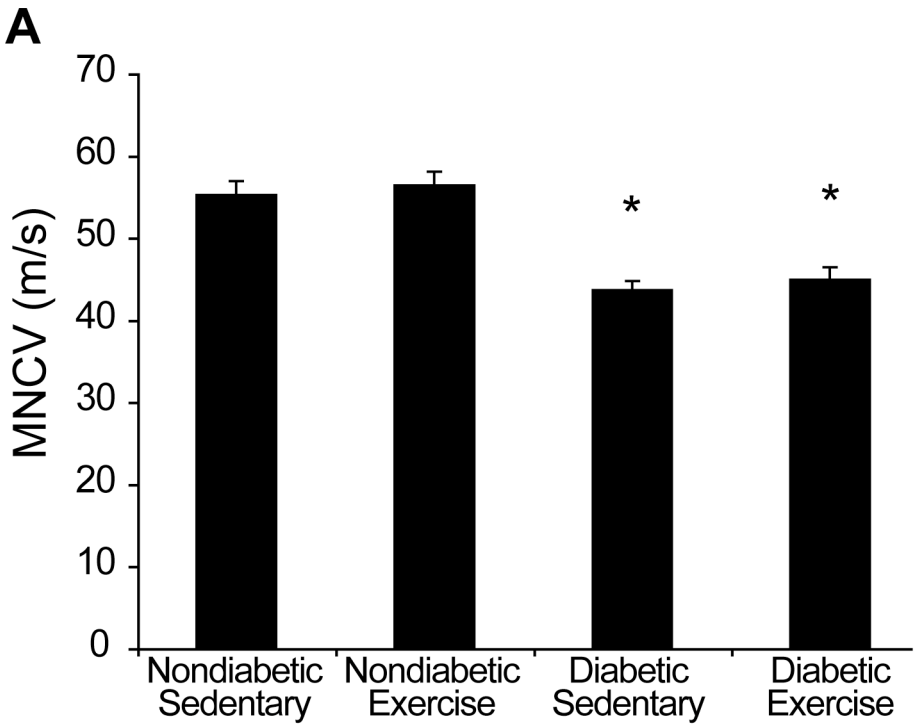
A
MNCV (m/s)
70
60
50
40
30
20
10
0
*
*
Nondiabetic Sedentary
Nondiabetic Exercise
Diabetic Sedentary
Diabetic Exercise

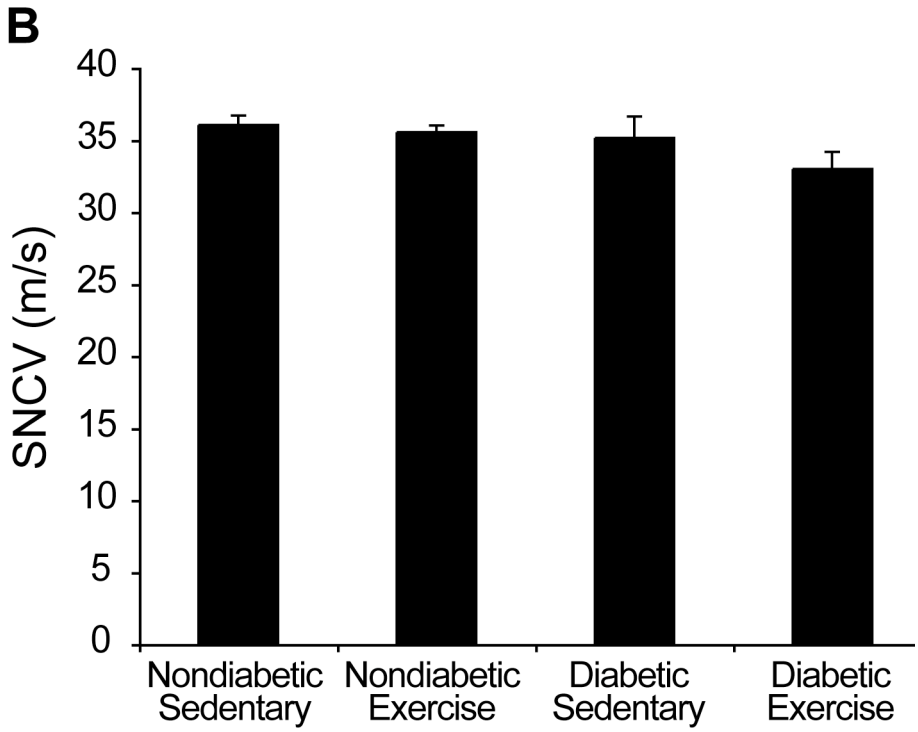
B
SNCV (m/s)
40
35
30
25
20
15
10
5
0
Nondiabetic Sedentary
Nondiabetic Exercise
Diabetic Sedentary
Diabetic Exercise

not affect MNCV in either nondiabetic ($p > 0.05$ ND-S vs. ND-E) or diabetic mice ($p > 0.05$ D-S vs. D-E; **Figure VIII-4A**). Similar to previous reports (Muller et al., 2008), there was no difference in the nerve conduction velocity of the digital nerve (SNCV) between diabetic and nondiabetic mice ($p > 0.05$ D-S vs. ND-S; **Figure VIII-4B**). Likewise, exercise had no effect on either nondiabetic ($p > 0.05$ ND-S vs. ND-E) or diabetic mice ($p > 0.05$ in D-S vs. D-E**; Figure VIII-4B**). These results suggest that diabetes alters MNCV, but not SNCV. In addition, this exercise therapy paradigm did not alter any of the electrophysiologic parameters measured here.

Diabetic sedentary muscle spindle Ia afferent morphology. As described previously in Chapters 2 and 3, diabetic muscle spindles display increased morphologic variability in mean axonal width and mean IRD compared to nondiabetic spindles. This finding was confirmed here; muscle spindle variability was greater in diabetic mice compared to nondiabetic mice. **Figure VIII-5** illustrates the differences in D-S muscle spindles compared to ND-S spindles. An example of a ND-S muscle spindle is shown in **Figure VIII-5A**. Diabetic Ia axons from sedentary mice can have a similar axonal width to ND-S mice (**Figure VIII-5B**), but interestingly they can also display much wider (**Figure VIII-5C**) or much thinner (**Figure VIII-5D**) axonal widths both in between diabetic animals and within the same muscle. However, this did not result in a difference in mean axonal width. The mean axonal width in D-S mice was 1.51 μm, which was not significantly different from ND-S mice (1.43 μm; $p > 0.05$; **Table VIII-1**). However, the range of mean axonal width in D-S mice was 2.56 μm, much greater than the range of 0.91 μm in ND-S mice (**Table VIII-1**). By plotting the number of muscle spindles with particular axonal widths in a histogram (**Figure VIII-5E**), it is apparent that the ND-S mice had a very tight range of axonal widths,

Figure VIII-5. Altered muscle spindle innervation in diabetic sedentary mice. (A) Confocal optical image from the equatorial region of the medial gastrocnemius muscle spindle from a nondiabetic sedentary mouse shows the typical axonal width and inter-rotational distance displayed by nondiabetic mice. (B, C, D) Confocal optical images from a diabetic sedentary mouse show that muscle spindles in diabetic mice can have axonal widths that are comparable with nondiabetics (B), that are much wider than nondiabetics (C), or even much thinner than nondiabetics (D). (B, C, D) These images highlight the variability in diabetic muscle spindle innervation morphology. Red visualizes slow tonic myosin heavy chain (S46) expression within spindle bag fibers, and green represents NF-H positive Ia axons with their characteristic annulospiral morphology. The white arrows denote very thin axons and the white arrowheads denote very thick axons. (E) Mean axonal width was more variable in diabetic sedentary mice compared to nondiabetic sedentary mice. Note that there are increased numbers of smaller or larger Ia axons in diabetic sedentary mice compared to nondiabetic sedentary mice. Diabetic sedentary mice have increased variability in axonal width in muscles of individual animals compared to nondiabetic sedentary mice (F). (G) Mean inter-rotational distance was also more variable in diabetic sedentary mice compared to nondiabetic sedentary mice. Diabetic sedentary mice also have increased variability in inter-rotational distance in individual muscles compared to nondiabetic sedentary mice (H). CoV is the coefficient of variation. Black circles represent 1 muscle, and black lines represent the mean CoV in each group (F, H).

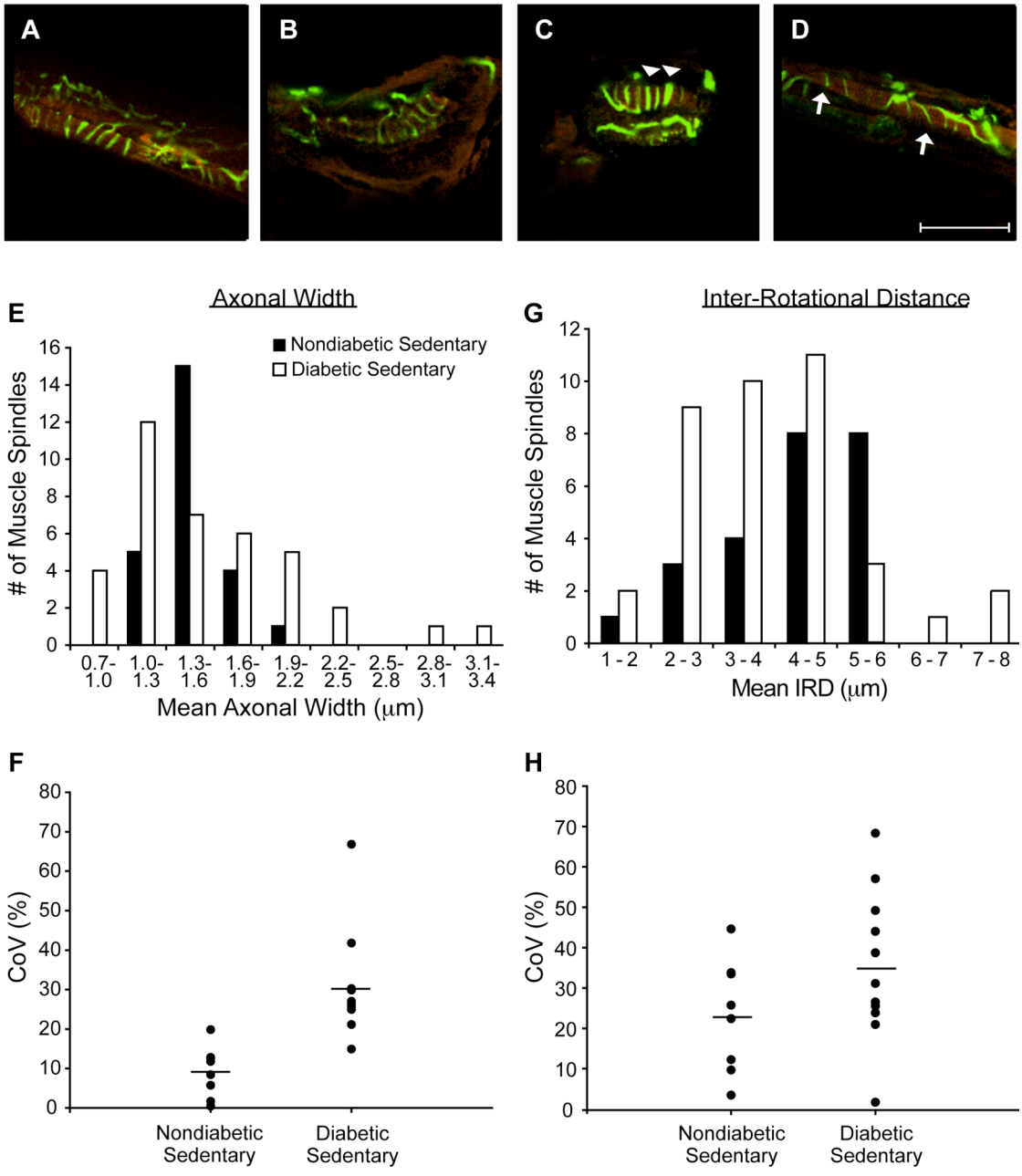
A
B
C
D
E
Axonal Width
Nondiabetic Sedentary
Diabetic Sedentary
# of Muscle Spindles
0.7-1.0
1.0-1.3
1.3-1.6
1.6-1.9
1.9-2.2
2.2-2.5
2.5-2.8
2.8-3.1
3.1-3.4
Mean Axonal Width (μm)
G
Inter-Rotational Distance
# of Muscle Spindles
1 - 2
2 - 3
3 - 4
4 - 5
5 - 6
6 - 7
7 - 8
Mean IRD (μm)
F
CoV (%)
Nondiabetic Sedentary
Diabetic Sedentary
H
CoV (%)
Nondiabetic Sedentary
Diabetic Sedentary

Table VIII-1. Summary of muscle spindle quantification

A. Axonal Width

	Mean	SEM	Minimum	Maximum	Range	Median
ND-S (n=8)	1.43	0.04	1.06	1.97	0.91	1.36
ND-E (n=8)	1.68	0.06	1.30	2.28	0.98	1.56
D-S (n=10)	1.51	0.08	0.93	3.49	2.56	1.39
D-E (n=9)	1.50	0.07	0.70	2.42	1.72	1.48

B. Inter-Rotational Distance

	Mean	SEM	Minimum	Maximum	Range	Median
ND-S (n=8)	4.34	0.25	1.58	6.43	4.85	4.14
ND-E (n=8)	4.87	0.30	2.56	8.07	5.51	4.51
D-S (n=10)	3.86	0.23	1.21	7.46	6.25	3.92
D-E (n=9)	3.44	0.24	1.18	7.63	6.45	3.38

Summary of muscle spindle quantification for axonal width and inter-rotational distance in nondiabetic sedentary (ND-S), nondiabetic exercise (ND-E), diabetic sedentary (D-S), and diabetic exercise (D-E) mice.

while the D-S mice had a wide range of widths. This indicates that there is a great deal of spread in mean axonal widths for diabetic mice. Furthermore, in order to examine the internal variability of muscle spindles within one animal, the coefficient of variation was calculated (CoV (%) = (Standard Deviation/Mean)*100). **Figure VIII-5F** reveals that the D-S mice had over 3 times more internal variability in axonal widths when compared to spindles from ND-S mice (30.7% vs. 9.2%).

Like axonal width, there was no significant difference between IRD in D-S mice (3.86 μm) and ND-S mice (4.34 μm; **Table VIII-1**). However, D-S mice did have a wider range of IRDs compared to ND-S mice (6.25 μm vs. 4.85 μm, respectively; **Table VIII-1** and **Figure VIII-5G**). Likewise, when examining the internal variability of IRDs in D-S mice, they had 1.5 times greater CoV compared to ND-S mice (**Figure VIII-5H**). These results show that D-S mice have greater variability in their axonal width and IRD as a group and within individual muscles. These data confirm our previous studies and set the stage to evaluate the results of 4 weeks of low-intensity exercise therapy on these mice.

Nondiabetic mice muscle spindle Ia afferent morphology after exercise. In nondiabetic mice, exercise therapy resulted in minimal changes to muscle spindle morphology. The mean axonal width of ND-E mice (1.68 μm) was not significantly different from that of ND-S mice (1.43 μm; $p > 0.05$), and the mean IRD of ND-E mice (4.87 μm) was also not significantly different from ND-S mice (4.34 μm; $p > 0.05$; **Table VIII-1**). Interestingly, in **Figures VIII-6A and -C** the histograms of ND-E mice have been slightly shifted to the right for both axonal width and IRD when compared to ND-S mice. However, the CoVs comparing ND-S and ND-E mice for axonal width and IRD are very similar (**Figures VIII-6B and -D**). These results reveal

Figure VIII-6. Ia axonal width and inter-rotational distance in nondiabetic sedentary and nondiabetic exercise mice. (A) There was a tight range of mean axonal widths in both nondiabetic sedentary and nondiabetic exercise mice. (B) Individual muscles from nondiabetic sedentary and nondiabetic exercise mice had similar low variability in mean axonal width. (C) There was also a tight range of mean inter-rotational distances in nondiabetic sedentary and nondiabetic exercise mice. (D) Individual muscles from nondiabetic sedentary and nondiabetic exercise mice had similar low variability in mean inter-rotational distance. CoV is the coefficient of variation. Black circles represent 1 muscle, and the black lines represent the mean CoV in each group (B, D).

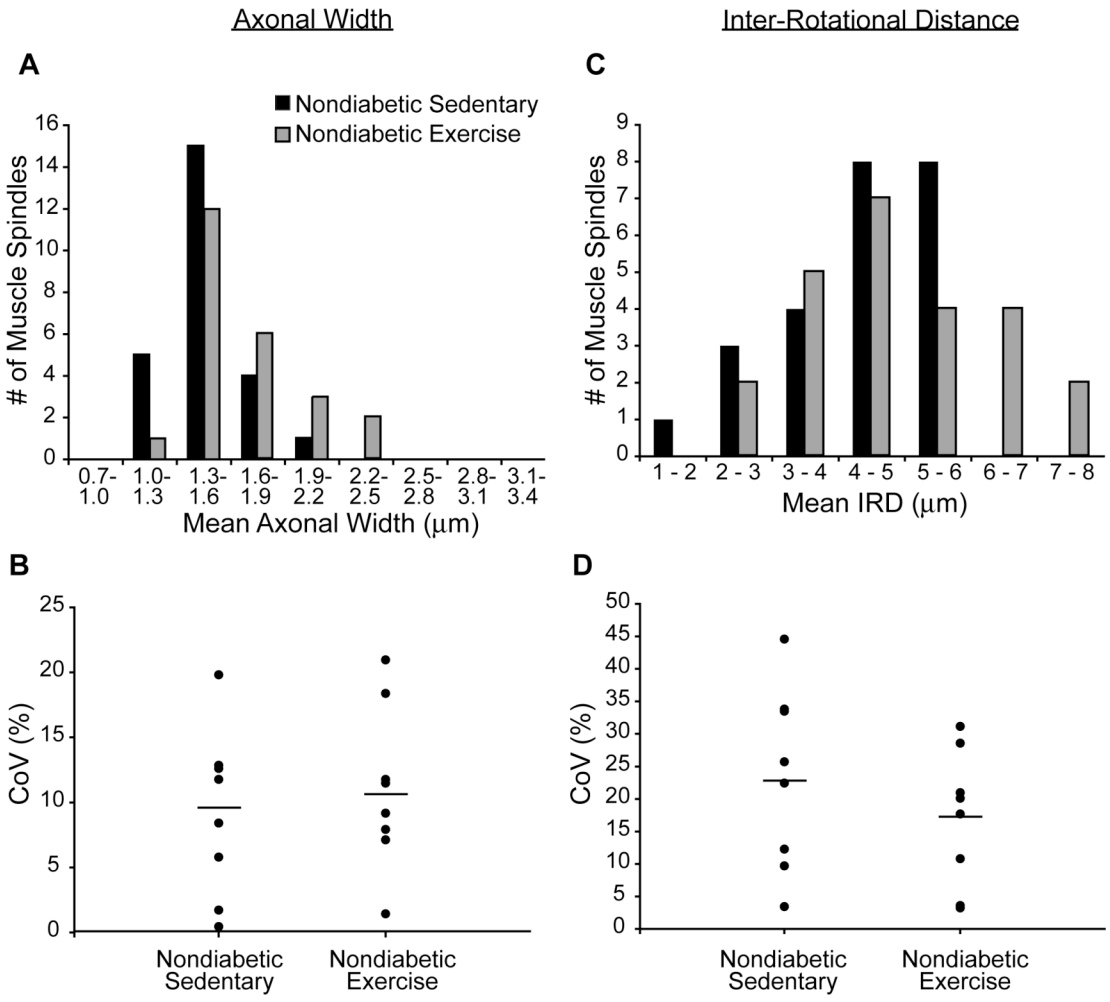
Axonal Width
Inter-Rotational Distance
A
C
Nondiabetic Sedentary
Nondiabetic Exercise
# of Muscle Spindles
0.7-1.0
1.0-1.3
1.3-1.6
1.6-1.9
1.9-2.2
2.2-2.5
2.5-2.8
2.8-3.1
3.1-3.4
Mean Axonal Width (μm)
1 - 2
2 - 3
3 - 4
4 - 5
5 - 6
6 - 7
7 - 8
Mean IRD (μm)
B
D
CoV (%)
Nondiabetic Sedentary
Nondiabetic Exercise

that exercise therapy in nondiabetic mice led to a slight increase in the axonal widths and IRDs of muscle spindles; however, the increase was not great enough to show significant increases in the variability of Ia axonal morphology. Therefore, 4 weeks of exercise therapy did not significantly affect muscle spindle Ia afferent morphology in nondiabetic mice.

Diabetic mice muscle spindle Ia afferent morphology after exercise. When examining the effects of 4 weeks of low-intensity aerobic exercise on diabetic mice, there were no differences in mean axonal width in D-E (1.50 μm) versus D-S (1.51 μm) mice, and no differences in mean IRD between D-E (3.44 μm) and D-S (3.86 μm) mice (**Table VIII-1**). When visualizing the histogram, the variability in axonal width in D-E animals was no different than the variability in D-S animals (**Figure VIII-7A**). Likewise, the CoV was similar in D-E and D-S mice (**Figure VIII-7B**), suggesting that exercise therapy did not alter the Ia innervation in diabetic mice as a group or within individual mice. In addition, the variability in IRD was the same between D-S and D-E mice (**Figure VIII-7C**), and the CoV was no different between the two groups as well (**Figure VIII-7D**). These results suggest that exercise did not decrease the high variability of diabetic muscle spindle Ia axonal innervation patterns.

5. Discussion

Results from this study reveal that 4 weeks of low-intensity aerobic exercise therapy in STZ-induced diabetic C57BL/6 mice repairs sensorimotor deficits without altering glucose or insulin levels, body weight, nerve conduction velocities, and,

Figure VIII-7. Ia axonal width and inter-rotational distance in diabetic sedentary and diabetic exercise mice. (A) There was a similar wide range of mean axonal widths in both diabetic sedentary and diabetic exercise mice. (B) Individual muscles from diabetic sedentary and diabetic exercise mice had similar high variability in mean axonal width. (C) There was also a wide range of mean inter-rotational distances in both diabetic sedentary and diabetic exercise mice. (D) Individual muscles from diabetic sedentary and diabetic exercise mice had similar high variability in mean inter-rotational distance. CoV is the coefficient of variation. Black circles represent 1 muscle, and the black lines represent the mean CoV in each group (B, D).

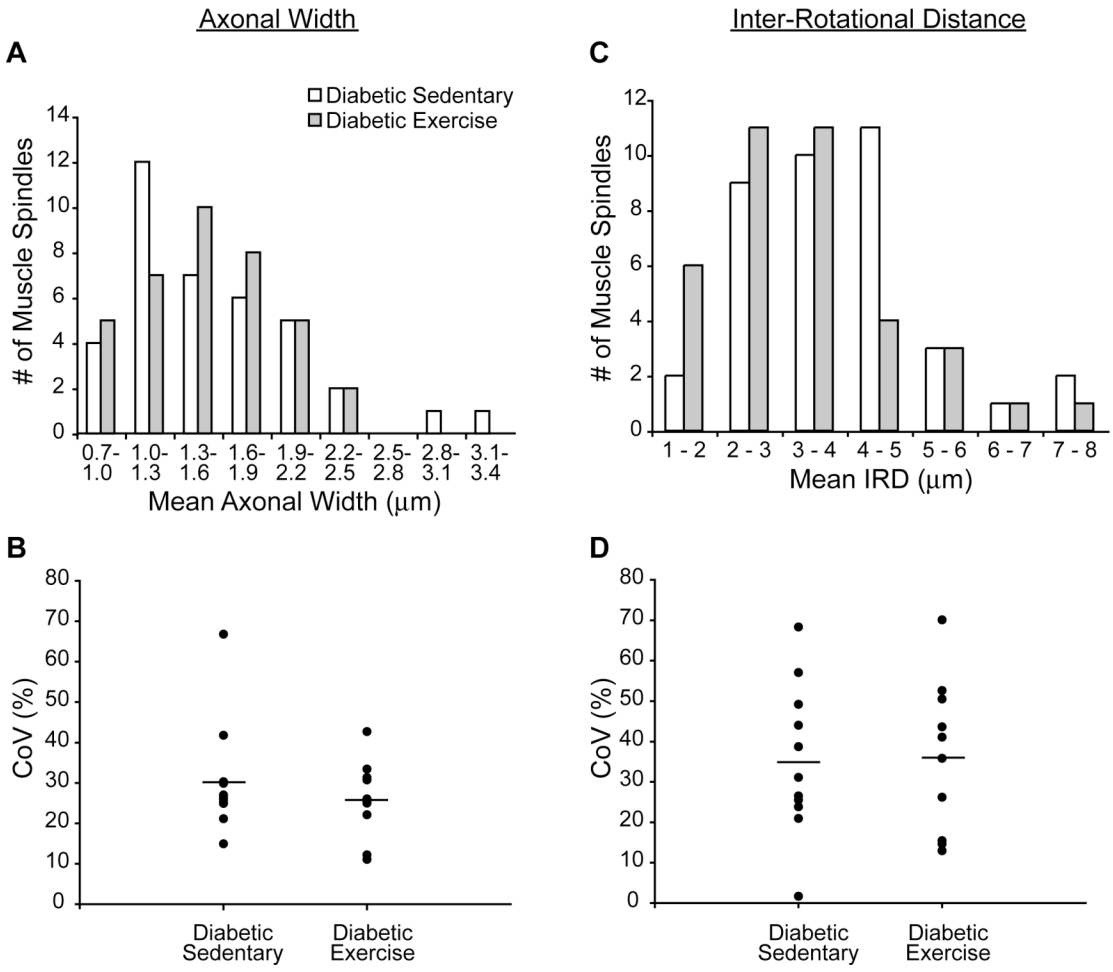
Axonal Width
A
Diabetic Sedentary
Diabetic Exercise
# of Muscle Spindles
0
2
4
6
8
10
12
14
0.7-1.0
1.0-1.3
1.3-1.6
1.6-1.9
1.9-2.2
2.2-2.5
2.5-2.8
2.8-3.1
3.1-3.4
Mean Axonal Width (μm)
Inter-Rotational Distance
C
# of Muscle Spindles
0
2
4
6
8
10
12
1 - 2
2 - 3
3 - 4
4 - 5
5 - 6
6 - 7
7 - 8
Mean IRD (μm)
B
CoV (%)
0
10
20
30
40
50
60
70
80
Diabetic Sedentary
Diabetic Exercise
D
CoV (%)
0
10
20
30
40
50
60
70
80
Diabetic Sedentary
Diabetic Exercise

interestingly, without changing muscle spindle Ia afferent axonal innervation. Based on findings from Chapters 2 and 3, diabetic mice with altered sensorimotor function display variations in Ia axonal morphology, and 4 weeks of insulin therapy not only decreased the behavioral deficits, but also substantially reversed the variability in muscle spindle innervation. To our knowledge, no studies to date have used exercise therapy to treat large-fiber diabetic neuropathy in a mouse model. In human diabetic neuropathy patients, exercise studies are commonly designed to improve the symptoms of both small- and large-fiber neuropathy (Balducci et al., 2006; Smith et al., 2006). Relating this goal to our current study, the sensorimotor symptoms in diabetic mice were improved by exercise; however, not through direct effects on muscle spindle afferents.

Glucose homeostasis. Exercise studies in diabetic humans show mixed results in regards to glucose homeostasis. Multiple studies in diabetic and pre-diabetic patients involving low-intensity exercise regimens (brisk walking) or exercise counseling reported no changes in fasting blood glucose or hemoglobin A_{1C} (HbA_{1C}) levels (Balducci et al., 2006; Fritz et al., 2006; Smith et al., 2006; Roumen et al., 2008). Others have reported that moderate-intensity exercise in diabetic patients results in significantly decreased HbA_{1C}, glucose, or glycated albumin levels (Sigal et al., 2007; Villa-Caballero et al., 2007; Nojima et al., 2008). Animal research on exercise and diabetes has also shown that low-intensity exercise in a type 2 diabetes mouse model had no effect on glucose levels (Moien-Afshari et al., 2008). Here, blood glucose concentrations in both diabetic and nondiabetic mice were not changed by 4 weeks of low-intensity exercise therapy consisting of brisk walking. Our results fit well with human and animal studies demonstrating that lower-intensity

exercise has little-to-no effect on glucose homeostasis. In addition, we have reported no effects of exercise on body weight or blood insulin concentrations in the current study, which is expected with a type 1 diabetes model in which the animals typically fail to gain weight and have decreased beta cells to produce insulin. Perhaps in type 2 diabetes obesity models in which insulin production is intact (such as the *db/db* or *ob/ob* mice), we might have expected changes in weight and insulin levels.

Nerve conduction velocities. As we have reported in Chapters 2 and 3, STZ-induced diabetic mice display significantly decreased sciatic motor nerve conduction velocities while showing no changes in sensory nerve conduction velocity. The current study is consistent with these findings, but demonstrates that low-intensity exercise therapy had no effect on deficits in MNCV and did not alter SNCV. This lack of effect is in accordance with our results that exercise had no direct effect on peripheral nerves. Balducci et al. (2006) completed a 4-year exercise intervention study in diabetic patients and found that peroneal MNCV significantly increased in the exercise compared to control groups, and found no increase in sural SNCV. However, MNCV in exercised patients was not significantly different than controls years 1-3 of the study. It is possible that our exercise intervention in diabetic mice was not of sufficient duration or intensity to induce electrophysiologic changes in peripheral nerves.

Sensorimotor improvement without action on nerves. The one parameter that was significantly improved by exercise therapy was the performance on the beam-walk apparatus. Improved sensorimotor function in exercised diabetic mice could be due to mechanisms involving many different systems: proprioceptive nerves, extrafusal muscle fibers, intrafusal muscle fibers (muscle spindles),

vestibular organs, or cutaneous afferents. Most likely, exercise has an effect on a combination of the above systems to induce improvements in sensorimotor control. As our previous results have showed, insulin treatment resulted in sensorimotor repair with concomitant muscle spindle innervation improvements. Therefore, we examined the Ia afferent innervation morphology in this study as well; however, Ia afferent innervation did not change after exercise therapy in diabetic mice. Consequently, our low-intensity 4 week exercise paradigm in STZ-treated diabetic mice produced animals with an improvement in sensorimotor behavior without directly affecting group Ia proprioceptor morphology.

Extrafusal fibers and sensorimotor function. One major question brought about by the current study is how does low-intensity exercise therapy in STZ-induced diabetic mice improve sensorimotor function? Our data suggests these positive actions are not through direct effects on muscle spindle proprioceptor innervation, which opens the door to other possibilities. Sensorimotor function, particularly based on the beam-walk task, is inherently complicated, and muscle spindles are completely surrounded by the extrafusal skeletal muscle environment. Extrafusal muscle lengthening leads to intrafusal lengthening causing proprioceptors to fire and monosynaptically signal to alpha motor neurons. Extrafusal skeletal muscle fibers are known to atrophy in the setting of diabetes (Cotter et al., 1989), and it is plausible to assume that their damage could lead to muscle spindle dysfunction. Importantly, it has been found that exercise after nerve injury can decrease muscle atrophy (Goldshmit et al., 2008), and exercise therapy can also increase muscle strength in type 2 diabetic patients (Praet et al., 2008). In addition, Richardson et al. (2001) performed intervention exercises on peripheral neuropathy patients directed at

improving ankle strength. They found that 3 weeks of exercise therapy was successful at increasing ankle muscle strength and resulted in improved balance. Therefore, it is feasible that exercise therapy can have a directly supportive effect on extrafusal muscle fibers, which can compensate for proprioceptive alterations and result in improved sensorimotor function.

Increasing exercise intensity. It is possible that a higher intensity exercise training program could lead to improved spindle morphology via decreased Ia afferent variability. As mentioned above, human studies utilizing moderate-intensity exercise resulted in improved glucose homeostasis (Sigal et al., 2007; Villa-Caballero et al., 2007; Nojima et al., 2008). Glucose toxicity is implicated as one of the primary causes of nerve dysfunction in the setting of diabetes (Duby et al., 2004; Tomlinson and Gardiner, 2008). Hyperglycemia leads to high glucose concentrations within neurons, which can lead to an increase in reactive oxygen species. Interestingly, Nojima et al. (2008) administered a moderate-intensity exercise protocol in diabetic patients and found a decrease in urinary 8-hydroxy-2'-deoxyguanosine, a product of DNA oxidative damage. If increasing exercise intensity decreases blood glucose levels and concomitantly oxidative stress, then it might result in a more positive impact on peripheral nerves directly.

Extending exercise duration. Not only could a more intense exercise protocol have a greater effect on peripheral nerves, but also could exercise training for a longer period of time. Our study consisted of 4 weeks of exercise therapy on the treadmill, while other animal exercise studies have varying lengths of exercise protocols ranging from 3 days – 7 weeks (Molteni et al., 2004; Ying et al., 2005; Moien-Afshari et al, 2008) with different results. Interestingly, only 3 days of voluntary

running significantly increased NT-3 mRNA levels in the DRG of rats (Molteni et al., 2004), but 7 weeks of moderate-intensity exercise was needed to improve endothelial function in *db/db* mice (Moien-Afshari et al., 2008). As mentioned previously, Balducci et al. (2006) did not record significant changes in NCV until 4 years of exercise training in human diabetic patients. Taken together, exercise studies have many different outcome measures requiring varied protocols, and perhaps with a longer protocol, we may be able to see muscle spindle anatomical changes after exercise.

In conclusion, we have identified a low-intensity exercise paradigm that is successful at reversing large-fiber sensorimotor deficits in diabetic mice. This is the first study, to our knowledge, that has utilized exercise therapy to treat large-fiber DPN in mice. Additionally, we have found that, in concordance with other studies, low-intensity exercise therapy does not modify blood glucose concentrations. Future studies could address molecular mechanisms by which exercise is improving behavior outcomes with the current protocol, and additionally extend the exercise paradigm to be of greater intensity and a longer amount of time. This study provides an animal model of treatment for large-fiber DPN that will allow for a more mechanistic approach to understanding how exercise improves the quality of life in diabetic patients.

IX. CHAPTER FIVE

Conclusions

Overall, the goal of this body of work was to characterize large-fiber diabetic sensorimotor polyneuropathy in a widely used animal model of diabetes, and explore the hypothesis that the symptoms of large-fiber DPN could be due, in part, to aberrant muscle spindle innervation. Through the development of novel techniques to visualize muscle spindle afferent innervation morphology, we have discovered alterations in diabetic mice that we think may translate to the pathogenesis occurring in diabetic humans. However, because visualization of muscle spindles in humans is extremely difficult, and only through indirect testing of muscle spindle afferents can any information be gained, our experimental paradigm will be of great benefit to future understanding and treatment of large-fiber DPN. In addition to characterizing large-fiber DPN in diabetic mice, we sought to test two treatments for the repair of large-fiber behavioral and anatomical deficits to get a better understanding of the pathophysiology taking place in DPN, and to direct future studies.

Chapter Two. Diabetic mice display sensorimotor deficits and altered muscle spindle Ia afferent innervation

This study was the initial characterization of large-fiber neuropathy in STZ-induced diabetic mice up to 10 weeks post-induction of diabetes and in type 2 diabetic *db/db* mice. These data suggest that diabetic mice undergo damage to large sensory axons that may contribute to deficits in large-fiber sensory feedback associated with balance and gait. Specifically, results from this study demonstrated that 1) STZ-induced diabetes leads to sensorimotor deficits involving both balance and gait. 2) STZ-induced diabetic mice display slowly progressive motor nerve conduction velocity deficits; however sensory nerve changes were not evident in the

digital nerve of the hindpaw. 2) Muscle spindle Ia afferent innervation is highly variable in diabetic mice, which differs from nondiabetic mice who display consistent innervation patterns. 3) Type 2 diabetic *db/db* mice also have similar alterations in their muscle spindle Ia afferent innervation morphology to STZ-induced diabetic mice.

We hypothesize that the altered muscle spindle innervation morphology observed in diabetic mice is likely due to varying rates of axonal degeneration and subsequent regeneration. It is known that accumulations of neurofilament and other neuroproteins can be seen in a degenerating axon, which may be reflective of the larger axons we visualized with neurofilament-H immunostaining. In addition, nerves that are in the process of regeneration can have multiple thin axonal sprouts, which may be indicative of the smaller axons we also visualized with neurofilament-H immunostaining. Neurodegeneration/regeneration has been reported in cutaneous nerve fibers in DPN, and muscle spindle afferents could be similarly affected. We also hypothesize that the alterations in the anatomy of spindle afferents are leading to electrophysiologic output disruption of those afferents in diabetic mice, which could be resulting in the sensorimotor changes observed in these animals. Electrophysiologic output disruption of muscle spindle afferents could result in deep tendon hyporeflexia due to the involvement of spindle afferents in the monosynaptic reflex arc. Interestingly, patients with diabetic neuropathy have been reported to have hyporeflexia and sometimes even areflexia. This could be due to alterations in muscle spindle afferents in human patients with DPN similar to the changes seen in our diabetic mice.

Future studies could examine the cell bodies of proprioceptors to determine if changes are visible in the dorsal root ganglion in addition to the axonal terminations in skeletal muscle. This could be done using alpha-3 Na/K+ ATPase, a channel that has been shown to be selective to muscle spindle proprioceptors and is easily visualized in the perikarya of DRG neurons. Co-labeling proprioceptors with activating transcription factor 3 (ATF3) would suggest that they muscle spindle sensory afferents are damaged from diabetes and increase expression of ATF3 to induce regenerative growth. In addition, future studies could be employed that test the electrical output of Ia afferents to determine if morphologic alterations do, in fact, lead to sensory afferent/motor efferent dysfunction. This could be performed using an acute isolated spinal cord preparation that recorded output of motor neurons after Ia afferent stimulation. Lastly, we would like to further understand the differences and/or similarities between type 1 and type 2 diabetic neuropathies. Our current study was limited by only examining the anatomical changes in type 2 diabetic mice, and we could further our understanding by examining behavioral and electrophysiologic changes in this animal model as well.

Chapter Three. Insulin treatment modifies development of sensorimotor deficits and repairs muscle spindle Ia afferent innervation in diabetic mice

This study was performed to determine whether sensorimotor, electrophysiological, and spindle deficits in a large-fiber type 1 diabetes mouse model were reversible after treatment with insulin. These data suggest that systemic treatment with insulin effectively reversed behavioral and anatomical large-fiber neuropathy deficits in mice. Specifically, results from this study demonstrated that 1)

sustained insulin release for 4 weeks in STZ-induced diabetic mice decreased blood glucose levels, increased body weights, and increased serum insulin concentrations to levels higher than nondiabetic mice. 2) Insulin increased motor nerve conduction velocity and altered sensory nerve conduction velocity. 3) Insulin decreased diabetes-driven pathologic muscle spindle Ia innervation variability.

Systemically, insulin can decrease glucose toxicity that is hypothesized by many to lead to neuropathy. However, others suggest that in a type 1 diabetes model the nerves are starved for insulin as a trophic factor, and perhaps giving insulin back to those nerves leads to healthier peripheral nerves. We hypothesize that insulin in this study was having an effect both systemically and more directly on peripheral nerves in order to improve sensorimotor behavior and spindle morphology. Interestingly, insulin is prescribed for human patients with diabetes, and yet these patients can still develop DPN. We think this may be decreasing the glucose toxicity in these patients; however, it may not be at high enough concentrations to be affecting the nerves directly. Perhaps giving intrathecal injections or near-nerve injections of insulin would lead to a decrease in the prevalence of DPN.

Future studies could deliver insulin intrathecally or directly to the sciatic nerve in order to tease out the effects of insulin being due to either decreasing hyperglycemia or due to a direct trophic effect on nerves. In addition, insulin signaling could be examined in specifically in proprioceptors to understand if downstream signaling pathways are disrupted after STZ-treatment.

Chapter Four. Aerobic exercise therapy improves sensorimotor deficits and has no effect on variability in muscle spindle Ia afferent innervation in diabetic mice.

This study was undertaken to examine the effects of exercise therapy on the symptoms of large-fiber DPN and muscle spindle morphologic variations. These data suggest that low-intensity aerobic exercise therapy improved sensorimotor deficits; however, without having an effect on large nerve fiber innervation of muscle spindles. Specifically, results from this study demonstrated that 1) 4 weeks of low-intensity aerobic exercise therapy repaired beam-walk performance without altering glucose or insulin levels or body weight. 2) Exercise therapy had no effect on motor or sensory nerve conduction velocity. 3) Exercise therapy had no effect on the high variability of Ia afferent axonal morphology.

We hypothesize that the improvement in sensorimotor function in diabetic mice after exercise is due to multiple factors. Although not measured in this body of work, improvements in extrafusal fiber strength and/or decreased atrophy of extrafusal fibers may have contributed to the repaired balance of diabetic mice. In addition, exercise is known to increase blood flow and have a positive effect on the vasculature, which is damaged in the setting of diabetes. Therefore, improvements in vascular flow could also have contributed to sensorimotor repair. These findings also suggest that the beam-walk task is reflective of measures other than spindle innervation, which need to be taken into consideration when examining the results of this behavioral task.

Future studies could examine the molecular mechanisms by which exercise improved large-fiber behavioral abnormalities. These studies could focus on

exercise's effect on extrafusal fibers, vascular flow, oxidative stress, and/or cutaneous innervation. In addition, a more intense and perhaps longer duration of exercise therapy in the same animals might be robust enough to induce spindle improvements.

Collectively, these studies demonstrate that STZ-induced diabetic mice are an excellent model of large-fiber diabetic sensorimotor polyneuropathy. Although behavioral changes in large-fiber DPN are subtle, they can be measured through the beam-walk task and, we hypothesize, through gait analysis, at 10 weeks post-STZ injection. Importantly, these behavioral changes may be due to altered muscle spindle Ia afferent innervation patterns, which could lead to aberrant spindle output. Insulin treatment repairs both behavioral and anatomical changes, while exercise therapy only has an effect on the sensorimotor behavior task. These studies give insight into human large-fiber DPN, and will hopefully be a stepping-stone from which future studies can discover the molecular mechanisms at play in both the mouse model and eventually in human patients. With understanding of the mechanisms, comes hope for better and more sophisticated treatments, which are currently lacking in the area of DPN. In addition, these studies also add to the body of literature on muscle spindles and their innervation and function, which will hopefully be applied to other diseases in which patients have difficulty with balance and gait that could be attributed to spindle dysfunction, such as Charcot-Marie-Tooth disease, myasthenia gravis, and Duchenne muscular dystrophy.

X. CHAPTER SIX

References

American Diabetes Association. Diagnosis and classification of diabetes mellitus. Diabetes Care 2006;29 Suppl 1:S43-S48.

American Diabetes Association. Diagnosis and classification of diabetes mellitus. Diabetes Care 2004;27 Suppl 1:S5-S10.

Andersen H, Gjerstad MD, Jakobsen J. Atrophy of foot muscles: a measure of diabetic neuropathy. Diabetes Care 2004;27(10):2382-2385.

Andersen H, Poulsen PL, Mogensen CE, Jakobsen J. Isokinetic muscle strength in long-term IDDM patients in relation to diabetic complications. Diabetes 1996;45(4):440-445.

Armstrong RB, Gollnick PD, Ianuzzo CD. Histochemical properties of skeletal muscle fibers in streptozotocin-diabetic rats. Cell Tissue Res 1975;162(3):387-394.

Balducci S, Iacobellis G, Parisi L, Di Biase N, Calandriello E, Leonetti F, Fallucca F. Exercise training can modify the natural history of diabetic peripheral neuropathy. J Diabetes Complications 2006;20:216-223.

Baskin YK, Dietrich WD, Green EJ. Two effective behavioral tasks for evaluating sensorimotor dysfunction following traumatic brain injury in mice. J Neurosci Methods 2003;129:97-93.

Bergin PS, Bronstein AM, Murray NM, Sancovic S, Zeppenfeld DK. Body sway and vibration perception thresholds in normal aging and in patients with polyneuropathy. J Neurol Neurosurg Psychiatry 1995;58(3):335-340.

Black JA, Langworthy K, Hinson AW, Dib-Hajj SD, Waxman SG. NGF has opposing effects on Na+ channel III and SNS gene expression in spinal sensory neurons. Neuroreport 1997;8(9-10):2331-2335.

Brewster WJ, Fernyhough P, Diemel LT, Mohiuddin L, Tomlinson DR. Diabetic neuropathy, nerve growth factor and other neurotrophic factors. Trends Neurosci 1994;17(8):321-325.

Brussee V, Cunningham FA, Zochodne DW. Direct insulin signaling of neurons reverses diabetic neuropathy. Diabetes 2004;53(7):1824-1830.

Cai F, Tomlinson DR, Fernyhough P. Elevated expression of neurotrophin-3 mRNA in sensory nerve of streptozotocin-diabetic rats. Neurosci Lett 1999;263(2-3):81-84.

Calcutt NA, Jorge MC, Yaksh TL, Chaplan SR. Tactile allodynia and formalin hyperalgesia in streptozotocin-diabetic rats: effects of insulin, aldose reductase inhibition and lidocaine. Pain 1996;68(2-3):293-299.

Cameron NE, Cotter MA. The neurocytokine, interleukin-6, corrects nerve dysfunction in experimental diabetes. Exp Neurol 2007;207(1):23-29.

Cameron NE, Eaton SE, Cotter MA, Tesfaye S. Vascular factors and metabolic interactions in the pathogenesis of diabetic neuropathy. Diabetologia 2001;44(11):1973-1988.

Casellini CM, Vinik AI. Clinical manifestations and current treatment options for diabetic neuropathies. Endocr Pract 2007;13(5):550-566.

Cavanagh PR, Derr JA, Ulbrecht JS, Maser RE, Orchard TJ. Problems with gait and posture in neuropathic patients with insulin-dependent diabetes mellitus. Diabet Med 1992;9(5):469-474.

Cavanagh PR, Simoneau GG, Ulbrecht JS. Ulceration, unsteadiness, and uncertainty: the biomechanical consequences of diabetes mellitus. J Biomech 1993;26 Suppl 1:23-40.

Centers for Disease Control and Prevention (2005). “National Diabetes Fact Sheet, United States, 2005.” http://www.cdc.gov.

Chen HH, Tourtellotte WG, Frank E. Muscle spindle-derived neurotrophin 3 regulates synaptic connectivity between muscle sensory and motor neurons. J Neurosci 2002;22(9):3512-3519.

Christianson JA, Ryals JM, Johnson MS, Dobrowsky RT, Wright DE. Neurotrophic modulation of myelinated cutaneous innervation and mechanical sensory loss in diabetic mice. Neuroscience 2007;145(1):303-313.

Cimbiz A, Cakir O. Evaluation of balance and physical fitness in diabetic neuropathy patients. J Diabetes Complications 2005;19(3):160-164.

Cnop M, Welsh N, Jonas JC, Jorns A, Lenzen S, Eizirik DL. Mechanisms of pancreatic beta-cell death in type 1 and type 2 diabetes: many differences, few similarities. Diabetes 2005;54 Suppl 2:S97-S107.

Copray JC, Brouwer N. Selective expression of neurotrophin-3 messenger RNA in muscle spindles of the rat. Neuroscience 1994;63(4):1125-1135.

Cotter M, Cameron NE, Lean DR, Robertson S. Effects of long-term streptozotocin diabetes on the contractile and histochemical properties of rat muscles. Q J Exp Physiol 1989:74(1):65-74.

Coulthard P, Pleuvry BJ, Brewster M, Wilson KL, Macfarlane TV. Gait analysis as an objective measure in a chronic pain model. J Neurosci Methods 2002;116(2):197-213.

Courtemanche R, Teasdale N, Boucher P, Fleury M, Lajoie Y, Bard C. Gait problems in diabetic neuropathic patients. Arch Phys Med Rehabil 1996;77(9):849-855.

Craner MJ, Klein JP, Renganathan M, Black JA, Waxman SG. Changes of sodium channel expression in experimental painful diabetic neuropathy. Ann Neurol 2002;52(6):786-792.

Dobretsov M, Romanovsky D, Stimers JR. Early diabetic neuropathy: triggers and mechanisms. World J Gastroenterol 2007;13(2):175-191.

Drel VR, Mashtalir N, Ilnytska O, Shin J, Li F, Lyzogubov VV, Obrosova IG. The leptin-deficient (ob/ob) mouse: a new animal model of peripheral neuropathy of type 2 diabetes and obesity. Diabetes 2006;55(12):3335-3343.

Drel VR, Pacher P, Vareniuk I, Pavlov IA, Ilnytska O, Lyzogubov VV, Bell SR, Groves JT, Obrosova IG. Evaluation of the peroxynitrite decomposition catalyst Fe(III) tetra-mesitylporphyrin octasulfonate on peripheral neuropathy in a mouse model of type 1 diabetes. Int J Mol Med 2007;20(6):783-792.

Duby JJ, Campbell RK, Setter SM, White JR, Rasmussen KA. Diabetic neuropathy: an intensive review. Am J Health-Syst Pharm 2004;61(2):160-176.

Dyck PJ. Nerve growth factor and diabetic neuropathy. Lancet 1996;348(9034):1044-1045.

Dyck PJ, O'Brien PC, Litchy WJ, Harper CM, Klein CJ, Dyck PJ. Monotonicity of nerve tests in diabetes: subclinical nerve dysfunction precedes diagnosis of polyneuropathy. Diabetes Care 2005;28(9):2192-2200.

Fernyhough P, Diemel LT, Tomlinson DR. Target tissue production and axonal transport of neurotrophin-3 are reduced in streptozotocin-diabetic rats. Diabetologia 1998;41(3):300-306.

Fernyhough P, Willars GB, Lindsay RM, Tomlinson DR. Insulin and insulin-like growth factor I enhance regeneration in cultured adult rat sensory neurons. Brain Res 1993;607(1-2):117-124.

Ferrer I, Kapfhammer JP, Hindelang C, Kemp S, Troffer-Charlier N, Broccoli V, et al. Inactivation of the peroxisomal ABCD2 transporter in the mouse leads to late-onset ataxia involving mitochondria, golgi and endoplasmic reticulum damage. Human Molecular Genetics 2005;14:3565-3577.

Fox GB, Fan L, Levasseur RA, Faden AI. Sustained sensory/motor and cognitive deficits with neuronal apoptosis following controlled cortical impact brain injury in the mouse. J Neurotrauma 1998;15:599-614.

Fritz T, Kramer DK, Karlsson HK, Galuska D, Engfeldt P, Zierath JR, Krook A. Low-intensity exercise increases skeletal muscle protein expression of PPARdelta and UCP3 in type 2 diabetic patients. Diabetes Metab Res Rev 2006;22(6):492-498.

Ganong WF (2005). Lange Review of Medical Physiology. McGraw-Hill Companies.

Goldshmit Y, Lythgo N, Galea MP, Turnley AM. Treadmill training after spinal cord hemisection in mice promotes axonal sprouting and synapse formation and improves motor recovery. J Neurotrauma 2008;25(5):449-465.

Hirschfeld H, Forssberg H. Development of anticipatory postural adjustments during locomotion in children. J Neurophysiol 1992;68(2):542-550.

Hogan P, Dall T, Nikolov P; American Diabetes Association. Economic costs of diabetes in the US in 2002. Diabetes Care 2003;26(3):917-932.

Horowitz SH. Recent clinical advances in diabetic polyneuropathy. Curr Opin Anaesthesiol 2006;19(5):573-578.

Hoybergs YM, Meert TF. The effect of low-dose insulin on mechanical sensitivity and allodynia in type I diabetes neuropathy. Neurosci Lett 2007;417(2):149-154.

Huang TJ, Price SA, Chilton L, Calcutt NA, Tomlinson DR, Verkhratsky A, Fernyhough P. Insulin prevents depolarization of the mitochondrial inner membrane in sensory neurons of type 1 diabetic rats in the presence of sustained hyperglycemia. Diabetes 2003;52(8):2129-2136.

Ishii DN. Implication of insulin-like growth factors in the pathogenesis of diabetic neuropathy. Brain Res Brain Res Rev 1995;20(1):47-67.

Jefferys JG, Brismar T. Analysis of peripheral nerve function in streptozotocin diabetic rats. J Neurol Sci 1980;48(3):435-444.

Johnson MS, Ryals JM, Wright DE. Diabetes-induced chemogenic hypoalgesia is paralleled by attenuated stimulus-induced fos expression in the spinal cord of diabetic mice. J Pain 2007;8(8):637-649.

Kararizou E, Manta P, Kalfakis N, Vassilopoulos D. Morphometric study of the human muscle spindle. Anal Quant Cytol Histol 2005;27:1-4.

Kearney JA, Buchner DA, De Haan G, Adamska M, Levin SI, Furay AR, Albin RL, Jones JM, Montal M, Stevens MJ, Sprunger LK, Meisler MH. Molecular and pathological effects of a modifier gene on deficiency of the sodium channel Scn8a (Na(v)1.6). Hum Mol Genet 2002;11(22):2765-2775.

Kennedy AJ, Wellmer A, Facer P, Saldanha G, Kopelman P, Lindsay RM, Anand P. Neurotrophin-3 is increased in skin in human diabetic neuropathy. J Neurol Neurosurg Psychiatry 1998;65(3):393-395.

Kishi M, Tanabe J, Schmelzer JD, Low PA. Morphometry of dorsal root ganglion in chronic experimental diabetic neuropathy. Diabetes 2002;51(3):819-824.

Kwon OY, Minor SD, Maluf KS, Mueller MJ. Comparison of muscle activity during walking in subjects with and without diabetic neuropathy. Gait Posture 2003;18(1):105-113.

Liu JX, Erikssonn PO, Thornell LE, Pedrosa-Domellof F. Fiber content and myosin heavy chain composition of muscle spindles in aged human biceps brachii. J Histochem Cytochem 2005;53(4):445-454.

Malik RA. Current and future strategies for the management of diabetic neuropathy. Treat Endocrinol 2003;2(6):389-400.

Menz HB, Lord SR, St George R, Fitzpatrick RC. Walking stability and sensorimotor function in older people with diabetic peripheral neuropathy. Arch Phys Med Rehabil 2004;85(2):245-252.

Mizisin AP, Calcutt NA, Tomlinson DR, Gallagher A, Fernyhough P. Neurotrophin-3 reverses nerve conduction velocity deficits in streptozotocin-diabetic rats. J Peripher Nerv Syst 1999;4(3-4):211-221.

Moien-Afshari F, Ghosh S, Khazaei M, Kieffer TJ, Brownsey RW, Laher I. Exercise restores endothelial function independently of weight loss or hyperglycemic status in db/db mice. Diabetologia 2008;51(7):1327-1337.

Molteni R, Zheng JQ, Ying Z, Gomez-Pinilla F, Twiss JL. Voluntary exercise increases axonal regeneration from sensory neurons. Proc Natl Acad Sci USA 2004;101:8473-8478.

Moore SA, Peterson RG, Felten DL, Cartwright TR, O'Connor BL. Reduced sensory and motor conduction velocity in 25-week-old diabetic [C57BL/Ks (db/db)] mice. Exp Neurol 1980;70(3):548-555.

Mueller MJ, Minor SD, Sahrmann SA, Schaaf JA, Strube MJ. Differences in the gait characteristics of patients with diabetes and peripheral neuropathy compared with age-matched controls. Phys Ther 1994;74(4):299-308.

Muller KA, Ryals JM, Feldman EL, Wright DE. Abnormal muscle spindle innervation and large-fiber neuropathy in diabetic mice. Diabetes 2008;57:1693-1701.

Nardone A, Schieppati M. Group II spindle fibers and afferent control of stance. Clues from diabetic neuropathy. Clin Neurophysiol 2004;115(4):779-789.

Nardone A, Galante M, Pareyson D, Schieppati M. Balance control in sensory neuron disease. Clin Neurophysiol 2007;118(3):538-550.

National Institute of Diabetes and Digestive and Kidney Diseases (2007). "National Diabetes Statistics, 2007." http://diabetes.niddk.nih.gov.

Nojima H, Watanabe H, Yamane K, Kitahara Y, Sekikawa K, Yamamoto H, Yokoyama A, Inamizu T, Asahara T, Kohno N. Effect of aerobic exercise training on oxidative stress in patients with type 2 diabetes mellitus. Metabolism 2008;57:170-176.

Onyszchuk G, Al-Hafez B, He YY, Bilgen M, Berman NE, Brooks WM. A mouse model of sensorimotor controlled cortical impact: characterization using longitudinal magnetic resonance imaging, behavioral assessments and histology. J Neurosci Methods 2007;160(2):187-196.

Praet SF, Jonkers RA, Schep G, Stehouwer CD, Kuipers H, Keizer HA, van Loon LJ. Long-standing, insulin-treated type 2 diabetes patients with complications respond well to short-term resistance and interval exercise training. Eur J Endocrinol 2008;158(2):163-172.

Ramji N, Toth C, Kennedy J, Zochodne DW. Does diabetes mellitus target motor neurons? Neurobiol Dis 2007;26(2):301-311.

Recio-Pinto E, Rechler MM, Ishii DN. Effects of insulin, insulin-like growth factor-II, and nerve growth factor on neurite formation and survival in cultured sympathetic and sensory neurons. J Neurosci 1986;6(5):1211-1219.

Richardson JK. Factors associated with falls in older patients with diffuse polyneuropathy. J Am Geriatr Soc 2002;50(11):1767-1773.

Richardson JK, Sandman D, Vela S. A focused exercise regimen improves clinical measures of balance in patients with peripheral neuropathy. Arch Phys Med Rehabil 2001;82:205-209.

Romanovsky D, Cruz NF, Dienel GA, Dobretsov M. Mechanical hyperalgesia correlates with insulin deficiency in normoglycemic streptozotocin-treated rats. Neurobiol Dis 2006;24(2):384-394.

Roumen C, Corpeleijn E, Feskens EJ, Mensink M, Saris WH, Blaak EE. Impact of 3-year lifestyle intervention on postprandial glucose metabolism: the SLIM study. Diabet Med 2008;25(5):597-605.

Russell JW, Berent-Spillson A, Vincent AM, Freimann CL, Sullivan KA, Feldman EL. Oxidative injury and neuropathy in diabetes and impaired glucose tolerance. Neurobiol Dis 2008;30(3):420-429.

Sacco IC, Amadio AC. Influence of the diabetic neuropathy on the behavior of electromyographic and sensorial responses in treadmill gait. Clin Biomech 2003;18(5):426-434.

Sherbel U, Raghupathi R, Nakamura M, Saatman KE, Trojanowski JQ, Neugebaumer E, et al. Differential acute and chronic responses of tumor

necrosis factor-deficient mice to experimental brain injury. Proc Natl Acad Sci USA 1999;96:8721-8726.

Sigal RJ, Kenny GP, Boule NG, Wells GA, Prud'homme D, Fortier M, Reid RD, Tulloch H, Coyle D, Phillips P, Jennings A, Jaffey J. Effects of aerobic training, resistance training, or both on glycemic control in type 2 diabetes: a randomized trial. Ann Intern Med 2007;147(6):357-369.

Sigal RJ, Kenny GP, Wasserman DH, Castaneda-Sceppa C. Physical activity/exercise and type 2 diabetes. Diabetes Care 2004;27:2518-2539.

Simoneau GG, Derr JA, Ulbrecht JS, Becker MB, Cavanagh PR. Diabetic sensory neuropathy effect on ankle joint movement perception. Arch Phys Med Rehabil 1996;77(5):453-460.

Singhal A, Cheng C, Sun H, Zochodne DW. Near nerve local insulin prevents conduction slowing in experimental diabetes. Brain Res 1997;763(2):209-214.

Sinnreich M, Taylor BV, Dyck PJB. Diabetic neuropathies: classification, clinical features, and pathophysiological basis. Neurologist 2005;11:63-79.

Skyler JS. Diabetes mellitus: pathogenesis and treatment strategies. J Med Chem 2004;47(17):4113-4117.

Smith AG, Russell J, Feldman EL, Goldstein J, Peltier A, Smith S, Hamwi J, Pollari D, Bixby B, Howard J, Singleton JR. Lifestyle intervention for pre-diabetic neuropathy. Diabetes Care 2006;29:1294-1299.

Smith AG, Singleton JR. Impaired glucose tolerance and neuropathy. Neurologist 2008;14(1):23-29.

Soukup T, Pedrosa F, Thornell LE. Influence of neonatal motor denervation on expression of myosin heavy chain isoforms in rat muscle spindles. Histochemistry 1990;94(3):245-256.

Stapley PJ, Ting LH, Hulliger M, Macpherson JM. Automatic postural responses are delayed by pyridoxine-induced somatosensory loss. J Neurosci 2002;22:5803-5807.

Stevens MJ, Obrosova I, Cao X, Van Huysen C, Greene DA. Effects of DL-alpha-lipoic acid on peripheral nerve conduction, blood flow, energy metabolism, and oxidative stress in experimental diabetic neuropathy. Diabetes 2000;49(6):1006-1015.

Sugimoto K, Murakawa Y, Sima AA. Expression and localization of insulin receptor in rat dorsal root ganglion and spinal cord. J Peripher Nerv Syst 2002;7:44-53.

Sullivan KA, Hayes JM, Wiggin TD, Backus C, Su Oh S, Lentz SI, Brosius F 3rd, Feldman EL. Mouse models of diabetic neuropathy. Neurobiol Dis 2007;28(3):276-285.

Swash M, Fox KP. The effect of age on human skeletal muscle: studies of the morphology and innervation of muscle spindles. J Neurol Sci 1972;16:417-432.

Swash M, Fox KP. The pathology of the human muscle spindle: effect of denervation. J Neurol Sci 1974;22:1-24.

Swash M, Fox KP. The pathology of the muscle spindle in Duchenne muscular dystrophy. J Neurol Sci 1976;18:175-184.

Taylor MD, Holdeman AS, Weltmer SG, Ryals JM, Wright DE. Modulation of muscle spindle innervation by neurotrophin-3 following nerve injury. Exp Neurol 2005;191:211-222.

Taylor MD, Vancura R, Patterson CL, Williams JM, Riekhof JT, Wright DE. Postnatal regulation of limb proprioception by muscle-derived neurotrophin-3. J Comp Neurol 2001;432(2):244-258.

Tomlinson DR. Aldose reductase inhibitors and the complications of diabetes mellitus. Diabet Med 1993;10(3):214-230.

Tomlinson DR, Gardiner NJ. Glucose neurotoxicity. Nat Rev Neurosci 2008;9(1):36-45.

Toth C, Brussee V, Martinez JA, McDonald D, Cunningham FA, Zochodne DW. Rescue and regeneration of injured peripheral nerve axons by intrathecal insulin. Neuroscience 2006;139(2):429-449.

Tourtellotte WG, Milbrandt J. Sensory ataxia and muscle spindle agenesis in mice lacking the transcription factor Egr3. Nat Genet 1998;20(1):87-91.

Tuomi T. Type 1 and type 2 diabetes: what do they have in common? Diabetes 2005;54 Suppl 2:S40-S45.

Uccioli L, Giacomini PG, Monticone G, Magrini A, Durola L, Bruno E, Parisi L, Di Girolamo S, Menzinger G. Body sway in diabetic neuropathy. Diabetes Care 1995;18:339-344.

van Dam PS, van Asbeck BS, Erkelens DW, Marx JJ, Gispen WH, Bravenboer B. The role of oxidative stress in neuropathy and other diabetic complications. Diabetes Metab Rev 1995;11(3):181-192.

van Deursen RW, Sanchez MM, Ulbrecht JS, Cavanagh PR. The role of muscle spindles in ankle movement perception in human subjects with diabetic neuropathy. Exp Brain Res 1998;120:1-8.

Villa-Caballero L, Nava-Ocampo AA, Frati-Munari AC, Rodriguez de Leon SM, Becerra-Perez AR, Ceja RM, Campos-Lara MG, Ponce-Monter HA. Hemodynamic and oxidative stress profile after exercise in type 2 diabetes. Diabetes Res Clin Pract 2007;75:285-291.

Vinik AI, Mehrabyan A. Diabetic neuropathies. Med Clin North Am 2004;88(4):947-999.

Vinik AI, Park TS, Stansberry KB, Pittenger GL. Diabetes neuropathies. Diabetologia 2000;43(8):957-973.

Wang ZC, Dohle JF, Friemann J, Green BS. Prevention of high- and low-dose STZ-induced diabetes with d-glucose and 5-thio-d-glucose. Diabetes 1993;42:420-428.

Wang J, McWhorter DL, Walro JM. Stability of myosin heavy chain isoforms in selectively denervated adult rat muscle spindles. Anat Rec 1997;249:32-43.

Waxman, SG (2003). Lange Clinical Neuroanatomy. McGraw-Hill Companies.

Weis J, Dimpfel W, Schroder JM. Nerve conduction changes and fine structural alterations of extra- and intrafusal muscle and nerve fibers in streptozotocin diabetic rats. Muscle & Nerve 1995;18:175-184.

White MF. Insulin signaling in health and disease. Science 2003;302(5651):1710-1711.

Wright DE, Zhou L, Kucera J, Snider WD. Introduction of a neurotrophin-3 transgene into muscle selectively rescues proprioceptive neurons in mice lacking endogenous neurotrophin-3. Neuron 1997;19(3):503-517.

Ying Z, Roy RR, Edgerton R, Gomez-Pinilla F. Exercise restores levels of neurotrophins and synaptic plasticity following spinal cord injury. Exp Neurology 2005;193(2):411-419.

Yokota T, Saito Y, Miyatake T. Conduction slowing without conduction block of compound muscle and nerve action potentials due to sodium channel block. J Neurol Sci 1994;124(2):220-224.

LIST OF MY PUBLICATIONS

Decker MJ, **Jones KA**, Solomon IG, Keating GL, Rye DB. Reduced extracellular dopamine and increased responsiveness to novelty: neurochemical and behavioral sequelae of intermittent hypoxia. Sleep 2005;28:169-176.

Levant B, Ozias MK, **Jones KA**, Carlson SE. Differential effects of modulation of brain docosahexaenoic acid content during development in specific regions of rat brain. Lipids 2006;41:407-414.

Muller KA, Ryals JM, Feldman EL, Wright DE. Abnormal muscle spindle innervation and large-fiber neuropathy in diabetic mice. Diabetes 2008;57:1693-1701.

Muller KA, Ryals JM, Wright DE. Low-intensity aerobic exercise therapy for large-fiber diabetic neuropathy in mice. (Under Review).

Muller KA, Wright DE. Large-fiber diabetic neuropathy: a review. (In Preparation)